A Spatial and Geophysical Exploration of Atlantic Eel Larval Distributions

A Spatial and Geophysical Exploration of Atlantic Eel Larval Distributions

Helen Andrée Périvier

A Thesis in the Field of Sustainability and Environmental Management

for the Degree of Master of Liberal Arts in Extension Studies

Harvard University Extension School

November 2015

Abstract

In the context of declining populations of freshwater eels in Europe and North America and inspired by observations of Japanese eel spawning near seamounts, this study explored a possible spatial relationship between spawning American and European eels (*Anguilla rostrata* and *A. anguilla*) and geophysical features in the Sargasso Sea. A spatial analysis of positive and null catch sampling data from 1863 to 2007 found observations of young eel larvae significantly clustered over magnetic anomalies with higher than average intensities. These larval clusters occurred above the southwest Bermuda Rise and in the vicinity of the Vema Gap, a constricted abyssal channel connecting the Nares and Hatteras Abyssal Plains and directing flow of the abyssal bottom current. In this area, newly hatched larvae were positioned on either side, but not within, a 170 km wide high-magnetic gradient band located on the M0 anomaly. This gradient separated the centers of the distributions of the two species when they were $\leq$ 5 mm in length. Standard deviations of directional trends indicated probabilities in dispersal patterns, highlighting a potential tool for modeling larval distributions. Like other species undergoing oceanic migrations, eels have demonstrated a magnetic sensory ability and may rely on magnetic cues for navigation. The geomagnetism of the ocean floor, which attenuates at a cubic rate with distance, may provide a clue to eel migratory routes and depth preferences or play a role in larval dispersal, metamorphosis and recruitment. Spatial analyses open new opportunities to study anguillid distributions in relation to geomagnetic and oceanographic features.

Acknowledgements

Lately when falling asleep, I have taken to imagining that I am an eel deep in the ocean. Since I am swimming a thousand meters below the surface, the water presses down heavily. There is no light, but I swim steadily in a darkness and enfolding silence towards something that I do not know but have never forgotten. Awake, I realize how different my own thesis journey has been from that of my imaginary eel. Twists and turns have brought me into the good company of a host of traveling companions, some sharing a portion of the journey and others keeping in step the entire way. It is a pleasure to now recognize those who have generously offered their helping hand and words of advice and encouragement at various junctions.

In particular, I thank both Adrian Jordaan, my thesis director, and George Buckley, my research adviser. I am deeply grateful to Dr. Jordaan at the University of Massachusetts in Amherst for taking me on as his advisee. As a director he has instilled a balance of critical assessment and curiosity that I think every graduate student hopes for in an adviser, sharpening inquiry without dampening the spirit of exploration. In addition, I would like to recognize Dr. Jordaan for imparting an appreciation for the “value of zero”, which has added an original dimension to this project that it would otherwise have lacked.

Shepard and mentor with his knowledge and long personal experience with the sea, Professor Buckley has provided a welcome source of inspiration and cheerful encouragement that has kept me moving in the right direction. His repeated advice to

students in his oceans environment course, one of my first in the program, and based on his own tumultuous experimentation in tilapia farming, “Know your species”, was a reminder that I have tried to keep in mind throughout my thesis process. I thank Prof. Buckley for letting his great enthusiasm and love of the ocean spill over in my direction.

It soon became clear beginning this project to what degree my prior courses in the Sustainability and Environmental Management program helped prepare me for the task. These included the ecology, conservation biology, and critical thinking and systems courses of Dr. Mark Leighton, who gave me the excellent advice to choose my thesis topic well because I was going to “have to live with it” for nine months. I am glad I kept his advice in mind when choosing my topic. It continues to fascinate and is even now hard to put down. I would also like to thank Dr. Ramon Sanchez for his preparation of thesis proposal writing and research in his proseminar and especially for his generous time talking informally between classes. As I took the deep breath and plunged in choosing my topic, Dr. Sanchez imparted confidence at a time filled with self-doubt, and gave some valued words that have kept me fierce in pursuing my research goals.

My good friends Karen Alexander and William Leavenworth have been central figures to my thesis story. As I was transitioning from a life in New Hampshire they helped me find the path that led me to Dr. Jordaan. During the winter I spent with them in an old farmhouse in New Hampshire, they inspired me with their work in historical ecology (or is it ecological history? I am never entirely sure), which I have had the opportunity to try a little myself in this project.

A new world also opened up to me during the course of my research giving me the new ambition to reincarnate in my next life as a research librarian. With patience and

the kindest words Dorothy Barr and Ronnie Broadfoot at the Ernst Mayr Library of the Museum of Comparative Zoology provided me their utmost professional help locating hard to find sources, helping me scan my way through a stack of hard-to-find books on several mad hot July days. This same spirit of generosity seems to be an occupational hazard of the research librarian. Bonnie Burns of the Harvard Map Collection, Ann Devenish and Audrey Mickel at the Woods Hole Oceanographic Institute Library, Angela Clark at the Rosenstiel School of Marine and Atmospheric Science, and Jim Bird at University of Maine Fogler Library without question assisted my search for sources.

Not all station data for eel research expeditions were in the library's reach. In this regard I am indebted to those eel researchers who not only shared their data but also much valued thoughts and motivation. My appreciation goes to Dr. James McCleave for sharing station data from his Cape Florida and Columbus Iselin expeditions and for his creation of the ICES Egg and Larvae data base, without which this project would not exist. I also thank Dr. Henrik Sparholt for generously sharing data from his Galathea III voyage and Dr. Michael Miller for his kind correspondence and thoughts on eels and their migration.

I have also relied on many online data tools and expert desks and would like to thank them for responding quickly to my pleas for help, notably Jason Roberts of the Marine Geospatial Ecology Lab, Brian Meyer with the NOAA National Geophysical Data Center, Pauline Weatherall with the British Oceanographic Data Center, and Stacy Bogan with the Harvard Center for Geographic Analysis.

As well, I would like to acknowledge Adrian Jordaan, Mark Leighton, George Buckley, and Valerie E. Gould, for their careful edits that have greatly improved the text

and format of this thesis.

Last but not least, I thank my family who gave me their love and support during this thesis journey and especially my husband, Ulf Birgander, who never doubted that I would find my way to the Sargasso Sea and back again.

Table of Contents

List of Tables

List of Figures

Chapter I

Introduction

Diadromous fish provide an important biological exchange of nutrients and energy between inland and estuarine ecosystems and the ocean environment. The catadromous anguillid American eel (*Anguilla rostrata*) and European eel (*Anguilla anguilla*), often referred to as freshwater eels, are North Atlantic Ocean species who spend the greater part of their life as juveniles in inland and coastal waters of the American and European continents. The only two anguillid species of the northwestern hemisphere, these eels inhabit freshwater lakes, rivers and brackish estuaries across a wide latitudinal range (Tesch, 2003). Yet despite geographic separation the two species are so closely related that their distinction was long subject of debate (Boëtius, 1980). The migrations of these far-ranging eels disperse from and re-converge in the Sargasso Sea, a sea defined not by shores, but by ocean currents and frontal systems in the southwest North Atlantic Ocean (McCleave & Kleckner, 1987; Schmidt, 1923; Schoth & Tesch, 1982). While the abundance of anguillids born and returning to the Sargasso Sea fall outside of human observation, eels are familiar inhabitants of continental freshwater ecosystems. Past estimates have calculated that American eels constituted as much as from 25% to 50% of the total biomass in some North American rivers, indicating some importance within riparian ecosystems (Dekker, 2004a; Ogden, 1970). Eels have featured in North American and European human culture for thousands of years and have traditionally supported inland and coastal food fisheries. However recent declines in eel

recruitment and abundance, most dramatically in Europe where recruitment of European eels in some regions has dropped to 90 percent of historical levels, have raised concern on both sides of the Atlantic (Casselman, 2003; Dekker, 2004a; Haro et al., 2000; ICES, 2008). Now new research has emerged indicating that abundances of eel larvae in the Sargasso Sea have declined significantly since the 1980s (Hanel et al., 2014).

A number of factors are known or believed to impact eel development, reproduction and survival, but none stands out as a single explanation for the widespread disappearance of eels from the North American and European continents. Land and coastal impacts include obstruction of eel migration routes by dams and other barriers that impede natural stream or river flows, toxic contaminants, invasive nematode parasites, and coastal commercial and illegal fishing (Dekker, 2004). This myriad of land-based impacts may reduce the number and health of maturing eels, negatively impacting spawning migration and reproduction. Eels migrate thousands of kilometers to reproduce and eels weakened by poor habitat and environmental conditions prior to migration may lack sufficient energetic resources to reach their spawning grounds (van den Thillart, Palstra, & van Ginneken, 2009). As well, oceanic factors during the larval marine phase of the eel's life cycle may impact early survival and migration and impact continental recruitment (Miller et al., 2009). For example, shifting ocean circulatory patterns induced by climate change may influence availability of food resources and drift patterns for migrating larvae (Bonhommeau, Chassot, & Rivot, 2008; Friedland, Miller, & Knights, 2007).

These uncertainties in the anguillid life cycle and its vulnerabilities to environmental and ecosystem factors weaken predictions of anguillid population

dynamics and distributions. The oceanic phase of the eel in both its larval and mature stages has proven the least accessible for study, and large gaps in knowledge leave many aspects of larval dispersal, spawning migration, and reproduction a mystery. Ever since Johannes Schmidt first followed a trail of eel larvae to their source in the early 1920s, researchers have sought to more precisely locate where eels spawn and migrate. Unlocking the mysteries of the oceanic life stages of the eel not only promises to inform anguillid conservation, but also to contribute to understanding of broader topics such as long distance ocean migration and the ecological function of the Sargasso Sea, an area of biologic importance for endemic and transient pelagic species. For practitioners, greater geographical precision of eel spawning and larval distributions would also help efforts to delineate areas of biological importance for conservation in the Sargasso region. However researchers have yet to observe an adult eel or anguillid egg within the Sargasso Sea, leaving the geography of eel spawning and its migration a largely deductive exercise relying on locations of larvae across a general area of approximately 1,000,000 km^2 (McCleave, 1993; Schmidt, 1923; Tsukamoto et al., 2011).

Despite a remarkable geographic dispersal as juveniles in rivers, streams, lakes and estuaries that for the American eel ranges from Venezuela to Greenland and for the European eel from the Black Sea to Finland, the random and aggregative spawning in the Sargasso Sea reduces each species into single breeding and genetically homogenous (panmictic) populations (Als et al., 2011; Volckaert, Maes, & Pujolar, 2005). The consequent absence of geographically isolated subpopulations limits the effectiveness of local and regional eel restoration measures and renders knowledge about eel reproduction all the more critical for eel conservation. Although no geographic barrier isolates the two

eel species from one another in the Sargasso Sea, the two species maintain a distinct morphological and genetic identity through offset breeding locations and seasons (Als et al., 2011; Kettle & Haines, 2006; McCleave, 2003; Munk et al., 2010; Schoth & Tesch, 1982; Tsukamoto, Aoyama, & Miller, 2002; Volckaert et al., 2005). However, the co-occurrence of newly hatched American and European eel larvae in field samples also shows that the breeding grounds and season of the two species overlap in time and space (Albert, Jonsson, & Bernatchez, 2006). The finding of multigenerational hybrid eels in Iceland provides evidence that this overlap leads to interbreeding between American and European eels and raises questions on how ocean currents and related variables influence American and European eel speciation (Albert, Jonsson, & Bernatchez, 2006). Efforts to model, or predict, how changing oceanic factors could affect future eel population structures would be aided by greater certainty of eel spawning behavior and geography.

Dynamic seasonal and thermal fronts in the southwest region of the Sargasso Sea are the primary oceanographic factors associated with eel spawning locations (Kleckner, McCleave, & Wippelhauser, 1983; Miller & McCleave, 1994). How Atlantic eels succeed in navigating up to 6000 km to locate these thermal fronts in the Sargasso Sea and aggregate for spawning is a mystery (Aarestrup et al., 2009; Tsukamoto, 2009). Eels have demonstrated magnetic and electromagnetic (Durif et al., 2013; Nishi & Kawamura, 2005; Nishi, Kawamura, & Matsumoto, 2004), as well as olfactory, (Huertas, Canario, & Hubbard, 2008) sensory abilities, as have other species that undertake long distance, oceanic migrations, such as loggerhead sea turtles (Lohmann, Lohmann, et al., 2008; Putman, Endres, Lohmann, & Lohmann, 2011) and salmon (Putman et al., 2014). Whether these sensory abilities, singly or in concert, play a navigational role is a key

question in animal migration. In the North Pacific Ocean, the Japanese eel (*A. japonica*), whose life cycle largely parallels that of its North Atlantic cousins, also migrates to reproduce along subtropical frontal systems, although in its case salinity rather than thermal gradients have been most strongly associated with spawning location (Kimura & Tsukamoto, 2006; Tsukamoto et al., 2011). Additional discoveries of *A. japonica* newly hatched larvae, eggs, and mature eels in proximity to seamounts in the West Mariana Ridge have further led researchers to hypothesize that the submarine topography may serve as landmarks orienting the movements of migrating Japanese eels into spawning aggregations (Aoyama et al., 2014; Chow et al., 2008; Tsukamoto, 2006; Tsukamoto et al., 2003; Aoyama, 1999). The southwest Sargasso Sea, however, lacks underwater sea features on the scale of the Mariana Ridge. This absence of prominent bathymetric features and depths of up to six kilometers have discouraged exploration of the potential influence of bathymetric and other geophysical cues in Atlantic eel migration.

From an ecological perspective, the Sargasso Sea is notable for an endemic ecological community that includes the world's only known wholly pelagic sea algae (*Sargassum*) and for its function as a nursery for pelagic species, such as sea turtles and porbeagle sharks (Butler, Morris, Cadwallader, & Stoner, 1983; Campana et al., 2010; Deacon, 1942; Laffoley et al., 2011). Recognizing the uniqueness and importance of the Sargasso Sea for global biological diversity, national governments, and intergovernmental and international organizations have proposed to create a pelagic marine reserve within its deep sea waters (Ardron et al., 2011; Dale, 2010; Laffoley et al., 2011; UNEP, 2008). The creation of a pelagic reserve in the Sargasso Sea poses unique challenges. Unlike coastal basins delineated by the continental shelf or a particular

bathymetry, the Sargasso Sea is deep, dynamic and defined by ocean currents (Ardron et al., 2011). Additionally, understanding the biophysical aspects of benthic and pelagic environments and how they interact is considered essential for planning reserves in the ocean landscape, even in a deep ocean environment (Harris & Whiteway, 2009).

With the aim of contributing to the knowledge of where eels go to spawn, this study explores whether a spatial relationship exists between eel spawning locations and geophysical features in the Sargasso Sea. A spatial analysis of anguillid larval distributions and their underwater landscape offers new perspectives on eel spawning migration and behavior that can inform conservation planning for the Atlantic eels and, more widely, the Sargasso Sea. As well, its many associations make eel spawning and migration relevant within fields of genetics, population dynamics, animal migration, and biological diversity of freshwater and marine ecological systems.

Background

The following sections introduce the North Atlantic eels, the Sargasso Sea, and anguillid larval distribution and spawning migration in its waters. Eel spawning migration is presented in the context of its relationship to geophysical surroundings, forming the thesis for this investigation.

Eels of the North Atlantic

The American eel and European eel are members of the Anguillidae family. The Anguillidae are made up of the single genus *Anguilla* and belong to the broader order of fish known as Anguilliformes. Anguilliformes are characterized by an elongated and

snake-like form with continuous dorsal and anal fins that merge into caudal fins and by their unique transparent and leaf-like larvae, known as leptocephali. Unusual among Anguilliformes species, which are otherwise fully marine, anguillids are catadromous, meaning they mature and live in inland freshwater rivers and streams and brackish estuaries and only spawn and hatch at sea (Lecomte-Finiger, 2003; Miller, 2009). For this reason, anguillids are often referred to as "freshwater eels", or "true eels", distinguishing them from their more distant and wholly oceanic relatives like the conger or moray eels. In actuality, adult anguillids demonstrate considerable flexibility in their preference and movements between habitats of varying salinity and so more accurately practice facultative catadromy (Daverat et al., 2006; Lamson, Cairns, Shiao, Iizuka, & Tzeng, 2009; Tsukamoto et al., 2002). Of the anguillid species inhabiting temperate environments, there are three in the northern hemisphere (*A. rostrata* and *A. anguilla* in the North Atlantic and *A. japonica* in the North Pacific Ocean) and three in the southern hemisphere in Australia and New Zealand, while other anguillids mature in tropical latitudes (Lecomte-Finiger, 2003). However, all anguillids including temperate species hatch and spawn either in tropical or subtropical waters (Aoyama, 2009; Lecomte-Finiger, 2003). Anguillids are semelparous, reproducing only at the end of their lifetime (Tesch, 2003).

The American and European eels (unless otherwise specified, "eels" in this paper refers only to anguillid eels and not marine species of Anguilliformes) are the only freshwater eels inhabiting the North Atlantic Ocean, while none inhabit the South Atlantic Ocean (Aoyama & Tsukamoto, 1997). Closely related, genetic analyses indicate that American and European eels have only relatively recently diverged into two species

(Lecomte-Finiger, 2003). The American and European eels were once debated as being a single species, but can be distinguished by their number of vertebrae, a feature for which anguillids demonstrate considerable plasticity (Tesch, 2003). Studying vertebrate counts of samples collected by Schmidt in 1913 and Ege in 1939, Tesch (2003) found American eels and European eels averaged 107 and 114 vertebrae respectively and that approximately 1.5% of the samples had overlapping vertebrae counts that made species identification more difficult.

Life cycle and biology. The life cycle of American and European eels includes several metamorphoses beginning as the larval type leptocephali and followed by a transformation into more eel-like glass eels off the continental shelves of North America and Europe (Lecomte-Finiger, 2003; Tesch, 2003). Leptocephali are unique to some 800 species of marine and freshwater eels and related fish and are distributed throughout the world's oceans (citing Nelson 2006, Miller 2009). Transparent and with laterally compressed bodies, leptocephalus larvae have a relatively large size and slow growth rate compared to other types of fish larvae. Leptocephali have an anguilliform swimming ability enabling them to swim forwards and backwards over short distances (Miller, 2009). The eyes of anguillid leptocephali are round, rather than telescoping or oval as is the case with some leptocephali species and have rod-like retinal photoreceptors that may indicate adaptation to depth where there is less available light (Miller, 2009). Leptocephali are born with olfactory organs and probably mechanoreceptor cells along lateral lines (Miller, 2009). Because of their large size, swimming ability, and possible visual acuity, leptocephali often succeed in avoiding capture in plankton nets, which are typically designed for smaller specimens (M. Miller et al., 2013). Difficulty in capture

and transparency poses challenges for the study of leptocephali with the result that they are not a well-known fish larvae (Miller, 2009).

The larval phase of anguillid leptocephali in the North Atlantic originates in the deep ocean environment of the southwestern area of the Sargasso Sea (Castonguay & McCleave, 1987; Kleckner & McCleave, 1988; McCleave, 2003; Schmidt, 1923; Schoth & Tesch, 1982). While no adult eels or eel eggs have been observed in the Sargasso Sea, the smallest leptocephali, some still containing yolk sacs, have been found in an area encompassing close to 1,500,000 km^2 as shown in Figure 1 (Castonguay & McCleave, 1987; Schmidt, 1923). Oliveira and Hable (2010) compared results of their artificial fertilization and maturation of *A. rostrata* studies with those of *A. anguilla* by Petersen in 2004 and Bezdenezhnykh in 1983. Ovulated eggs of *A. rostrata* and *A. anguilla* ranged from 960 to 1030 µm and from 1000 to 1600 µm respectively (Oliveira & Hable, 2010). Hatching periods for *A. rostrata* (32–45 h) were somewhat shorter than for *A. anguilla*, measured from 48 to 50 h by Pedersen, and from 46 to 110 h by Bezdenezhnykh (as cited by Oliveira & Hable, 2010). Upon hatching, *A. rostrata* larvae measured 2.7 ± 0.2 mm, growing to 3.8 ± 0.3 mm in four days (Oliveira & Hable, 2010). Newly hatched *A. anguilla* were 2.7 mm and 2.35 mm as measured by Bezdenezhnykh and Pedersen respectively (as cited by Oliveira & Hable, 2010). After hatching and during an initial preleptocephalus stage, larvae feed off an attached yolk sac that sustains them for up to a week as they develop head, teeth, and eyes and initiate active feeding (Miller, 2009).

Anguillid leptocephali undergo a lengthy and variable period of oceanic development. Feeding on the bottom of the food chain at the bacterial level, the leptocephali ingest larval cases, marine snow and other particulate carbon matter (Miller,

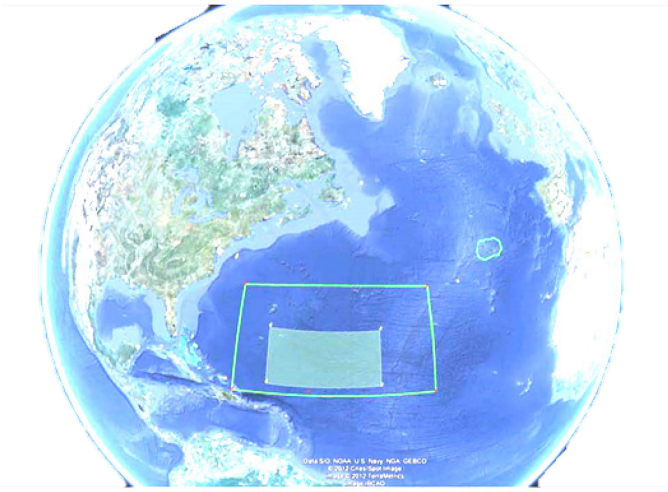

Figure 1. The Sargasso Sea and Schmidt's discovered eel breeding grounds. The outer box represents the rough perimeter of the Sargasso Sea, an area of 4,163,500 km^2 (Laffoley et al., 2011). The inner shaded area is where Schmidt (1923) found the smallest leptocephali and encompasses approximately 1,500,000 km^2.

2009). Larval duration varies with the strength, direction and distance of the ocean currents that transport them towards the continental shelves (Munk et al., 2010). The larval migration of *A. rostrata* can vary between eight months and one year before recruitment to the North American continent, while it can take *A. anguilla* larvae one to two years to complete their from 5000 to 6000 km migration to Europe (Kettle & Haines, 2006; Kleckner & McCleave, 1985; McCleave et al., 1998; McCleave et al., 1987). As leptocephali approach the continental shelf, they reduce in size and metamorphose into tiny transparent and serpentine glass eels, subsequently gaining pigment and growing into elvers as they enter coastal, estuarine and freshwater habitats (Fahay, 1978; Tesch, 2003). During transformation into glass eels, leptocephali lose water and a considerable

amount of weight, about an order of magnitude, so that just over one gram of leptocephali reduces to approximately 0.1 g of glass eels (Fahay, 1978). Entering inland waters, elvers develop into juvenile yellow eels. Females of both species generally grow to be larger than males (Fahay, 1978). Krueger and Oliveira (1999) found that American yellow eels from a river in Rhode Island differentiated into males and females after exceeding a mean size of 251 mm and that males had a smaller mean size than females. Yellow eels inhabit inland and coastal fresh or brackish habitats typically for between 3 and 20 years before maturing and migrating back to sea. Some eels that become landlocked and unable to migrate have been known to live up to 80 years in freshwater environments (Fahay, 1978).

At the onset of sexual maturity, juvenile yellow eels begin to "silver". The silvering metamorphosis prepares the eel for ocean migration, while full sexual maturation may only complete later during migration or when reaching spawning grounds (Fahay, 1978; van Ginneken et al., 2007). During silvering and prior to reentering the deep sea environment, the eel fattens, pectoral fins elongate, gonads develop, growth hormone, gonadotropin, blood lipids and cortisol levels rise, the eye size relative to length (eye index) increases, and the eel ceases to eat as its body begins to absorb its digestive tract (Durif, Dufour, & Elie, 2005; van den Thillart et al., 2009; van Ginneken et al., 2007). The elimination of the digestive system and cessation of feeding means silver eels must rely on endogenous reserves of fat for energy during their long migration to the Sargasso Sea (Palstra, van Ginneken, & van den Thillart, 2009; van den Thillart et al., 2009). Lack of sufficient fat reserves may cause an eel to starve or otherwise weaken it to the point of impairing it from spawning (Clevestam, Ogonowski,

Sjöberg, & Wickström). For this reason, fat reserves of maturing eels are considered to be an indicator of reproductive fitness. While there have not been any spawning eels observed in the North Atlantic Ocean, observations and collections of thin and weakened post-spawning Japanese eels, which also undergo a long oceanic migration prior to reproduction, support this assumption (Tsukamoto et al., 2011).

Range and population dynamics. The American eel is the most wide-ranging fish in North America and can be found over 10,000 km of coastline between 7° N and 55° N, from Venezuela to Iceland, as well as spawning in the subtropical Sargasso Sea (COSEWIC, 2012; Tesch, 2003). A small proportion (from 0.1 % to 0.4 %) of American eel larvae have additionally been found intermixed with elvers arriving into northern European waters (Boëtius, 1980). European eels range from Scandinavia, including Iceland, throughout western Europe to northern Africa and the Mediterranean Sea, and as far inland as Switzerland (Dekker, 2004a). Despite this wide geographic dispersal, random mating within American and European eel aggregations in the Sargasso Sea renders each species into a single, genetically homogenous (panmictic) population across their entire range (Aoyama, 2009; Mank & Avise, 2003; Palm, Dannewitz, Prestegaard, & Wickstrom, 2009; Wirth & Bernatchez, 2001). Côté et al. (2013) found strong evidence of panmixia with "virtually zero" global differentiation in a comprehensive genetic assessment of American eels. Consequently conservation of the Atlantic eels requires their species be considered as a single population (Wirth & Bernatchez, 2003). The discovery of *A. rostrata* and *A. anguilla* multigenerational hybrids in Iceland raises questions about the relation of ocean currents and migration routes to this mixing of species (Albert et al., 2006; McCleave, 1993). Further, despite being panmictic across

their range, some genetic heterogeneity exists within the Atlantic eels that may reflect genetic differentiation acquired through the varying environmental factors of habitats or breeding between different cohorts, i.e., eels do not migrate or reproduce at a uniform age and males migrate and reproduce earlier than females (Als et al., 2011; Gagnaire, Normandeau, Côté, Møller Hansen, & Bernatchez, 2012; Pujolar, Maes, & Volckaert, 2006). This heterogeneity, albeit weak, plays a potential role in eel population dynamics and may influence fitness and fecundity and male-to-female ratios of local stocks (EELREP, 2005; Gagnaire et al., 2012; ICES, 2008). Individuals with greater genetic heterogeneity appear to be fatter and larger, and more fecund as a result, suggesting that despite panmixia some genetic variation is important for eel conservation (EELREP, 2005).

Random mating and larval dispersal of eels in the Sargasso Sea challenge the effectiveness of locally or regionally targeted conservation efforts since new generations of eels do not recruit from local stocks. On the other hand, the cost of migration may vary with how far an eel is located on the continent from the spawning grounds in the Sargasso Sea, raising regional considerations for conservation. For example, a shorter and less demanding migration route to the Sargasso Sea could possibly explain why male European eels, which are smaller and have less fat reserves than the females, tend to concentrate in southwestern Europe (Kettle, Asbjørn Vøllestad, & Wibig, 2011). The discoveries of second and multi-generational *A. anguilla–A. rostrata* hybrids in Iceland and that only hybrids and European eels inhabit Iceland, while American eels have been exclusively found in Greenland, also highlights regional issues that can arise in managing panmictic eel populations (Albert et al., 2006). Changes in eel population structures in

Greenland and Iceland may be monitored to see how changing ocean circulation patterns can affect these regional population dynamics. Understanding how underlying oceanographic conditions determine or contribute to these two species distributions and their interactions, and the ability to apply predictive models, will undoubtedly improve with greater knowledge on eel spawning migration and larval dispersal patterns in the Sargasso Sea.

Evolution and regional perspectives.The genetic tree, or phylogeny, of the freshwater eels, also known as the "true eels" or anguillids, reflects their geographical distribution and divergence into different species (speciation) over the course of millions of years and can provide some clues to the migratory behavior and patterns of the Atlantic anguillids of today. Tsukamoto, Aoyama and Miller (2002) hypothesize that "migration loops", shifts in migrations route and lifecycle timing, may explain anguillid speciation. Referring to earlier molecular phylogenetic analyses (Aoyama, Nishida, & Tsukamoto, 2001) and to the concentration of anguillid diversity in tropical Pacific waters around Indonesia, Tsukamoto et al. (2002) hypothesize that anguillid species radiated genetically and geographically from *A. borneensis*, a primitive eel species endemic to Borneo. From there, the authors believe that the geographic range of a branch of early anguillids gradually shifted, moving across the ancient Tethys Sea Corridor some 70 million years ago. Under their "Tethys hypothesis" tropical eels maintained shorter migration routes to spawning grounds in deep waters relatively close to coastal areas, while extending ocean migration loops led the ancestors of today's temperate eels in the Northern hemisphere to diverge from tropical eels in Mozambique into distinct species. The ancient paleo-circumglobal equatorial current that would have facilitated this shift in larval migration

patterns did not enter the then considerably smaller South Atlantic Ocean, possibly explaining modern day absence of *Anguillid* species in the South Atlantic Ocean basin (Tsukamoto et al., 2002).

Theories of the evolution of the American and European eels species also point to a shared ancestry (Mank & Avise, 2003). As continental drift opened the Atlantic Ocean and widened the distance between the Sargasso Sea and the continental shelves, temperate Atlantic eels would have had to undergo longer migrations. These expanding eastward and westward migrations would have slowly diverged and led to speciation of American and European eels (Aoyama, 2009; Mank & Avise, 2003). Longer ocean migration distances may explain why temperate eel larvae develop more slowly compared to tropical anguillids (Aoyama, 2009; Miller, 2009). Shorter migration distances to islands and land may permit patterns of geographic isolation that explain why tropical anguillid species are not panmictic and support geographically distinct subpopulations (Aoyama, 2009).

The Cretaceous-Eocene period shifts in eel migration patterns as described above are thought to ultimately have led to speciation of the North Atlantic eels from their relatives in the tropical waters of the Pacific Ocean. However, despite their evolved differences, all anguillids spend at least part of their life in subtropical waters, within 30 degrees of either side of the Equator (Aoyama, 2009). Kettle et al. (2008) suggest that Pleistocene glaciations some 2.6 million to 11,700 years ago (Cohen, Finney, & Gibbard, 2012) drove eels from northern latitudes into refuge areas in southwestern Europe and the Caribbean, a hypothesis with considerations in the contemporary context of climate change. Along these regional lines, Kettle, Vollestad and Wibig (2011) propose that the

Iberian peninsula and northern Morocco were a likely area for early colonization by European eels and suggest that this region is the most efficient launching point for a European silver eel migration to the Sargasso Sea.

Population status, regional considerations and conservation. Historically, American eels have been abundant in eastern rivers and streams, accounting for up to 25% of total fish biomass (Ogden, 1970; Smith & Saunders, 1955). Eel biomass for some European rivers has been estimated to have been as high as 50% (Dekker, 2004a). Yet declines in recruitment of eel populations have been experienced since the 1990s on both sides of the North Atlantic Ocean (Haro et al., 2000; ICES, 2008). In Europe, recruitment of glass eels in recent years has declined between 1% and 10% of historical levels, and has been compounded by high mortality among juvenile and adult stages (ICES, 2008).

In North America, declines have also been observed in both Canada and the United States (Casselman, 2003; Haro et al., 2000). Ontario has experienced a decline of about 90% of their eel stock (COSEWIC, 2006), and a decline of 99% has been observed in the Saint Lawrence River (Castonguay, Hodson, Couillard, et al., 1994). Changes in the abundance of Atlantic eels have typically been observed in freshwater and estuarine surveys or based on coastal recruitment. A comparative study by Hanel et al. (2014) concluded that 2011 catch rates of anguillid leptocephali in the subtropical zone of the Sargasso Sea had declined by 71% and 63% for *A. rostrata* and 89% and 64% for *A. anguilla*, relative to catch rates in 1983 and 1985 (Hanel et al., 2014). As some areas of Europe had already started to observe initial declines in eel recruitment by 1983, the authors surmise that leptocephali abundances could have already begun to decline by the early 1980s.

Multiple anthropogenic factors are believed to contribute to the mortality of

Atlantic eels. While impacts have been documented at local scales, no single cause has proven to be a determining factor for global declines (COSEWIC, 2006; Dekker, 2004a; Haro et al., 2000). The obstruction of natural river flows by dams and other barriers has been shown to cause high level of eel mortalities (Carr & Whoriskey, 2008; Castonguay, Hodson, Couillard, et al., 1994). Restoration of water flows by removing dams in Virginia has reopened tributaries and led to a repopulating by eels of headwater streams in Virginia, a response indicating the past impact of obstructions (Hitt, Eyler, & Wofford, 2012). Such measures may not only be important to maintain local stocks, but also have wider implications for the species reproductive potential since larger, longer lived, and more fecund females appear to prefer upstream habitats (Belpaire et al., 2009).

Commercial fishing harvests eels across life stages and includes illegal exports of glass eels from North America and Europe to Asian markets. However the impact of overfishing exploitation on eel abundance remains inconclusive (Castonguay, Hodson, Couillard, et al., 1994; COSEWIC, 2006; Dekker, 2004a, 2004b; Haro et al., 2000; ICES, 2008; USFWS, 2007).

Eel fat reserves accumulate concentrations of persistent pollutants over their long lifetimes and have been studied as bio-indicators of pollution (Castonguay, Dutil, & Desjardins, 1989; Santillo, Allsopp, Walters, & Johnston, 2006). Dioxin-like compounds, including PCBs, have been shown to negatively impact egg quality and impair fertilization and embryonic development of eels under laboratory conditions (Palstra, van Ginneken, Murk, & Thillart, 2006). The release of stored toxins from metabolized fat reserves during the long migration to the spawning grounds could therefore negatively impact reproduction and viability of offspring (Robinet & Feunteun, 2002; van den

Thillart et al., 2009; van Ginneken, Bruijs, Murk, Palstra, & van den Thillart, 2009).

Invasive viruses and parasites introduced by aquaculture or ship ballast water pose additional threats that could impair spawning migrations. The parasitic nematode, *Anguillicola crassus*, native to East Asia, has been introduced in Europe and North America. The nematode infests the swimbladder of the American and European eels who suffer reduced swimming ability and buoyancy control, weakening or killing infected eels and raising the potential that silver eels fail to survive their migratory journey to the Sargasso Sea (Clevestam et al.; COSEWIC, 2006; EELREP, 2005; Kirk, 2003). Viruses create additional pathological threats. The rhabdovirus Eel Virus European X and Eel Virus America (EVEX and EVA), and *Herpesvirus anguillae* have spread globally through aquaculture. In separate swim tunnel experiments European eels infected with *Anguillicola crassus* and the EVEX virus demonstrated significantly weakened swimming endurance, in simulation of conditions experienced during long-distance migration, compared to non-infected eels, raising concern for their migratory capacity (Palstra, Heppener, van Ginneken, Székely, & van den Thillart, 2007; van Ginneken et al., 2005).

Climate and oceanic factors may also drive fluctuations in eel recruitment. A number of studies have provided evidence of a negative correlation between a positive North Atlantic Oscillation (NAO) index and recruitment of European eels in the following year (Friedland et al., 2007; Kettle, Bakker, & Haines, 2008; Knights, 2003). Silver eel migration peaks during periods of high rainfall and may also vary with changing continental weather patterns (Côté et al., 2013; Kettle, Bakker, et al., 2008). However, their spatial and temporal scale make climate influences difficult to verify,

while the elusive life history of the eel and its whereabouts at sea challenge their assessment even further.

An analysis of historical eel harvest data finds that male *A. anguilla* concentrate in the southern latitudes of their range, while females represent the greater proportion of European eels in northern latitudes (Kettle & Haines, 2006). This disproportional distribution of female eels in northern latitudes has also been observed with American eels (Oliveira, 1999). Despite the lack of genetic differentiation across their geographic range, disproportionate regional distributions of males and females may heighten the conservation value of eels from particular areas due to their greater importance to population dynamics of the species. The Committee on the Status of Endangered Wildlife in Canada, for example, has assessed that the abundance and size of the large female eels in Lake Ontario and Lake Champlain and tributaries represents from 26% to 49% of the entire American eel egg production and recommends regional conservation as a strategy for protecting the global population (Busch & Braun, 2014; COSEWIC, 2012). Larger females also reportedly concentrate farther upstream in headwaters and in more northern latitudes, while males, which are smaller than females, appear to prefer latitudes with shorter migration routes (Fahay, 1978; Kettle et al., 2011; Oliveira, 1999). Diverging from the concept that conservation measures should focus on ensuring successful migration of larger female eels due to their higher fecundity, Kettle et al. (2011) suggest that male European eels may represent the weakest link in eel conservation because their smaller size and more limited fat reserves raise the risk of mortality before and during migration. Under this argument, a concentration of vulnerable European eel males in southern Europe would have greater conservation value than that wider-ranging female

eels in more northern latitudes. Regional impacts on habitat caused by drought, pollution, or water flow obstructions in the Iberian Peninsula or Morocco would consequently assume greater relevance for the reproductive success of the European eel as a whole (Kettle et al., 2011; Kettle & Haines, 2006).

The International Union for Conservation of Nature and Natural Resources (IUCN 2015) lists *A. anguilla* as "critically endangered" and *A. rostrata* as "endangered" on its global Red List of Threatened Species, and estimates that recovery of the European eel population could require from 60 to 200 years considering declines in recruitment, disappearance of older eels and the life span of the species. The Convention on International Trade in Endangered Species of Wild Fauna and Flora (CITES) lists *A. anguilla* in its Appendix II to control trade incompatible with the survival of the species (CITES, n.d.). In response, the European Commission has mandated river basin eel management plans with the goal of attaining a 40 percent escapement of silver eel to their ocean spawning grounds, restocking depleted areas, removing barriers to make rivers passable and habitat accessible, reducing predation pressure, temporarily switching off hydroelectric turbines and aquaculture, reducing commercial and recreational takes and monitoring stocks (EC, 2007). In North America, the United States and Canada have adopted separate eel management strategies. The federal agency responsible for managing the eel commercial fishery in the United States, the Atlantic States Marine Fisheries Commission (ASMFC), expressed concern in 2004 over the extreme declines of American eel stocks in the Saint Lawrence River and Lake Ontario range and requested that the U.S. Fish and Wildlife Service (USFWS) and the National Oceanic Marine Fisheries Service conduct a status review of the species under the provisions of the

Endangered Species Act (USFWS, 2007). The ASMFC has also asked the USFWS to evaluate the appropriateness of listing the regional eel stock as a distinct population segment (USFWS, 2007). At the conclusion of a twelve month review the USFWS concluded that listing the American eel under the Endangered Species Act was unwarranted under the argument that as a panmictic population the eel would not be threatened by regional extirpations and that there was a lack of evidence of a global decline in American glass eel recruitments (USFWS, 2007). Since then a new petition was put forward and in 2010 the USFWS decided that sufficient new information had been put forward for a second status review of the American eel, scheduled for publication in the Federal Register in September 2015 (USFWS, 2011). The Canadian government meanwhile has responded to American eel declines by listing the species as threatened due to "dramatic declines over a significant portion of its distribution" in Lake Ontario and the upper St. Lawrence River, pointing to loss of habitat, dams, pollution and fisheries as obstacles threatening recovery of regional eel stocks (COSEWIC, 2012). Ontario has named the American eel as "endangered" under its Species at Risk in Ontario List (OMNR, 2009) and has adopted a management program that bans eel harvests, mandates construction of eel ladders at hydroelectric dams on the St. Lawrence River and institutes stocking programs (COSEWIC, 2006). In both Canada and the United States measures have been put in place to gather data for more accurate assessments of the status of the American eel population (ASMFC, 2008; COSEWIC, 2006).

In addition to these land based measures, the Sargasso Sea itself has become a focus of conservation. An initiative through the Convention on Biological Diversity supports the establishment a global network of marine protected areas in open ocean

waters and deep-sea habitats and names the Sargasso Sea as a candidate ocean reserve due to its ecological significance to many species (UNEP, 2008). The government of Bermuda is leading an international initiative for a Sargasso Sea pelagic marine reserve in partnership with the Sargasso Sea Alliance non-governmental organization (Dale, 2010). In March 2014, the Azores, Bermuda, Monaco, United Kingdom, and United States signed the Hamilton Declaration, a non-binding governmental agreement to collaborate for the protection of the Sargasso Sea, outside of the Bermuda Territorial Sea and Exclusive Economic Zone. The collaboration includes agreeing to minimize adverse effects from shipping and fishing and protect habitats of threatened and endangered species from harmful anthropogenic activities.

The Sargasso Sea

The circulation of the world's ocean currents revolve in gyres around their ocean basins, driven by prevailing wind belts and offset by the Coriolis force of the revolving Earth (Sverdrup & Armbrust, 2008). The Earth's west-to-east rotation propels an anti-cyclonic, or clockwise, oceanic gyre in the northern hemisphere and piles waters towards the western continental edge of the ocean basins (Nybakken & Bertness, 2005). Fed by the Antilles, Caribbean and Florida Currents, the Gulf Stream system intensifies the subtropical gyre within the North Atlantic basin, circulating warm waters from the subtropical North Equatorial current (around 15° N) upwards along the continental shelf until veering northeast from Cape Hatteras to the Newfoundland Rise at around 50° W (Sverdrup & Armbrust, 2008). As it weakens, the gyre deflects westwards below the Azores frontal system to the European continent, where it then travels as the Portugal and

Canary currents down the coastline until it merges with the westward flowing Equatorial current (Tomczak & Godfrey, 2003).At the eye of the North Atlantic gyre is the Sargasso Sea, a convex "lens of clear, warm, downwelling water." This lens is created by the Ekman Transport in which wind driven surface water drags deeper layers of water and in combination with the rotation of the Earth creates a downward spiral that extends about 100 m deep (Sverdrup & Armbrust, 2008). The downward spiraling forces of the Atlantic gyre deflect the surface water of the Sargasso Sea inwards and raises its level above that of the surrounding ocean, adding pressure on the deeper water below and increasing its density (Sverdrup & Armbrust, 2008). The boundary edge of the Sargasso Sea forms where the inward and outward pressure of its lens balances into a smooth flowing geostrophic current (Sverdrup & Armbrust, 2008).

The Sargasso Sea both feeds into and receives water from the Gulf Stream when portions of the northward flowing Gulf Stream waters break off from its main current and create eddies that are then recaptured (Tomczak & Godfrey, 2003). When these eddies of the Gulf Stream enter colder or warmer bodies of water they form distinctive anticyclonic or cyclonic rings of warm or cold water temperature (Figure 2) that form distinct and biologically important areas of up- and downwelling waters (Cornillon, Evans, & Large, 1986; Richardson, 1993; Richardson, Strong, & Knauss, 1973; The Ring Group, 1981). Upwellings raise nutrients to the upper waters forming spots of enhanced primary productivity, downwellings in the Sargasso Sea accumulate large mats of free floating *Sargassum* weed supporting unique ecological communities (Nybakken & Bertness, 2005; The Ring Group, 1981). Productive cyclonic upwelling eddies typically

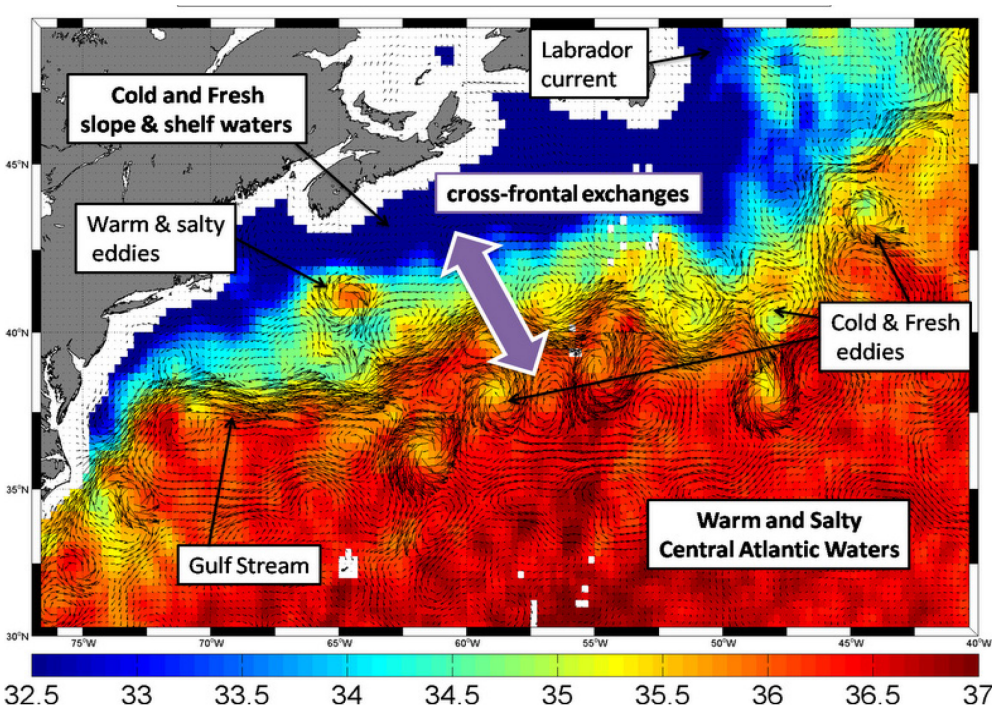

Figure 2. Eddy formation along the Gulf Stream. The image shows eddy formation and temperature related cross-frontal exchanges of salinity along the Gulf Stream. Remote sensing by the Soil Moisture and Ocean Salinity (SMOS) program of the European Space Agency. Color bar units are Practical Salinity Units, or PSU (1g kg^{-1}). Average salinity of world's oceans is 35.5 PSU, with rivers less than 15 PSU and Dead Sea exceeding 40 PSU (Reul & Chapron, 2013).

concentrate in the northern half of the Sargasso Sea, while anti-cyclonic eddies tend to concentrate towards the Southwest corner, although this is somewhat of a generalization (Ardron et al., 2011).

A distinctive feature of the Sargasso Sea, the seasonally driven subtropical convergence zone (STCZ) is a meandering band of frontal waters where the cooler water mass of the northern North Atlantic converges with warmer equatorial water of the southern part of the sea (Ullman, Cornillon, & Shan, 2007). The convergence creates steep thermal gradients that effectively divide the Sargasso Sea between cooler northern waters and warmer southern waters during the late autumn and winter through to early

spring, and which weaken during the late spring and summer (Ardron et al., 2011; Ullman et al., 2007). This subtropical convergence occurs between 22° N and 32° N along the latitudes where the Westerlies transition into easterly Trade Winds. The latitudinal band of this dynamic convergence zone extends on a northeast directional axis, from the Gulf Stream to beyond 60° W, at which point it begins to dissipate and merge into a frontal system near the Azores (Figure 3; Ullman et al., 2007).

Besides thermal boundaries, the STCZ is also characterized by gradients of associated parameters such as salinity, nutrients, and water densities. Together these gradients function as barriers that differentiate ocean systems and create areas of elevated primary productivity and diverse marine life (Belkin, Cornillon, & Sherman, 2009). Fronts are dynamic areas and are influenced by mesoscale and submesoscale eddy systems that characterize the Sargasso Sea (Ullman et al., 2007). An 18 year time series study found that the stronger and more predictable fronts with steepest gradients occur in the westernmost part of the STCZ (from 23.5° N to 34° N, and from 74° W to 6° W) as shown in Region 1 of Figure 3. This western region of the STCZ has the greatest seasonal variation in frontal occurrence and strength in the spring (Ullman et al., 2007). To the east, the STCZ weakens and shows less seasonal variation, peaking later and merging with the frontal zone in the Azores current (Ullman et al., 2007).

Bathymetry

The Sargasso Sea circulates above the North Atlantic plate and within the North.

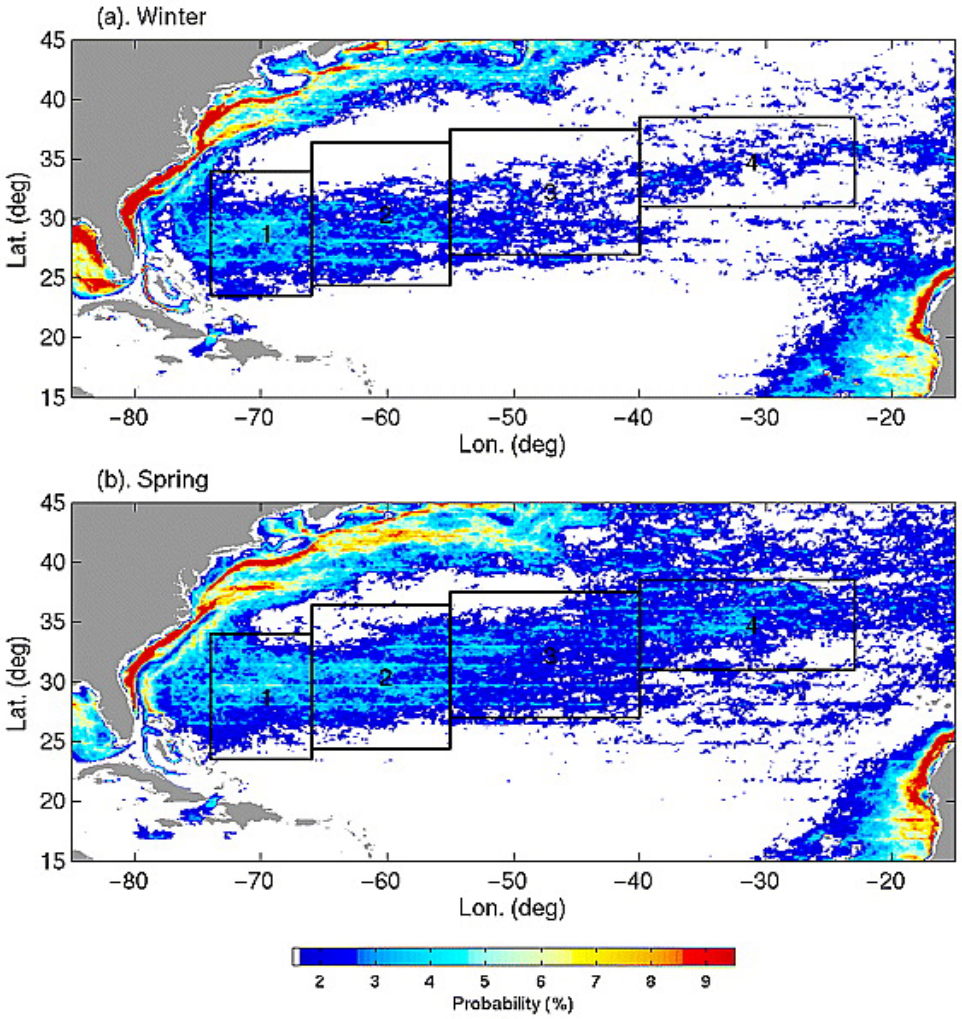

Figure 3. Seasonal trends of the subtropical convergence zone (STCZ). Winter (top) and spring (bottom) images show the northeastern and regional trends of the frontal system. The frontal system shows regional variation (boxes) with stronger and more frequency in the western part of the zone. From Ullman (2007).

Depths in the Sargasso Sea descend from 2000 m at the edge of the continental slope and 4000 m at the mid-Atlantic ridge to below 6000 m at its deepest points (Parson & Edwards, 2011).

The ocean floor of the Sargasso Sea is characterized by 20–30 km wide northwest trending fracture zones, most notably the Blake Spur, and the Kane and Atlantis Fracture zones (Parson & Edwards, 2011; Pushcharovskii, 2004). Prominent features of the Sargasso Sea are the New England Seamount and Corner Seamounts to the north; the island of Bermuda and its swell, the Bermuda Rise, on its western side; and the surrounding Hatteras, Sohm and Nares abyssal plains (Parson & Edwards, 2011; Pushcharovskii, 2004). The New England and Corner Seamounts begin approximately 120 km from the continental shelf to the northern Bermuda rise and rise to 1,000 m below sea surface (Parson & Edwards, 2011). These northern seamounts are characterized by flat eroded tops that increase in age from east to west following their formation over the moving North America Plate (Parson & Edwards, 2011). The Bermuda Rise, by contrast, possibly originated as a thermal uplift over an active hot spot and attains shallower depths (800–1000 m), extending from 1000 to 1500 km in length and from 100 to 500 km in width (Driscoll & Laine, 1996; Pushcharovskii, 2004).

The three abyssal plains are pronounced features in the North American basin and fall within a 5000 m contour line, with the deepest being the Nares Abyssal Plain (5700–5,900 m), followed by the Hatteras (5,400–5,600 m) and the Sohm (5,100–5,000 m) Abyssal Plains (Pushcharovskii, 2004). The Hatteras Abyssal Plain to the west has well-defined sediment patterns with no flow obstructions (Parson & Edwards, 2011).

The northern Sohm Abyssal Plain has comparatively more vigorous turbidity and active currents that leave less regular sedimentation, as well as nearby seamounts that obstruct its seaward flow (Parson & Edwards, 2011).

While volcanic seamounts are widespread on and to the east of the Bermuda Rise, and prominently in its northern region, their numbers and the percent of existing seamounts and surveyed bathymetric features are uncertain (Pushcharovskii, 2004; Vogt & Jung, 2007). In addition to seamounts Vogt and Jung (Vogt & Jung, 2007) describe a number of depth anomalies characterizing the region. The geological composition of the Sargasso Sea includes polymetallic sulphide deposits emitted from hydrothermal sites along the actively spreading plate boundaries of the Mid-Atlantic Ridge system and zinc, copper, iron, and other ore deposits formed by subsequent cooling and spreading of the crust (Parson & Edwards, 2011). Polymetallic manganese nodules on the deep sea floor and cobalt rich ferromanganese crusts coating seamounts, as well as hydrocarbons, aggregates and gas hydrates are reported although they remain largely unexplored (Parson & Edwards, 2011).

The Bermuda Rise. On the western side of the Mid-Atlantic Ridge, one of the most prominent features in the central Atlantic Ocean is the island of Bermuda and its underlying swell, the Bermuda Rise. Unlike ocean ridges which are steep and narrow and characterized by central rift valleys, ocean rises have gentler slopes with their highest elevation occurring at its center (Sverdrup & Armbrust, 2008). The Bermuda Rise is a seismically active uplift that extends on a south-southwest and north-northeast axis perpendicular to the motion of the western North Atlantic tectonic plates and resulting fracture zones (Vogt & Jung, 2007). The four most prominent features along this axis are

the Bowditch Seamount, Bermuda, Challenger Bank and Argus or Plantagenet Bank (Vogt & Jung, 2007). The geologic formations are thought to have formed during the Middle Eocene from 47 to 40 Ma concomitant to the closing of the ancient Tethys Sea (Vogt & Jung, 2007). The singularity of the Bermuda Rise and the lack of a distinct geological chain that would have formed in tandem with the tectonic motion of the seafloor has made the origins of the Bermuda Rise a subject of debate and led to theories that it was formed by the pulsing of a thermal hot spot stationary under the shifting mantle of the Earth (Vogt & Jung, 2007).

To the south of Bermuda and extending into the presumed area of the eel spawning grounds, the swell of the southwest Bermuda Rise lifts 1 km closer to the surface than the surrounding basin topography (Driscoll & Laine, 1996). An investigation of the morphology and sediment of the southwest Bermuda Rise (65 W°–72° W and 23° N–30° N) found that the Rise bifurcates the abyssal Antarctic Bottom Water Current and directs its main flow around and through the Vema Gap at its southern end, channeling the current from the Nares into the Hatteras Abyssal Plain (Figure 4; Driscoll & Lane, 1996). The steep and rough Vema Gap is a 32 km wide and 112 km long constricted passageway with a northwest–southeast orientation (Driscoll & Laine, 1996). Its average gradient of 1:300 is much steeper than either the Nares Abyssal Plain (1:3500) to its east or the Hatteras Abyssal Plain (1:3000) to its west (Heezen, Tharp, & Ewing, 1959).

The western slope of the Bermuda Rise descends smoothly to the Hatteras Abyssal Plain, while towards the south of the rise the topography of its descent into the Vema Gap is steep and rough (Driscoll & Laine, 1996). The bathymetry of the southwest

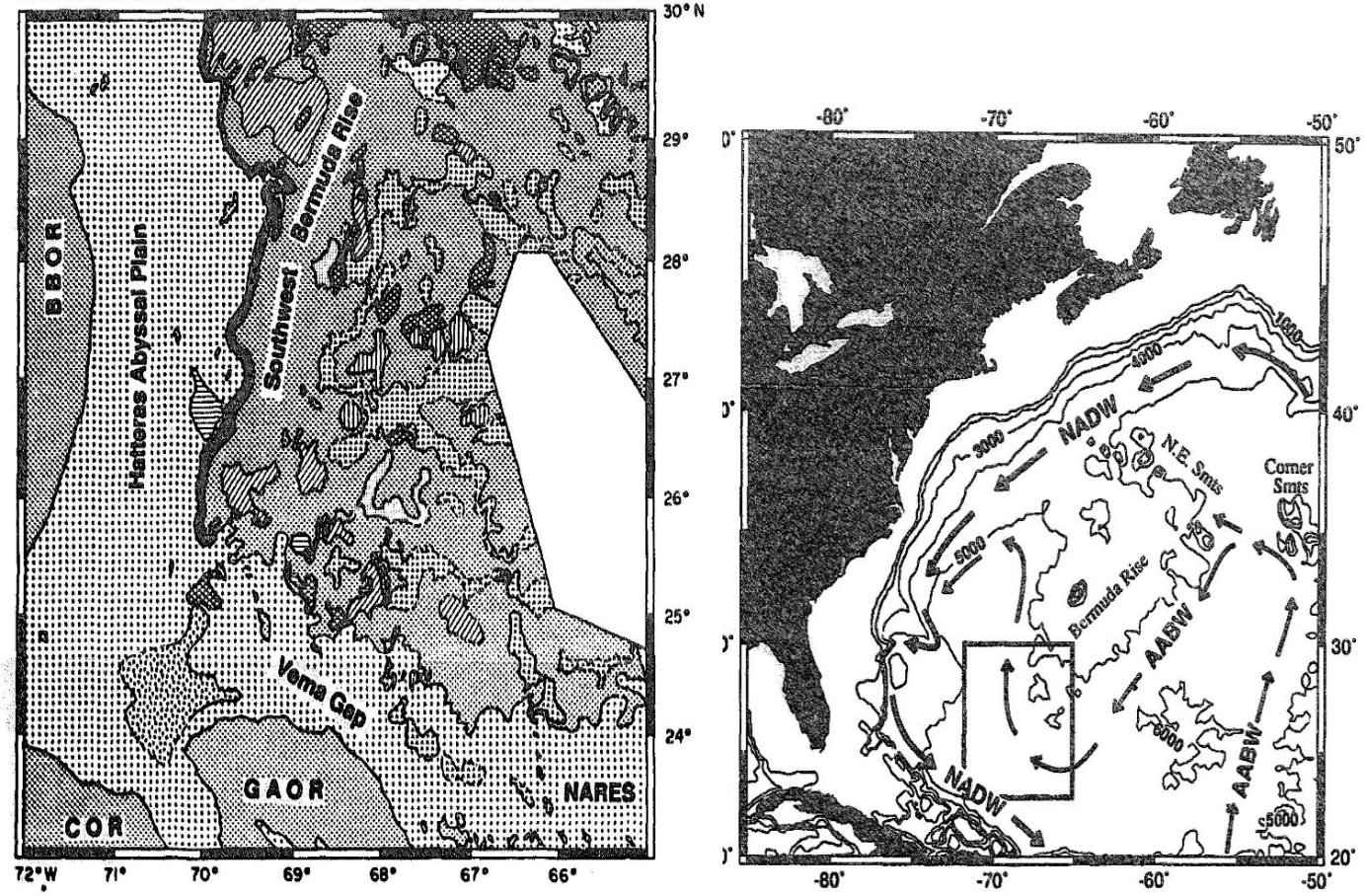

Figure 4. The southwest Bermuda Rise, Hatteras Abyssal Plain and Vema Gap (left). The figure on the right illustrates the diversion of the abyssal Antarctic Bottom Water Current around the rise and through the gap. Figures from Driscoll & Laine (1996).

Bermuda rise has raised questions regarding its potential influence on eddies and ocean circulation and was a subject of the Mid-Ocean Dynamics Experiment (MODE-I) project (Bush, 1976). The MODE-I data contrasted the rugged bathymetry of the southwest Bermuda Rise to the featureless Hatteras abyssal plain where depths descend to a 5500 m isobath. Features of the southwest Bermuda Rise profiled in the Mode-I study area are the Researcher Seamount, rising some 1100 m from the seafloor, Swallow Knoll to its east, Vanguard Knoll to its north and Discovery Ridge to its south. The area also includes the twin-peaked Independence Knolls which rise on a 30° gradient approximately 1000 m off the seafloor on the edge of the Bermuda Rise and contains Eastern Knoll. As described by Bush (1976, p. 7), "the entire structure is a complexity of ridges and channels, hills and valley". The description of the MODE-1 study area concludes that currents on the western edge of the Bermuda Rise increase in speed and "tend to be more meridional with increasing depth", and that bottom topography may influence "energetic mesoscale motions" measured in earlier *Aries* current measurement studies (Bush, 1976, p. 1111).

Magnetic map. The Bermuda Islands have high amplitude magnetic anomalies that are attributed to high levels of titanium and iron. The island of Bermuda and the Bermuda Rise lie along the axis of the magnetic anomaly associated with the M0 iscochron, as shown in Figure 5 (Johnson & Vogt, 1971; Vogt & Jung, 2007). As presented in the landmark article by Vine and Matthews (1963) and elaborated upon by Sverdrup and Armbrust (2008), the world's oceans are characterized by stripes of magnetic anomalies of alternating positive and negative amplitudes derived from the magnetic forces embedded in the minerals of the ocean crust. The magnetic properties of these fields are remnant from the cooling of hot magma erupting along oceanic ridges as they enter the

lithosphere. Unlike the magnetic meanderings of the Earth's poles, periodic polar reversals and shorter term variations caused by activity in the ionosphere, the ocean floor retains fixed magnetic properties within its crust. This "remnant" magnetism of the ocean floor retains the imprint of periodic polar reversals and is the basis of plate tectonic theory, serving both as a geophysical map of the oceans of today and a temporal map of the opening and spreading of the ocean floor (Vine & Matthews, 1963).

Ocean Migrations

Although eels have contributed to human diets and cultures in North America and Europe for thousands of years (Tsukamoto & Kuroki, 2014), Italian biologists Grassi and Calandruccio in 1896 were the first to realize that a strangely flat and transparent fish larvae arriving on the coasts of the Mediterranean, European and North African coasts each spring were in fact an early life form of the European eel (Grassi, 1896; McCleave, 2003).

> Four years of continual researches made by me in collaboration with my pupil, Dr. Calandruccio, have been crowned at last by a success beyond my expectations…[and] have enabled me to dispel in the most important points the great mystery which has hitherto surrounded the reproduction and the development of the Common Eel (*Anguilla vulgaris*)…[and that] has occupied the attention of naturalists since the days of Aristotle…The most salient fact discovered by me is that a fish, which hitherto was known as *Leptocephalus brevirostris*, is the larva of *Anguilla vulgaris* (Grassi, 1896, p.261-262).

Only some 40 years prior to this discovery that leptocephali were the larvae of the eels, Johann Kaup in 1856 had identified the larvae as a distinct species, naming them Leptocephalus brevirostris in reference to their flat, tapering, and leafy structure (McCleave, 2003; Schmidt, 1923). Referring to the importance of the eel industry in his

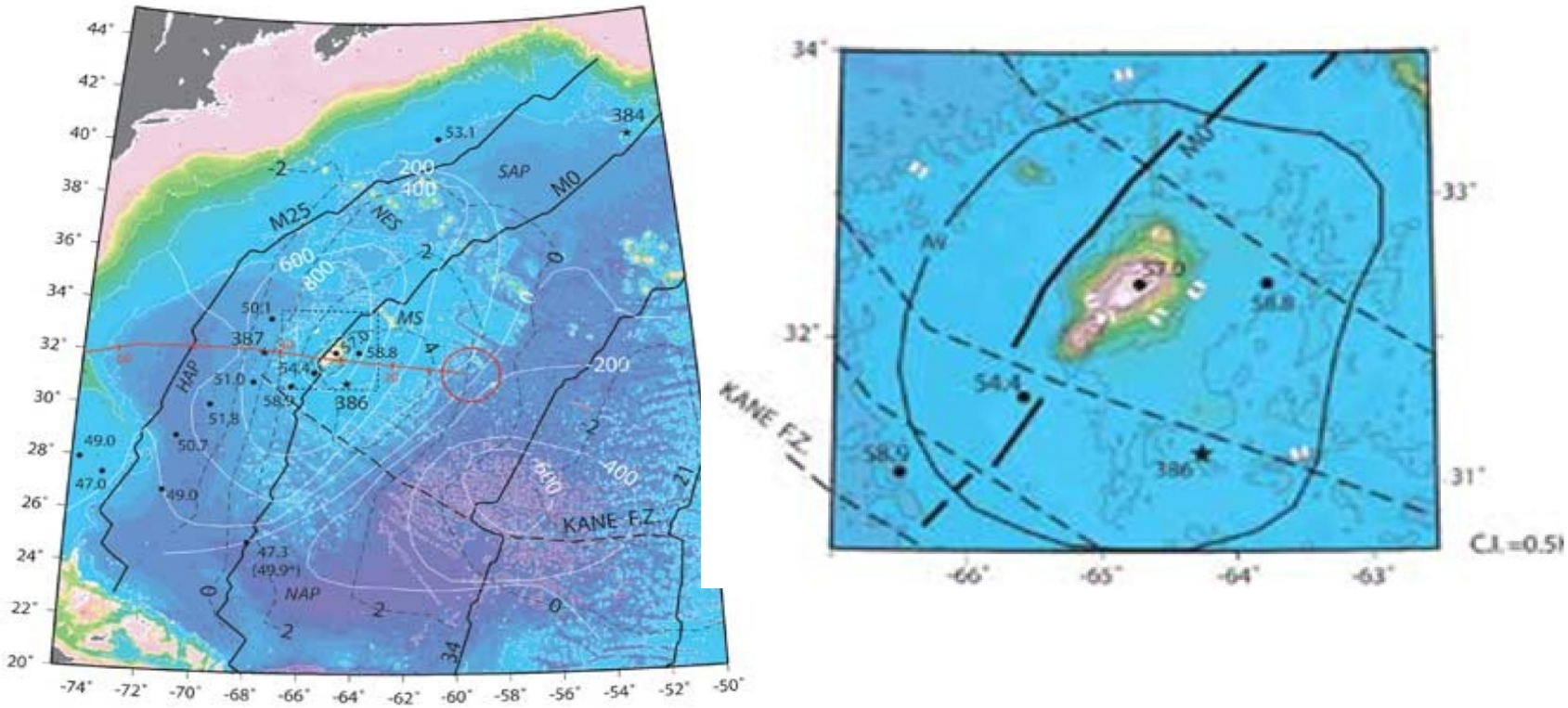

Figure 5. The Island of Bermuda along the axis of the M0 marine magnetic anomaly. The axis of the Bermuda Rise and Island of Bermuda (right) are shown in the context of the magnetic anomalies M0 and M25 and with that of the prominent east–west running Kane Fracture Zone. The Island of Bermuda and the M0 anomaly (right). From (Vogt & Jung, 2007).

home country of Denmark and presumably driven by his own innate curiosity as a naturalist, Johannes Schmidt initiated in 1903 what was to become a series of oceanic voyages, scraping together money and ships of all description, in a 20 year investigation to find the spawning ground of the European eel (McCleave, 2003; Schmidt, 1923). The discovery of the spawning grounds, Schmidt noted, was essential to understanding larval development, to know how long a period the larvae spent at sea and their age when arriving off the coasts of Europe (Schmidt, 1923). Observing that leptocephali off the coast of Europe were typically about 7 cm in length and much larger than newly hatched larvae of other known fish species, Schmidt concluded that the eel larvae must have already spent a lengthy period at sea by the time they recruited to European coastal waters (Schmidt, 1923). Between 1903 and 1922 Schmidt followed a trail of larvae of increasingly diminishing size across the Atlantic to where their smallest specimens aggregated in an area bounded from 22˚ N to 30˚N and from 48˚ W to 65˚W in the southern Sargasso Sea (Figure 6; Schmidt, 1923). At around the same time as Schmidt began his research, Eigenmann and Kennedy were collecting *Leptocephalus grassii*, the larvae of the American eel, in the Atlantic Ocean some 200 miles offshore (Eigenmann & Kennedy, 1902; McCleave, 2003).

Larval distribution and migration. The Sargasso Sea fluctuates with surrounding currents and so has no fixed boundary, but has been calculated to occupy an area of approximately 4,163,500 km^2 (Laffoley et al., 2011). Schmidt (1923) discovered the smallest leptocephali in a smaller area within the sea of approximately 1,500,000 km^2. Schmidt (1923) found American and European eel larvae comingled in the center of this immense area, although with differences in their overall spatial distribution (Figure 6) and in the

timing of their reproduction cycles. The distribution of European eel leptocephali extended farther towards the east, while American eel leptocephali were found more towards the western part of the southwest Sargasso Sea and never east of 50˚W. In Schmidt's (1923) observations this line of longitude (50° W) also marked a division between earlier and later stages of European eel leptocephali, since none larger than 50 mm were found to its east and only fully developed larvae to its west. Schmidt (1923) himself marveled over what he estimated was a 5000 km migration of the European larvae and his remarkable discovery that all European eels originated from the North American continent.

Other oceanographic expeditions have since refined and largely reconfirmed the general location of larval emergence, and by deduction, eel spawning grounds in the Sargasso Sea. These expeditions also sought to answer perplexing questions regarding the dispersal, development and motility of the eel larvae, the migratory and spawning behavior of mature eels, as well as their environmental preferences and vulnerabilities (Castonguay, Hodson, Moriarty, Drinkwater, & Jessop, 1994; Kleckner & McCleave, 1985; Kleckner et al., 1983; McCleave et al., 1985; Munk et al., 2010; Schoth & Tesch, 1982; Tesch & Wegner, 1990; Wippelhauser, McCleave, & Kleckner, 1985). The findings of these later expeditions have supported Schmidt's original findings that the American and European eel leptocephali overlap in one area of the Sargasso Sea, and that otherwise their geographical distributions are separated with European eel leptocephali extending to the east and the American eel to the west (McCleave, 1993; Schmidt, 1923; Schoth & Tesch, 1982).

Similarly, the spawning season of the two species overlap, but with the American

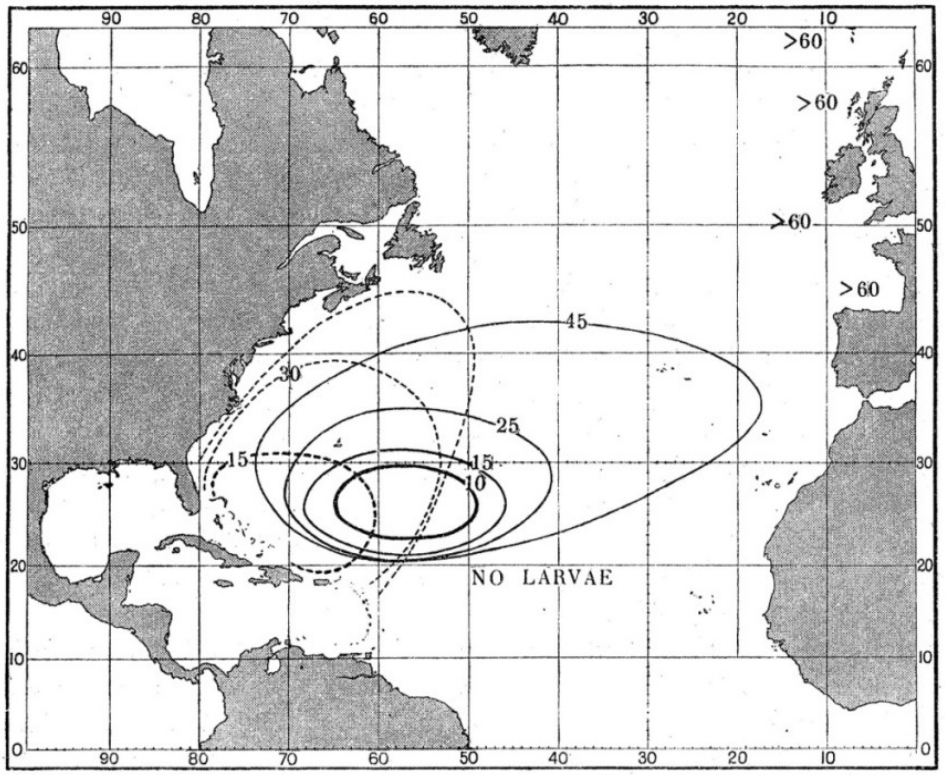

Figure 6. Schmidt's leptocephali ellipses. Observations of European eels (solid lines) and American eels (hatched lines), with overlapping areas for the two species (solid bold) are designated with circles representing larval size (mm) (Schmidt, 1923).

eels beginning and ending spawning earlier than the European eels. Accumulated field sampling data indicates that peak spawning period for *A. rostrata* occurs in February and March, extends through April and into June (Kleckner & McCleave, 1985; Kleckner & McCleave 1988; McCleave, 2008). By contrast, based on field sampling data, the European eel peak spawning occurs in March and April, and extends into July (McCleave, 2008). The thermal gradients of the frontal subtropical convergence zone have been strongly associated with eel spawning, presumably providing optimal conditions of water temperature, triggering spawning and favoring reproduction, and

possible beneficial conditions that retain larvae in an area with reliable food resources (Castonguay, Hodson, Moriarty, et al., 1994; Kleckner & McCleave, 1985; Kleckner et al., 1983; McCleave et al., 1985; Munk et al., 2010).

The smallest American and European leptocephali are found along latitudes in the southern part of the Sargasso Sea where the subtropical frontal system separates the warmer waters of the southern Sargasso Sea from cooler waters to its north (Kleckner & McCleave, 1988; Schoth & Tesch, 1982). Schoth and Tesch (1982) found that the distribution of 0-group leptocephali, first year larvae sized at ≤ 30 mm, had a northern limit at 20° N with a correlated sea surface temperature of 18°C, and a southern limit at the warmer (< 25°C) Antilles current. The distributions of both species of the 0-group leptocephali (≤ 30 mm) had a western limit of 69° W (Schoth & Tesch, 1982). However, while identifying an eastern limit of the 0-group *A. rostrata* at 52° W and a northeast limit for *A. anguilla* at 50° W, the researchers continued to find *A. anguilla* up to the eastern edge of their study area and so could not determine an eastward boundary for the *A. anguilla* ≤ 30 mm larval distribution (Schoth & Tesch, 1982).

Estimating that leptocephali smaller than 10 mm in total length were less than one month old, Wippelhauser et al. (1985) surveyed for *A. rostrata* in February and March 1981, finding specimens ≤ 9 mm between 20° N and 26° N, and 63° W and 76° W, and larger specimens only west of 69°W (Wippelhauser et al., 1985). A review of American eel larval collections by Kleckner and McCleave (1985) found *A. rostrata* leptocephali less than 10 mm in length only within a 550 km arc east of the Bahamas and north of Hispaniola. McCleave (1993) illustrated an overlapping area of American and European leptocephali within a bounded area from 22° N to 30° N and from 50° W to

79° W (Figure 7). In a comprehensive review of the ICES data, published during the course of this research, Miller et al. (2014) found newly hatched *A. rostrata* (≤ 6 mm) distributions occurred between 75° W and 60° W and *A. anguilla* (≤ 6 mm) from 74° W to 51° W; and that although slightly larger larvae (6.0–10.9 mm) had a wider distribution they were centered over the same locations as the smaller larvae (Figure 8). Using frequency plots of lengths of larval size to latitude and longitude, the authors predicted that *A. rostrata* primarily spawns from 23° N to 28° N and from 75° W to 58° W, and *A. anguilla* primarily from 23° N to 28° N and from 70° W to 51° W (Miller et al., 2014).

Anguillid leptocephali are distributed in the water column and undergo a daily vertical migration, descending to darker water by day and rising towards the surface at night. Reviewing vertical migration data of American and European eel leptocephali from five expeditions between 1983 and 1985, Castonguay and McCleave (1987) concluded that anguillid larvae ≤ 5 mm in length do not vertically migrate and likely lack the motility to adjust their position in the water column. They also found the smallest size larvae spread across a greater depth range (50–350 m) than larger sizes and in greater density at the deepest depths (250–300 m). Larvae with lengths from 5 to 20 mm concentrated at a nighttime shallow depth from 50 to 100 m and descended to a depth of from 100 m to 150 m at day with maximum daytime ranges around 200 m, indicating an average daily migration of 50 m (Castonguay & McCleave, 1987).

The artificial fertilization of eel eggs and their hatching under laboratory conditions inform age estimates of the larvae in the water column. Artificially fertilized eggs of *A. japonica* hatched from 38 to 45 h, and those of *A. anguilla* from 50 to 60 h, and their larvae grew to 5 mm in five days (Yamamoto and Yaumachi as cited by

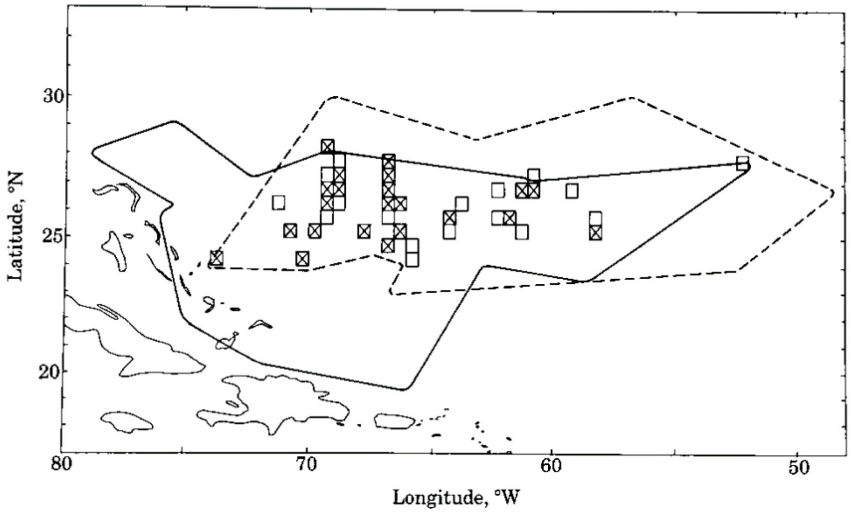

Figure 7. Overlapping distribution of anguillid leptocephali ≤ 10 mm. Hatched lines indicate *A. anguilla* and solid lines, *A. rostrata*. Crossed boxes are where both species < 7 mm were found and empty boxes larvae from 7 to 10 mm. From McCleave (1993).

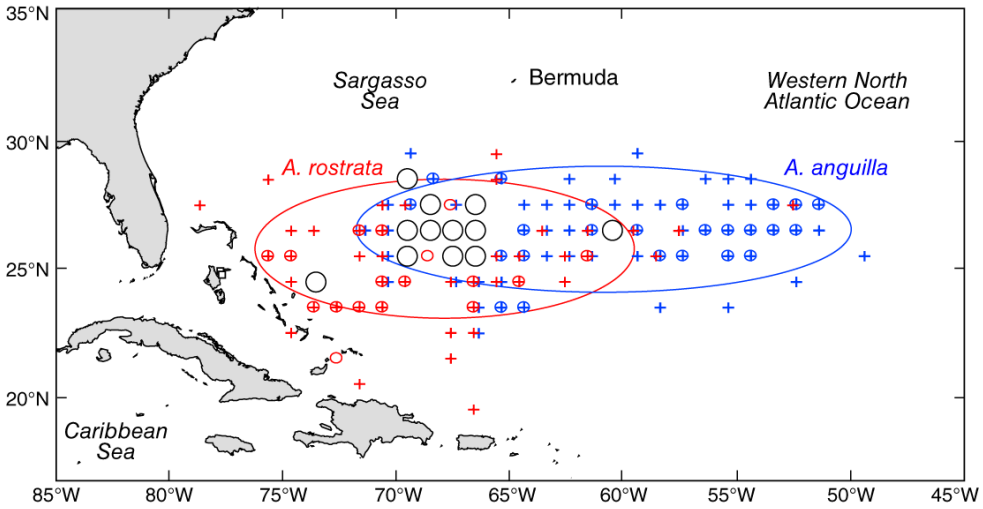

Figure 8. Locations of small larvae (3.0–10.9 mm). The projected spawning grounds of the two species are shown in the ellipses with crosses. Small circles show the location of larvae ≤ 5.9 mm and crosses larvae from 6.0 to 10.9 mm. Large circles show overlap of larvae ≤ 6 mm. *A. rostrata* represented in red and *A. anguilla* in blue. From Miller et al. (2014).

Castonguay & McCleave, 1987). Castonguay and McCleave (1987) surmised that the depths where the smallest larvae had been found (300–250 m) approximated that of spawning activity, and that spawning likely occurred at depths under 50 m because no small larvae had been found closer to the surface. The absence of vertical mixing below the mixed layer of water (50–100 m) may benefit preleptocephali, which lack motility (Castonguay & McCleave, 1987). However Castonguay and McCleave (1987) hesitated to estimate a lower depth limit for eel spawning, citing observations by Coombs, the Research Group on Eel Production, and Bezdenezhnykh et al., that anguillid eggs are positively buoyant and that their rising rates are unknown. Additionally, leptocephali are born without swim bladders and so have a specific gravity, i.e., ratio of larval density to seawater (Tsukamoto et al., 2009). From their measurements of artificially raised Japanese eel leptocephali, Tsukamoto et al. (2009) calculated that their specific gravity would maintain buoyancy above a 26°C thermocline, which would correspond to a depth of 100 m in the North Equatorial Current (NEC). After larvae initiated feeding, their specific gravity increased so that the larvae would sink lower below a 20°C thermocline, corresponding to an approximate 200 m depth in the NEC (Tsukamoto et al., 2009).

In their expedition of larval distributions in the Atlantic subtropical ocean frontal system, Munk et al. (2010) determined that the fronts retain young eel larvae in a band close to advection towards favorable currents and with reliable food resources. Based on observations of Yamamoto and Yamuchi that 7 mm anguillid leptocephali are from 7 to 14 days old, and citing Wegner that currents in the central Sargasso Sea can move at a rate of 102 cm/sec, Schoth & Tesch (1982) calculated that newly spawned larvae (7 mm) would occur within 13 nm (24.1 km) from where they had hatched. However, Kleckner

and McCleave (1988, pp. 649–650) also comment that mesoscale cyclonic and anticyclonic eddies in the Sargasso Sea STCZ reach deeply into the water column and can create currents that can travel 20 km day^{-1}, potentially transporting two to three week old larvae "tens to hundreds" of kilometers from their spawning area. *A. rostrata* leptocephali migrate to the American coast predominantly via the Florida Current and Gulf Stream (McCleave, 1993). While *A. anguilla* and *A. rostrata* leptocephali travel with the Gulf Stream and North Atlantic currents during their migrations, questions remain if those currents are the sole vehicle for *A. anguilla* dispersal. The horizontal distribution of European eel leptocephali along a narrow east–west axis and their proximity to easterly frontal currents and possible subtropical counter currents have led some researchers to hypothesize the possibility of an additional shorter and more direct eastward larval migration route to Europe (Friedland et al., 2007; Kettle & Haines, 2006; McCleave, 1993; Munk et al., 2010). Modeling of European eels by Kettle and Haines (2006), predicted that many European eel larvae would migrate eastwards from the southeast corner of the Sargasso Sea spawning area, although the model also projected their dispersal to equatorial Africa where no freshwater eels have been found. While a more direct route for the European eel remains unconfirmed, the recruitment of smaller leptocephali in southern latitudes of Europe than in the north has also supported the hypothesis that easterly jets or an equatorial counter current may facilitate an alternative more direct and easterly larval migration (McCleave, 1993; Munk et al., 2010).

Reliance on physical oceanographic factors for dispersal renders eel recruitment highly dependent on the strength and position of ocean currents (Wirth & Bernatchez, 2003). The lack of information on spawner escapement, egg production and larval

survival make it difficult to ascertain a definite link between ocean conditions and impacts on recruitment and reproduction (Friedland et al., 2007). Dissolved and particulate organic matter are a food resource for leptocephali (Miller, 2009) and primary production of organic matter may exert a bottom up control on the development and survival of leptocephali in both the Pacific and Atlantic Oceans (Bonhommeau, Chassot, & Rivot, 2008). Kettle and Haines (2006) modeled availability of food using ocean data for chlorophyll α as a proxy and determined that during their first three months leptocephali drift into areas with greatest food resources, at latitudes 30 N and 55 N, after they have consumed their yolk sac but are still too small to swim actively.

Over a 40 year period, from 1971 to the 2000s, the sea temperature of the upper 100 m layer of the Sargasso Sea warmed from an average below 21.2°C to over 22°C (Bonhommeau, Chassot, Planque, et al., 2008). Changes in ocean temperature gradients, winds and the surface layering could potentially affect spawning, larval transport and the larval food resources (Friedland et al., 2007). Studying historical data over an 11 year period (1994–2004) and using temperature as a proxy for primary productivity, Bonhommeau, Chassot and Rivot (2008) concluded that glass eel recruitment correlated with long term and interannual short term changes in ocean currents and food productivity. European eel recruitment has been negatively correlated with changes in the North Atlantic Oscillation (Friedland et al., 2007; Kettle, Bakker, et al., 2008), while American eel abundance and recruitment have been found to have a highly significant positive correlation (Côté et al., 2013).

Most research on eel migration has been in the spirit of refining Schmidt's analysis of the Atlantic eel breeding grounds rather than directly challenging his

assumptions. However there have been some exceptions. Stating that Schmidt had done much to prove where the smallest anguillid leptocephali were, but not enough to prove where they were not, Boëtius and Harding (1985) tested the probability of the geographic latitudes and longitudes of Schmidt's newly hatched larvae observations occurring in a wider area. Their analysis found statistical evidence supporting Schmidt's estimated north–south limit for the distribution of the 10 mm leptocephali, but insufficient to support his delineation of its eastern boundaries (1985). In their field work, Schoth and Tesch (1982) concurred with this assessment, noting that they continued to find Group 0 larvae (≤ 30 mm) up to the southeastern limit of their study area and could find evidence to support an eastern limit to the spawning area.

Spawning migration. Little is known about the behavior and navigation of migrating adult Atlantic eels and their aggregation in the Sargasso Sea. Temperature and salinities in the subtropical convergence zone may orient navigation, as well as influence maturation rates and trigger spawning (McCleave, 1993). Eels have an olfactory ability, and the southern Sargasso Sea may emit a distinctive odor from its unique *Sargassum* algae that helps orient the eels in its direction (McCleave, 1993; Tesch, 2003; Tsukamoto, 2009). There is also the possibility that the Atlantic eels, which have demonstrated an ability to sense the Earth's magnetic field, may be born with or acquire a geomagnetic imprint that guides their return migration as adults to the Sargasso Sea (Durif et al., 2013).

Challenges to answering some of these questions include unknown migration routes, high costs of oceanographic field work, and technological limitations in satellite tagging that persist despite promising advancements (Righton et al., 2012). Pop-up radio

transmitters have shed insights into the swimming patterns and initial directions of migration, but have not until recently succeeded in remaining attached to the eels beyond the first 1300 km of their 5000 km migration (Aarestrup et al., 2009). Pop-up satellite tags added a two-fold energetic swimming cost when tested on eels in a swim tank, and so the interpretation of their data is subject to some qualification (Burgerhout et al., 2011). In his review of eel spawning migration, Tsukamoto (2009) refers to research by Tesch, Westerberg et al., and Westin that found maturing silver European eels released in the Baltic, North Sea and Mediterranean Sea demonstrated preferred directional headings, although not necessarily towards the Sargasso Sea. However, more recently, researchers successfully tracked one American eel 2,400 km from the Scotian Shelf of Canada to the northern limit of the spawning areas in the Sargasso Sea (Beguer-Pon, Castonguay, Shan, Benchetrit, & Dodson, 2015). The same study found that eight eels, naturally matured and released within a few days of capture, maintained consistent migratory behavior and trajectories to the edge of the continental shelf (Beguer-Pon et al., 2015).

Some studies have indicated that silver eels swim at a varying depth of about 200 m. Tracking of the New Zealand temperate eel, *A. dieffenbachia*, found that it swims to a depth of 980 m during the day. Using miniaturized pop-up satellite archival transmitters to track migrating silver European eels, Aarestrup et al. (2009) similarly found that eels swam as deep as 1000 m during the day, rising to swim at 200 m during the night. European eels released off the coast of France and Europe swam at depths from 470 to 700 m (Wahlberg et al., 2014). Artificially matured silver female eels released in the Northeastern Atlantic Ocean and Sargasso Sea swam at depths reaching 1000 m, with two eels in the southern Sargasso Sea swimming at a mean depth of 900 m during the day

and 450 m at night (Wysujack et al., 2015). One American eel tracked to the northern limit of the known spawning grounds in the Sargasso Sea swam at an average depth of 141 ± 14 m at night and 618 ± 16 m during the day, with a maximum depth of 699 m (Beguer-Pon et al., 2015). An Alvin submersible photographed a tentatively identified anguillid eel in an apparent pre-spawning condition (swollen abdomen) at a depth of 2000 m on the bottom of a deep sea trough near the eel spawning area in the Atlantic Ocean (Robins, Cohen, & Robins, 1979), however doubts regarding the accuracy of the identification leave this as an unconfirmed but intriguing observation.

The diel vertical migrations of plankton and fish are often attributed to avoidance of visual predators by day and surface feeding under relatively safer conditions at night (Nybakken & Bertness, 2005). Adult eels, however, lose their digestive tract before migrating and so do not need to rise to the surface at night to feed during their migration. Migrating silver eels may rise vertically at night to regulate their body temperatures in warmer surface water (Aarestrup et al., 2009). Additional factors that may influence depth preference are densities in deeper water that increase swimming efficiency (van Ginneken et al., 2005), and cooler temperatures that may delay sexual maturation until reaching the Sargasso Sea (Boetius & Boetius, 1967, as cited by Haro, 1991).

Tracking of eight migrating American silver eels released in the Gulf of Saint Lawrence led researchers to infer that porbeagle sharks were eating migrating eels (Béguer-Pon et al., 2012). By statistically comparing known diving patterns of sharks and tuna, the main fish predators in the Gulf of Saint Lawrence, the researchers concluded that two of the eels had been consumed by porbeagle sharks. Porbeagle sharks dive to depths of up to 400 m and the eels were consumed at depths estimated to range from less

than from 20 to 50 m. While the eight released eels at first remained in the surface, two began an inverse diel migration by swimming close to the surface at day. This abnormal behavior of swimming close to the surface in daylight may have been caused by tagging and have increased the vulnerability of the eels to shark predation. Interestingly, female porbeagle sharks also migrate to birth their pups in the Sargasso Sea (Béguer-Pon et al., 2012; Campana et al., 2010). Béguer-Pon et al. (2012) speculate that at least in the Saint Lawrence eels may represent a reliable food source for porbeagle sharks. A similar study of released European eels off the coasts of France and Ireland also gave results in predation of eight eels tags suddenly reporting a sudden raise of temperature and a change in dive pattern that the researchers was consistent with predation by a toothed whale (Wahlberg et al., 2014).

Research on long-distance migration by other pelagic species may offer insights into eel navigation. A sizeable body of research supports the hypothesis that loggerhead turtles (*Caretta caretta*) and other sea turtles that migrate thousands of miles are able to sense and orient to the Earth's magnetic cues (Lohmann, 2007; Lohmann, Lohmann, Ehrhart, Bagley, & Swing, 2004; Lohmann, Lohmann, & Putman, 2007). Loggerhead sea turtles demonstrate a response to magnetic fields and ability to orient in both a magnetic north–south and east–west direction, a directional response that may help keep them on a migratory track in the weak and variable currents of the Caribbean, or avoid straying into the Guinea or Canary currents when entering the westward equatorial current (Lohmann, Cain, Dodge, & Lohmann, 2001; Lohmann et al., 2004; Putman et al., 2011). Migrating salmon also show evidence of a geomagnetic sense. A 56 year time series of salmon in the Fraser River showed salmon altered their migratory routes between years, changing

their approach around Vancouver Island in correlation to with shifts in the earth's magnetic field (Putman et al., 2014). Other research suggests that cetaceans rely on magnetic cues to orient their movements. A geographic information analysis of four years of migrating fin whale sightings found a seasonally-based statistical correlation between non-feeding fin whales and magnetic field intensities and gradients (Walker, Kirschvink, Ahmed, & Dizon, 1992). On the other hand, evidence of a relationship between the beaching of fin whales and dolphins in areas of abnormal magnetic activity has been found inconclusive (Hui, 1994; Walker et al., 1992). Notably, by referring to locations where geomagnetic field and intensity were relatively independent of the bathymetry, methodologies for such fin-whale and dolphin studies allowed have for a separate analysis of these two potential factors on subject behavior (Hui, 1994).

Geomagnetism in the marine environment may help orient adult eels in their migration. McCleave and Power (1978) found that American eel elvers responded to even weak changes in magnetic intensity and polarity at levels that corresponded to those found in salt and even fresh water. Japanese glass eels, yellow and silver eels from rivers, farms and oceans exhibited conditioned responses to an imposed 21° easterly shift in the magnetic field (Nishi et al., 2004). Glass eels slowed heart beats when exposed to high levels of geomagnetic intensity ranging from 12,000 to 190,000 nT (Nishi & Kawamura, 2005). Various studies have found that American and European eels demonstrate preferred orientations to the magnetic field in natural and laboratory environments, and will change their orientations in accordance with manipulations in the magnetic field (Souza, Poluhowich, & Guerra, 1988; Tesch & Lelek, 1973). A field study on the effect of electromagnetic fields on sixty migrating silver eels in the Baltic found that eels

swimming close to a 130 kv AC power cable significantly slowed their swimming compared to those who swam in zones farther to the east and south, finding no external factors other than the change in the electromagnetic field to explain the difference in behavior (Westerberg & Lagenfelt, 2008). European eels from freshwater environments not only re-oriented their original headings to manipulated changes in magnetic North, but also adjusted their magnetic preferences with water temperature (Durif et al., 2013). In cooler temperatures below 12°C, the eels oriented themselves in line with their previous heading, but in warmer temperatures (12°C to 17°C) the eels oriented themselves perpendicular to the axis of their previous heading (Durif et al., 2013).

Seamount Hypotheses

The three temperate species of eels in the Northern Hemisphere all spawn near seasonal frontal systems in subtropical ocean gyres of the North Pacific and North Atlantic Ocean (Tsukamoto, 2009; Tsukamoto et al., 2002). Observations of newly hatched leptocephali have narrowed the spawning area of the Atlantic eels to the seasonal subtropical frontal area that divides the north and south parts of the Sargasso Sea, however no spawning eels or eggs have ever been seen there (McCleave, 1993; Schmidt, 1923). By charting and analyzing data of small *A. japonica* leptocephali collected in oceanic cruises in the North Pacific Ocean in 1986, 1995, and 1998, researchers have located the spawning grounds of the Japanese eel on the edge of the west flowing North Equatorial Current near 15˚ N and 140° E (Tsukamoto, 2009; Tsukamoto et al., 2003). Discoveries of anguillid eggs and pre- and post-spawning Japanese eels in 2008 and 2009 have provided further evidence that Japanese eels spawn along a salinity front in the North Equatorial Current (NEC) and at a latitude where the Kuroshio Current will

transport larvae northward after the NEC bifurcation from the southerly Mindanao Current (Aoyama et al., 2014; Tsukamoto, 2009). Notably, this spawning location of the Japanese eel overlaps geographically with the spawning grounds of the tropical anguillid giant mottled eel *Anguilla marmorata,* although their larval migration takes them in different directions (Kuroki et al., 2009). Annual variations in the strength of the salinity front have encouraged questions regarding the means by which silver Japanese eels navigate to and aggregate within their preferred spawning areas (Aoyama et al., 2014). The location of the frontal area near the southernmost end of the West Mariana Ridge further places the Japanese eel spawning close to where three seamounts (Sugura, Arakane and Pathfinder) rise three to four kilometers from the ocean floor as shown in Figure 9 (Aoyama et al., 2014; Tsukamoto et al., 2002; Tsukamoto et al., 2003).

As a result of these findings, researchers of the Japanese eel have proposed a "Seamount Hypothesis" that spawning Japanese eels aggregate along the southern seamounts of the West Mariana Ridge and that, concurrent with a "New Moon Hypothesis", spawning occurs during the phase of the new moon (Tsukamoto et al., 2002). This new moon hypothesis was subsequently supported by a study of otoliths, small inner ear bones that indicate age of small leptocephali and pre-leptocephali, which narrowed Japanese eel spawning to the new moon period during summer months (Tsukamoto et al., 2003). As for the relationship between spawning activity and proximity to seamounts, Tsukamoto (2009) has provided evidence that both supports and qualifies his hypothesis. Newly hatched leptocephali found in 1998 near the Suruga Seamount had been collected during an El Niño year characterized by complex currents and likely unusual ocean characteristics (Tsukamoto, 2009). Further, a large number of

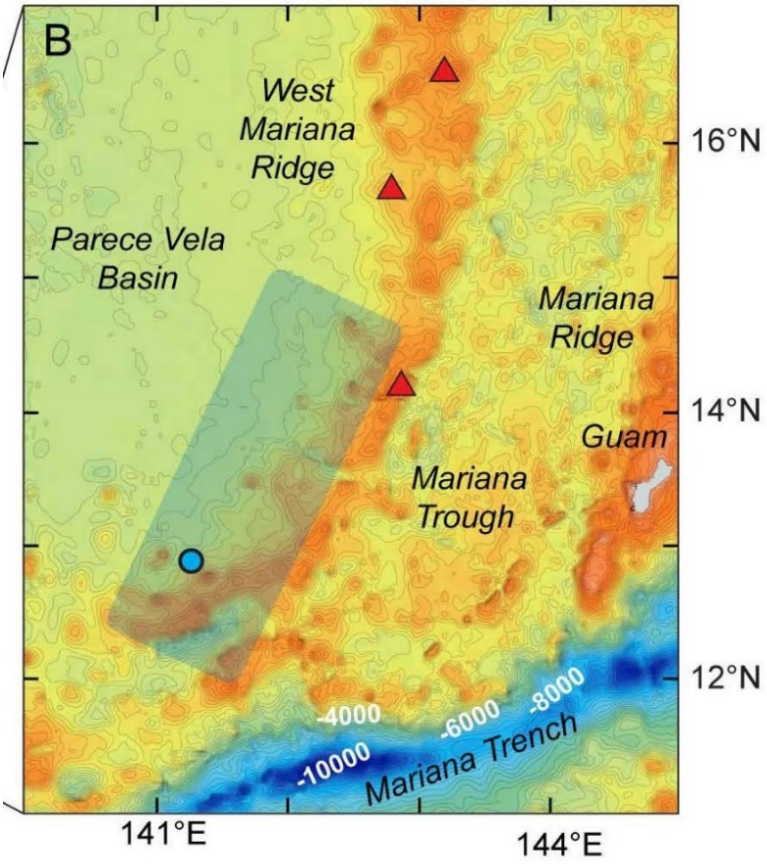

Figure 9. Japanese eel spawning area and the West Mariana Ridge. The blue shaded rectangle indicates the spawning area and blue circle where eggs were collected (Aoyama et al., 2014).

preleptocephali and the remarkable discovery of two male silver eels at 130 km south of the nearest seamount in 2008, indicated that Japanese eels spawning can occur in the open ocean farther from the seamounts (Tsukamoto, 2009). Spawning of the Japanese eel appears to shift within narrow salinity fronts, but the possibility that seamounts play a role in aiding navigation and aggregation of migrating eels, possibly through olfactory or

magnetic cues, remains a topic of research (Aoyama et al., 2014; Tsukamoto, 2009).

It is not known whether Atlantic anguillids, after spending the greater part of their lives in geographically dispersed and relatively isolated freshwater, estuarine, and coastal habitats, migrate singly or in schools before aggregating to spawn in the Sargasso Sea. If they migrate singly to deep oceanic spawning grounds they presumably would require some type of orientation mechanism that would help them locate other spawning eels, for example through geomagnetic or olfactory cues due to water properties, pheromones, or some combination thereof (Fricke & Tsukamoto, 1998; McCleave et al., 1985; Tsukamoto, 2009; Tsukamoto et al., 2011). Referring to the Japanese seamount hypothesis, Fricke and Tsukamoto (1998) have speculated that Echo Bank, a seamount charted in 1898 some 270 miles northeast of Barbuda Island and reported to rise to 62 m below the ocean surface, and other offshore banks near the Antilles may be a spawning site for Atlantic eels. However, Echo Bank has only been identified once in 1946 since its original discovery, and its presence lacks verification (Fricke & Tsukamoto, 1998). In 1977 an expedition on the R/V Westward attempted to find the Echo Bank seamount without success, leading Arthur Gaines, Jr., the head of the expedition to call it a shoal of "questionable existence" (Gaines, 1977, p. 8), although also acknowledging that the ship position two miles from the uncertain location of the bank limited chances of finding the slope of a bank less than 5 miles wide. An alternative theory for the elusive seamount was also put forward:

> Dr. Howard Winn of University of Rhode Island believes that sightings of colored water near Echo Bank from airplanes may tie this mystery to a seemingly unrelated one—the breeding ground of the American eel, *Anguilla rostrata*. Winn suggests that massive "shoals" of eels congregating for spawning could explain sightings of "bottom" in water of oceanic depth. And Eels could also be responsible for midwater sonar reflectors (Gaines, 1977, p. 46).

Other than these speculative references, however, attempts to correlate the spatial distribution of Atlantic eel leptocephali with geological features in the Sargasso Sea appear lacking. Tsukamoto (2009) comments on the relatively featureless landscape of the Sargasso Sea in comparison to that of the North Pacific area of the southern end of the West Mariana Ridge where summits of seamounts reach to just below the water surface.

Spatial Analysis Approach

Spatial analysis is based on the fundamental principal of geography that "everything is related to everything else, but near things are more related than distant things" (Tobler, 1970). A spatial analytical approach explores the spatial distribution of events, features, and their attributes to distinguish how their trends, relationships and patterns differ from otherwise random occurrences. The use of geographic information systems offers opportunities to explore, manipulate, analyze and visualize such patterns and trends in continuous and discrete spatial data (Congalton & Green, 1992). In 1984, the U.S. Joint Committee on Geographic Education defined five themes of geography: location, place, human-environment interaction, movement or the relationship between places, and regions (Boehm & Petersen, 1994). In view of this description, the extraordinary phases of dispersal and aggregation of the life cycle of the eel make an apt subject for spatial and geographic analysis.

The potential association between eel spawning and migration in the Sargasso Sea with nearby geophysical features remains relatively new territory. Spatial analyses provide the means to assess the randomness and patterns of larval distributions in relation

to each other and to the bathymetry and other geophysical features of the ocean floor. On the one hand, planning of pelagic marine reserves, as is underway for the Sargasso Sea, must focus on dynamic boundaries to accommodate preferences of pelagic species following seasonally recurring frontal zones or ephemeral eddies and frontal jets (Hyrenbach, Forney, & Dayton, 2000). However, the success of such planning will be supported by understanding the underlying bathymetry, its relation to hydrodynamics, and its connection between benthic and pelagic environments (Harris & Whiteway, 2009; Sale et al., 2005). The following analysis attempts to find such connections by investigating historical observations and null catch data for a pelagic species of larvae and exploring their relationship to geophysical features in the deep sea environment. The disappearance of a once common species from freshwater and estuarine ecosystems and current efforts to delineate a pelagic conservation area in the Sargasso Sea where they reproduce make this a timely investigation.

Chapter II

Methods

This research employed geographic information system (GIS) analytical tools to assess spatial distributions of larvae in relation to bathymetric depth and slope and the intensities and gradients of geomagnetic anomalies. A collection of "null data", stations and haul locations where eel expeditions did not report eel findings, supplemented an existing and published global set of Atlantic larvae observations. Because prior research has associated small larval distributions, an indication of adult spawning locations, with the temperature gradients of the subtropical frontal zone, data on sea surface temperature and chlorophyll for regression analyses were also anticipated and acquired. A literature review of freshwater eel evolution, spawning behavior and their migrations provided background for interpretation of the analytic results and their implications.

Assumptions

Data acquired for this project included hauls and stations where eel sampling activity took place but no eels were reported. This study makes the assumption that eels were absent at these locations, or researchers would otherwise have reported them as present. A broader assumption in this project and in eel research generally is that eel spawning location is inferable from locations of the smallest, newly hatched leptocephali. As no eel eggs or silver (adult) eels have been observed in the Sargasso Sea, results from experiments that have created artificial conditions, e.g., spawning behavior of hormonally

treated eels, durations of egg fertilization and pre-larval development in the laboratory, swimming behavior of eels wearing tracking devices, etc. are assumed to provide useful material that can inform natural processes or behavior. While these assumptions are necessary and applied throughout, the literature review, analysis, and discussion have attempted to remain conscious of limitations. As well, while the American eel and European eel are discussed in tandem and have many parallel life histories and biology, the extent of their differences and similarities are not fully known. The treatment and discussion has tried to apply caution in generalizing similarities by including separate and comparative analyses for both species.

Study Areas

Spatial distributions were studied at several progressively smaller scales to gain insights into the overall distributions of larval sampling and observations. Initially, all sampling and larvae sampling locations west of 19° E were explored over an area that extended from the middle of the Mediterranean Sea to the east coast of North America. A subsequent study area was made by creating a 200 km buffer around the convex minimum boundary polygons of locations where larvae ≤ 30 mm had been found present. A second study was formed in a similar fashion by creating a 200 km buffered rectangle around the minimum convex polygon of the ≤ 10 mm larval distributions. The rationale for the buffered areas was to avoid edge effects with the population of interest (smaller, younger larvae) and to include the results of sampling around the perimeter of their extent.

Data Sources

Data on larval captures were accessed from the International Council for Exploration of the Sea (ICES) Egg and Larvae Data Base (McCleave, 2011), which contains a comprehensive compilation of Atlantic anguillid larvae observations records. The ICES data set was organized by counts of larval lengths that were categorized by species, sample number and haul numbers. In addition to larvae size, species and counts, sample and haul numbers, the ICES data set provided information on date, time, geographic coordinates, ship and ship station, principle researchers and primary and secondary sources. Additionally, some records included information on gear type and haul duration.

The ICES data were supplemented with station and haul data from ship expeditions where sampling was documented but no larvae reported. For the purpose of this study, these "null" stations or hauls represented locations where larvae were considered to have been absent. The null station data were acquired from cruise reports obtained via a variety of online and library sources and personal files of eel researchers. Sources of the null data used in this study are shown in Appendix D.

The null haul data were appended to that of positive hauls found for stations in the ICES data set. The observations were then coded as "positive" or "null" hauls and later condensed into "positive" and "null" stations. Data were summarized to provide a station list that included total counts of larvae by species and increments of 10 mm size groups. Locations finding both species present were coded to facilitate analysis of species overlaps. Minimum, maximum, mean and standard deviations per station were also

recorded. The end result was to create two data sets, one with single records of individual larvae observations and the other summarized into station data as described. Stations with both positive and negative hauls were counted as a "positive" station.

Bathymetric Data

Bathymetric data were acquired from the General Bathymetric Chart of the Oceans (GEBCO) Digital Atlas project (IOC, IHO, & BODC, 2008) and the ETOPO1 Global Relief Model (Amante & Eakins, 2009). GEBCO is a collaboration between the Intergovernmental Oceanographic Commission, International Hydrographic Organization, British Oceanographic Data Centre and other scientific and academic institutions. The GEBCO_2014 30 arc-second grid and GEBCO Digital Atlas one arc-minute grid were downloaded from the British Oceanographic Data Center in ASCII and NetCDF grid formats. Vector data of bathymetric contour lines were acquired from the GEBCO Digital Atlas compact disc. The ETOPO1 1 minute grid is produced by the National Oceanic and Atmospheric Administration (NOAA) National Geophysical Data Center (NGDC) and was retrieved as a binary ASCII file from their website.

Bathymetric slope was calculated from the GEBCO_2014 data using the ESRI Slope Tool.

Geomagnetic Data

The global Earth Magnetic Anomaly Grid (EMAG2) provided crustal geomagnetic intensities (nT) in 2-arc-minute resolution that is compiled from satellite, ground and ship survey data (Maus et al., 2009). The grid anomaly data were downloaded

in ASCII and GeoTIFF files from the Cooperative Institute for Research in Environmental Sciences (CIRES), which hosts the main EMAG2 website and data portal.The magnetic gradients were calculated from the EMAG2 data using the ESRI Slope Tool.

Oceanographic Data

NASA Ocean Color L3 Sea surface (SST) and chlorophyll *a* (Chl) data for available years were acquired with tools provided by the Marine Geospatial Ecology Lab (Roberts, Best, Dunn, Treml, & Halpin, 2010). This data included Aqua MODIS Chlorophyll concentration, CZCS Chlorophyll concentration, Sea WiFS Chlorophyll concentration, and AVHRR Pathfinder Version 5 SST data. Ultimately, these data sets were not used in the analysis.

Analytical Tools

ArcGIS Desktop software version 10.2 was the primary analytical program employed for analyses. It was later updated to ArcGIS 10.3 towards the end of the study. The software supports spatial and geostatistical analysis and modeling, data management, editing, and mapping (ESRI, 2011). The Marine GeoSpatial Ecology Tools (MGET), produced by the Duke University Marine Geospatial Ecology Laboratory, provided open source tools that facilitated the retrieval and extraction of oceanographic HDF files and their interpolation to point sampling locations (Roberts et al., 2010). MGET tools are integrated with R statistical software and MATLAB. They were also used to check for initial collinearity between variables in preparation for general additive and generalized

linear modeling. IBM SPSS Statistics software supported additional basic statistical analysis.

Analysis

Larvae and station data were imported into ArcGIS v.10.2 and transformed into vector point features with accompanying attribute tables. The GEBCO and EMAG2 data were converted into useable ArcGIS raster formats. All layers were projected to a WGS 1984 plate carrée coordinate system.

Larvae data were subsequently classified into various categories (null/positive stations, species, and different size groups) so that patterns according to size, species, year and other groupings of interest could be explored. Data exploration and analysis were undertaken at various scales with an eventual focus on ≤ 10 mm larvae. Spatial operations included transformation, selection, categorization and visualization of data, creating layers and joining data. The spatial analyses proceeded from descriptive to inferential and initial stages of regression analysis. Descriptive statistics analysis measured geographical distributions of size categories and species and identified their mean and median centers, central features, standard distance and directional trends.

Inferential statistics analysis explored the probabilities of significant clusters versus a random distribution. Tests included calculating nearest neighbor indices globally and at incremental distances, providing confidence levels for clustering of larval lengths and associated features with the Getis-Ord Gi* statistic, and probabilities of autocorrelation of high and low value clusters with the global and Anselin local Moran's I statistic. Initial regression analysis explored possible correlations between

feature attributes of depth and crustal geomagnetic intensity using ArcGIS ordinary least squares and the MGET Cleveland Plot Table tools.

A proposed model of the data analyses presented in Figure 10 outlines a sequential roadmap leading from data selection and preparation to data exploration, spatial operations and analysis, and initial statistical tests.

Geographical Distributions

Geographical statistical distributions were measured for different size groupings of larvae. These measurements included the following measurements (ESRI, 2015):

- Mean Center – the means of the x and y coordinates (latitudes and longitudes in this study) latitude and longitude of all features.
- Median Center – the location with the shortest total distance to all features. The median center is less influenced than the mean center by outliers.
- Central Feature – the feature in the data set with the shortest accumulated distance to all other features.
- Standard Distance – the dispersal or compactness of features represented as a circle around the mean center. The standard distance circle can represent one, two or three standard deviations to respectively capture 68%, 95% and 99% of a normally distributed population.
- Directional Distribution (or Standard Deviational Ellipse) – calculates the directional trend for the x and y coordinates (latitudes and longitudes in this study) and represents them as an ellipse around their axes. The one, two, or three standard deviational ellipses respectively show the directional trends for

68%, 95% and 99% of a normally distributed population.

The geographic centers were measured using both unweighted and weighted features for comparison. Weighting features shows how attributes such as counts or other values affect their spatial distribution.

Nearest Neighbor Index

Nearest neighbor averages were calculated for the distribution of larvae across the study area. The nearest neighbor average calculates the average observed difference between features across a designated area and compares that average to an expected random distribution (ESRI, 2015). The tool provides a Nearest Neighbor Index, or ratio, that can then be used to produce a *z*-score and associated probability value (*p*-value) of randomness within that area. A *z*-score of zero indicates randomness, while a positive *z*-score is a sign of dispersal and a negative one of clustering.

Ripley's K-function

Nearest neighbor indices are sensitive to the scales at which they are measured and do not provide information on where spatial patterns occur within an area.
For example, a pattern of points dispersed across an area may only reveal clustering at a larger scale. Nearest neighbor averages were tested across incremental ranges and *z*-scores compared with the Ripley's K-function tool to see at what scale larval distributions showed maximum dispersal or clustering.

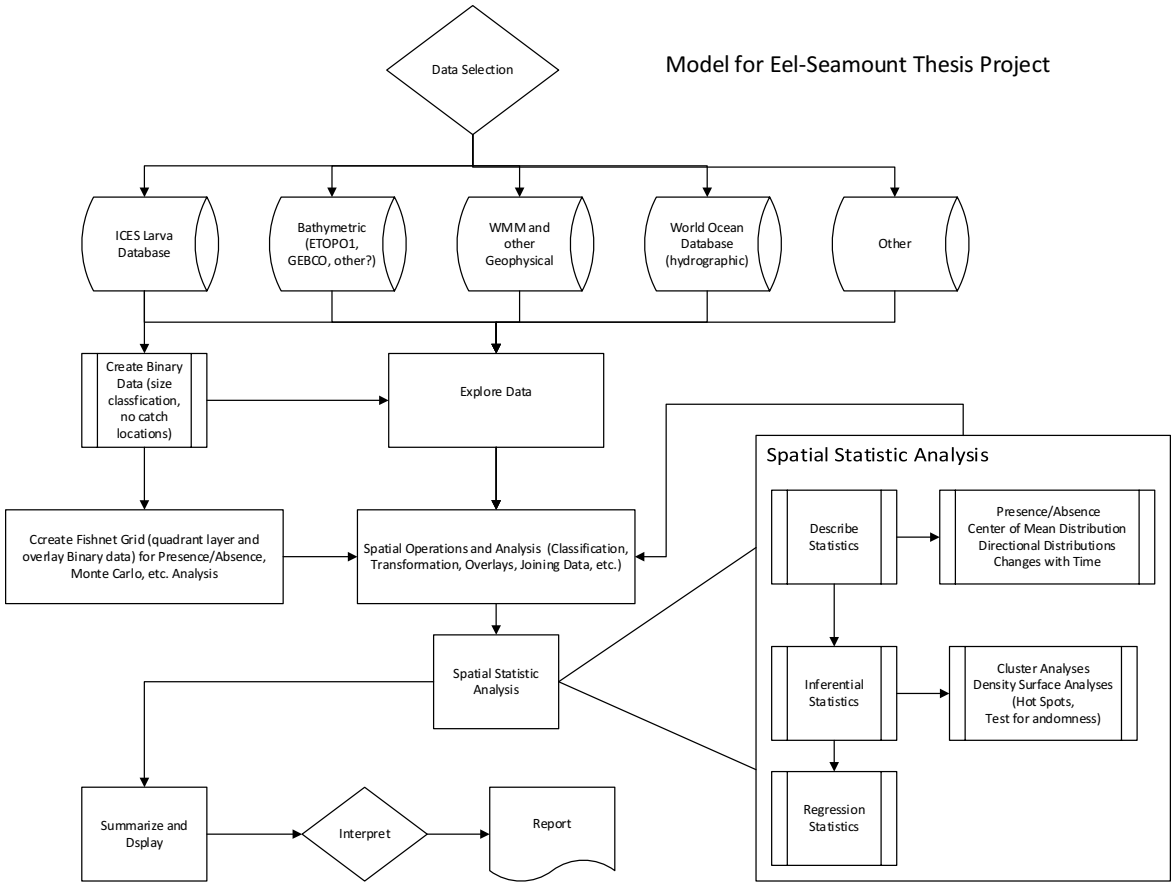

Figure 10. Proposed model for eel project spatial analysis.

Global Moran's I and Spatial Autocorrelation

This ArcGIS spatial autocorrelation tool was used to identify the distances at which larval distributions exhibited higher variation between expected and random distributions, i.e. where their patterns were most distinguished from a random distribution. Applying a fixed increment across a range of distances, this tool applies user input fixed distance bands to test for non-random spatial dependency between features or attributes, a phenomenon referred to as spatial autocorrelation. The observed spatial patterns were compared over a series of incremental distances using the ArcGIS tool for multi-distance spatial autocorrelation, providing a series of probability ratios over the range of distances. Rows of the variables in the data set were standardized as recommended to remediate potential sampling bias. Outliers that could confound results were identified as those whose nearest neighbor was three standard distances greater than the mean. This was accomplished using the Near Proximity tool to find the nearest neighbor distance for each point and calculating their mean and standard deviations. This analysis for autocorrelation of larvae sizes across a range of distances was performed to gauge at what distance clustering and dispersal would best come into focus and also to inform on appropriate fixed distance bands that ensure each feature approach an optimum number of neighbors for later analyses.

Clustering and Hot Spots

The Nearest Neighbor Index is a general value that applies to the entire study area but does not indicate areas of clustering or dispersal within the sampling area. ArcGIS

provides inferential tools for measuring and mapping areas of significant non-random clustering and dispersal using a Getis-Ord General GI* index and using a Local Moran's I statistic. The analyses for local spatial distributions may need inputs to specify scale for the analysis.The Anselin Local Moran's Index (Moran's I) weights numerical attributes of adjacent features and then compares them to their global average to determine areas with significant levels of spatial clustering and dispersal (ESRI, 2015).

The Getis-Ord Gi* hot spot analysis produces an index based on whether a feature with high or low values are surrounded by neighbors with similar values. Neighboring features with higher than the expected sum are considered statistically significant (ESRI, 2015).

The local clustering analyses require a choice of spatial conceptualization. The recommended and default conceptualization is a fixed band analysis. The fixed band is based on a user determined scale of analysis and only considers the features within that scale. An inverse distance spatial conceptualization anticipates that all features in the data set exert influence on one another but at a diminishing rate of influence with distance. This study applied both the recommended fixed band and inverse distance spatial conceptualizations for comparison.

Data Limitations

Sampling data were collected from different expeditions across a wide range of years, in various seasonal time frames, and with individual purposes, methods and biases. Their variation in sampling design, methods, and environmental factors qualify the analyses. Null data were not available for all expeditions. Bathymetric data were limited

by the extent to which the area has been surveyed. While coastal bathymetry is often produced with high resolution data, the deep sea bathymetric grids and derived shape contours typically represent smoothed and interpolated data that can miss variations in depth at smaller scales (Kearns & Breman, 2010). These limitations were kept in mind throughout the study.

Chapter III

Results

This chapter presents the results of this study as it progressed through data exploration, analysis of spatial patterns, and initial investigation of relationships between variables. The first part describes the distributions found in the sampling and larvae data at the scale of the North Atlantic Ocean. The second section reviews results of the spatial analysis of a buffered area that encompassed the extent of all larvae ≤ 30 mm in total length. The last section explores the area defined by the buffered extent of small larvae (≤ 10 mm in length), detailing their distributions in relation to depth, slope, geomagnetic intensity and gradient, and the surrounding landscape.

Sampling and Larvae Data

Atlantic anguillid larvae observations were accessed from the International Council for the Exploration of the Sea (ICES) Eggs and Larvae Dataset (McCleave, 2011) which contains counts of larvae by length, dates, geographic locations, species, sample and haul numbers, primary and secondary sources, and for some records, type of gear and haul duration. Only larvae observations west of 19° E were downloaded into an Excel spreadsheet. The downloaded data contained 15,700 records of frequency (counts) of larvae lengths at sampling locations. An Excel macro then extracted 31,284 records of individual larvae observations from these aggregated counts. Records of 344 individual glass eel observations, including 239 stations that only reported finding glass eels, were

removed from the dataset, a step that left 30,940 observations of anguillid leptocephali from 1476 stations remaining for analysis.

Null Stations

The data included 697 stations where sampling activities did not report any larvae observations. This "null data" was added to the dataset of larvae observations. Some of the observations recorded included data on individual hauls, gear and haul duration. Time constraints precluded transcription of all the available null data set, and its full compilation and analysis remain a work in progress. Sources for null data used in this study are shown in Appendix D. The added data expanded the dataset to a total of 32,935 records of sampling activities on 77 ships at 2,173 station locations (Figure 11). Records in the data set were then then coded with a binary 1 or 0, with 1 indicating a "positive" haul and 0 a "null", or empty, haul. Because many stations had more than one haul, this information was condensed to the station level, counting any station with at least one positive find a "positive" station (Figure 12).

Temporal Distribution

Sampling activities took place over a range of 145 years in 66 individual years, distributed between 1863 and 2007. Sampling years were not evenly distributed during this period. Data collected during 23 of the 66 years represented 90.3% of all sampled locations. The greatest number of locations were sampled in the years of 1922 (9.1%), 1984 (8.7%), 1964 (8.1%), 1979 (7.2%) and 1921 (6.7%) with peaks occurring in the 1920s, 1960s, late 1970s and 1980s (Figure 13). Greater detail of

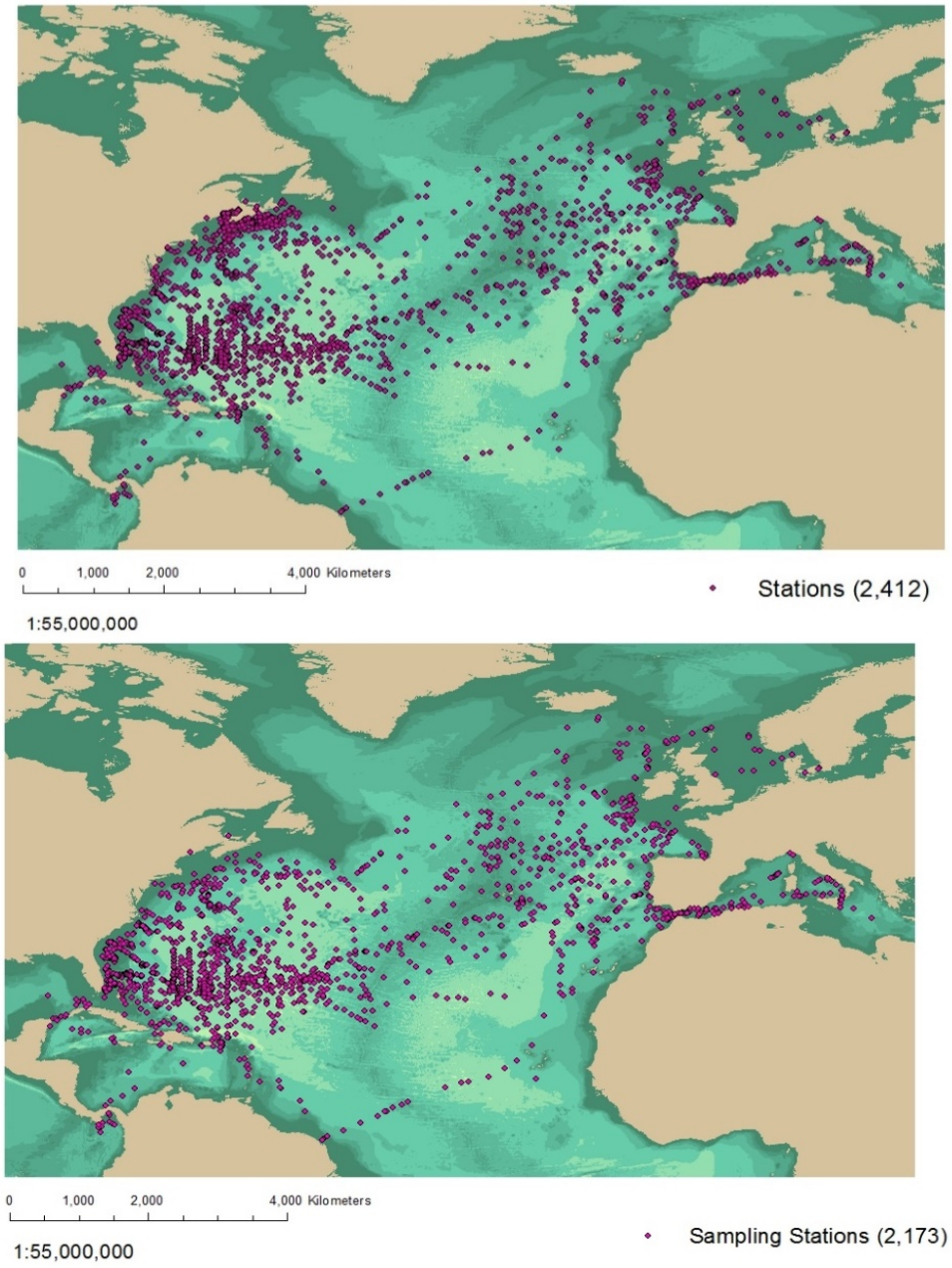

Figure 11. Sampling locations (with and without glass eels). Distributions of downloaded sampling locations with glass eel data (top) and excluding glass eels (bottom). There were 2,173 sampling locations after removing the 239 stations that only found glass eels. Their removal is particularly noticeable in Nova Scotia and the Bay of Fundy. Figures include both null and positive stations.

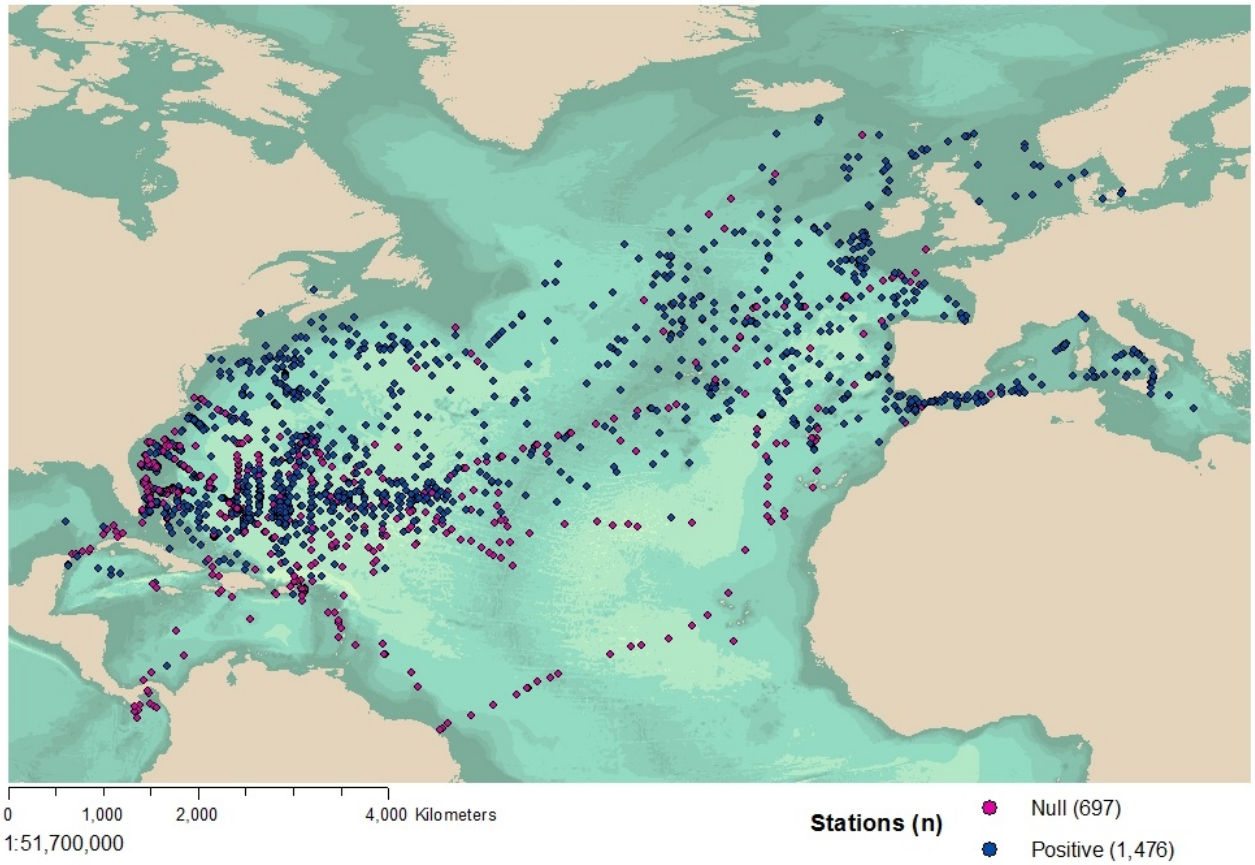

Figure 12. Null and positive stations. The distribution of 2,412 sampling stations included 1,476 positive stations (blue) where anguillid larvae were found and 697 null stations (magenta) that did not record any larvae observations. Stations with both positive and null hauls were counted as a positive station.

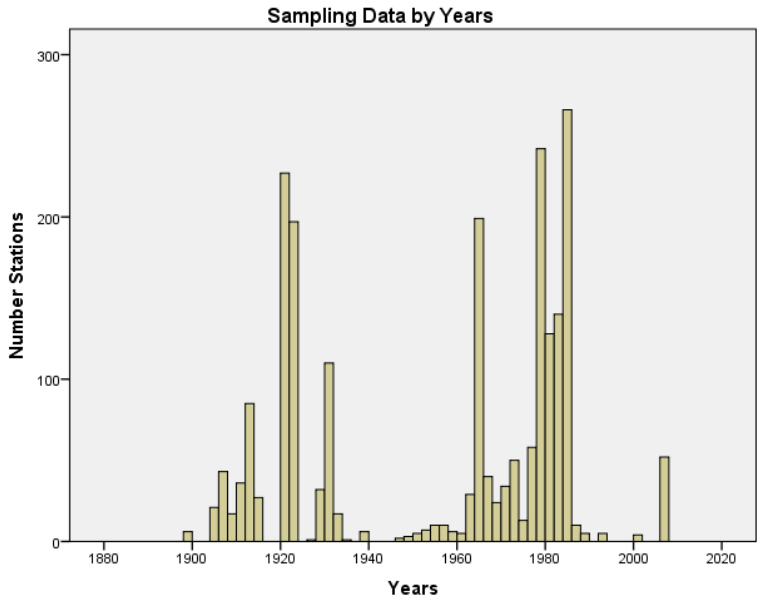

Figure 13. Sampling data by years. The histogram shows the distribution of sampling activity as counted by number of stations across the years covered in the ICES data base.

sampling years is found in Appendix C. Some problems with date formats were encountered when inconsistent month and date formats were introduced into the data set. This problem was not entirely resolved before the end of the project and so seasonal and annual analyses were not included.

Sampling Distribution

Geographic positions of sampling stations (Figure 11) ranged from the eastern entrance to the Panama Canal to a western-most cutoff point in the Mediterranean Sea. Stations with only recorded observations of later-staged glass eel larvae were then removed from the data set, resulting in a visible difference off the coast of Nova Scotia and in the Bay of Fundy. All sampling positions were in the northern hemisphere.

Latitudes ranged across 57.7 decimal degrees between 5.05° N and 62.75° N (Table 1). Longitudes of sampling locations in the data set ranged across 106.8 decimal degrees from 19.47° E to 87.33° W. The mean latitude and longitude was at 31°.71 N and 53°.00 W (Table 1). A histogram of the latitude and longitudes of sampling locations show sampling stations were most numerous at latitudes from the mid- to high 20s (degrees of latitude) and between 55° W and 80° W (Figure 14).

Species Distribution

Data included records of 21,483 *A. anguilla* leptocephali constituting 65.2% of all larvae observations (including glass eels). *A. rostrata* represented 28.7% of the total with 9,458 observations. Mapped distributions are shown in Figure 15. In addition, 1,994 (6.1%) anguillid leptocephali were not identified to the species level. The lack of identification was often a factor of a myomere count falling within the range of overlap between the two species, e.g. a myomere count of 111. Moreover, out of the total 2,173 stations, both species coincided at 300 stations, or 13.8% of the total number of locations (Figure 16).

Size Distribution

Total lengths of larvae ranged from 3 to 190 mm. Five stations in the Mediterranean Sea recorded larvae larger than 90 mm. The mean larval length was 31.39 mm (*SD* = 22.10 mm) with a median of 24.00 mm. A frequency analysis showed 12.0 mm to be the most frequent measurement for both species (Figure 17). Length distributions of *A. rostrata* leptocephali ranged from 3 to 77 mm with a mean length

Table 1. Distribution of geographic coordinates for sampling stations.

Coordinates	Stations (*n*)	Range	Minimum	Maximum	Mean
Latitude	2,173	57.7	5.05	62.75	31.71
Longitude	2,173	106.8	-87.33	19.47	-53.00

The range, minimum, maximum and mean distribution of 2173 sampling locations by latitude and longitude.

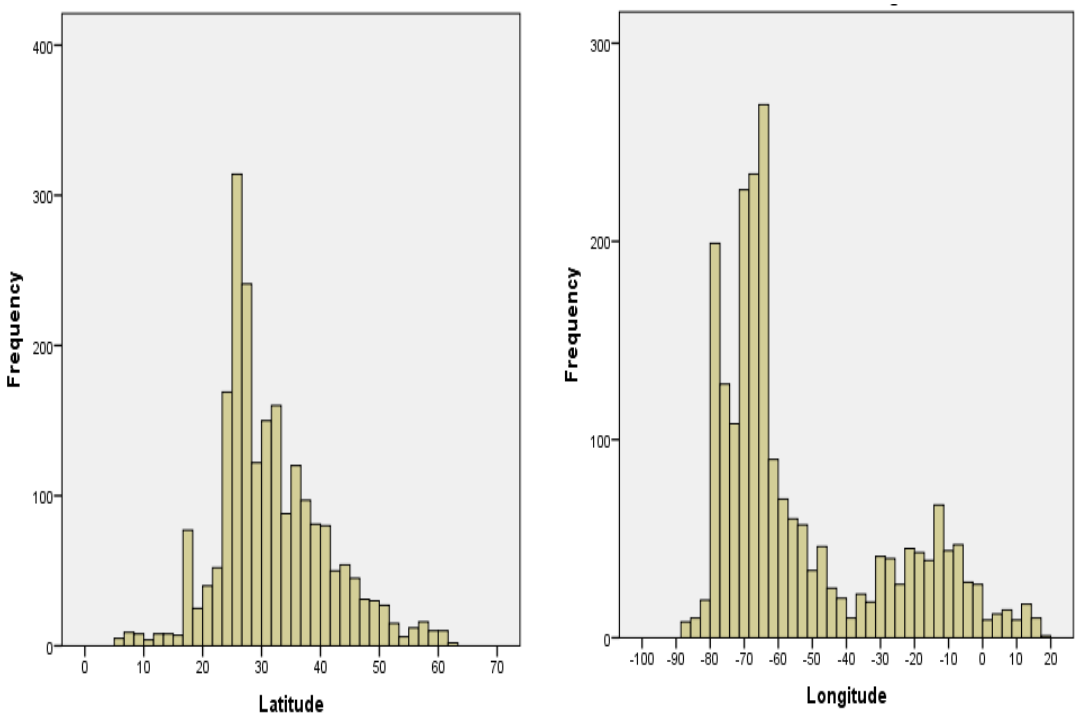

Figure 14. Histograms of station latitudes and longitudes. Sampling occurred most frequently from latitudes 24° N to 28° N and from longitudes 80° W and 60° W.

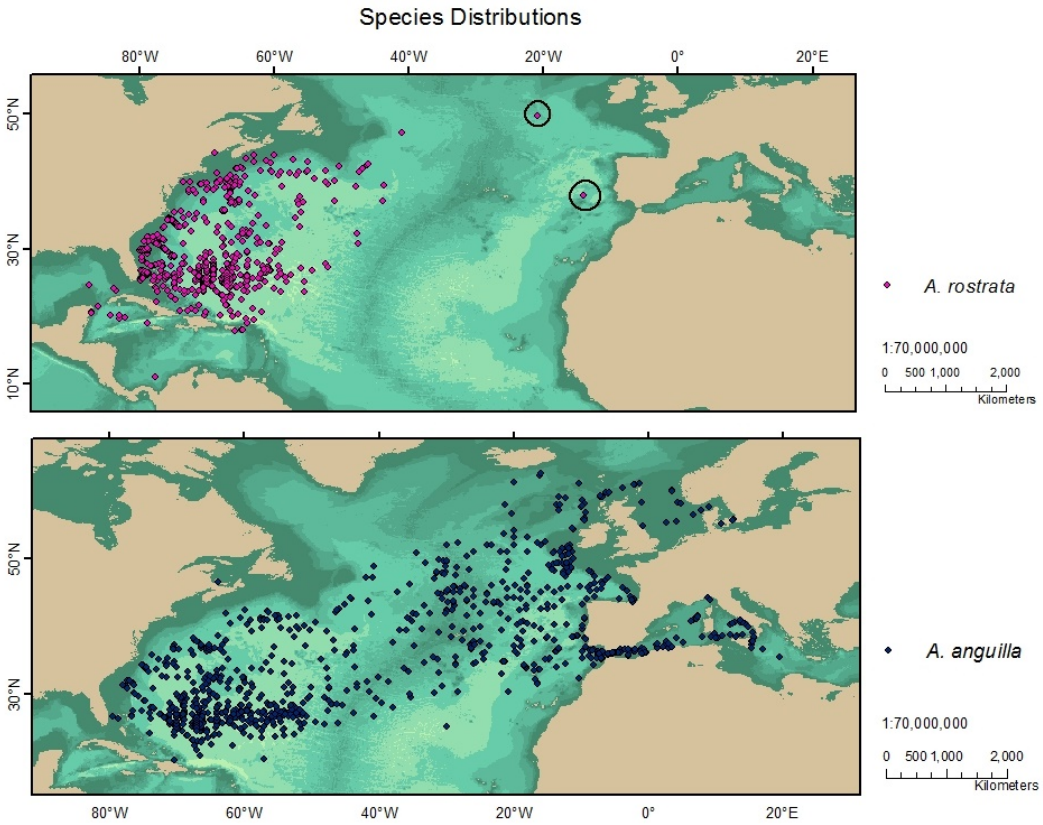

Figure 15. American and European larval distributions. While the distribution of *A. rostrata* leptocephali (top) stayed mainly within the confines of the eastern Atlantic, two outlying larval leptocephali can be spotted off the coat of Portugal and the North Sea (circled). Leptocephali of *A. anguilla* (bottom) reflect their migration to the European continent; however their larvae are also spotted off of both Florida and Hispaniola to the south and north at the entrance to the Saint Lawrence River.

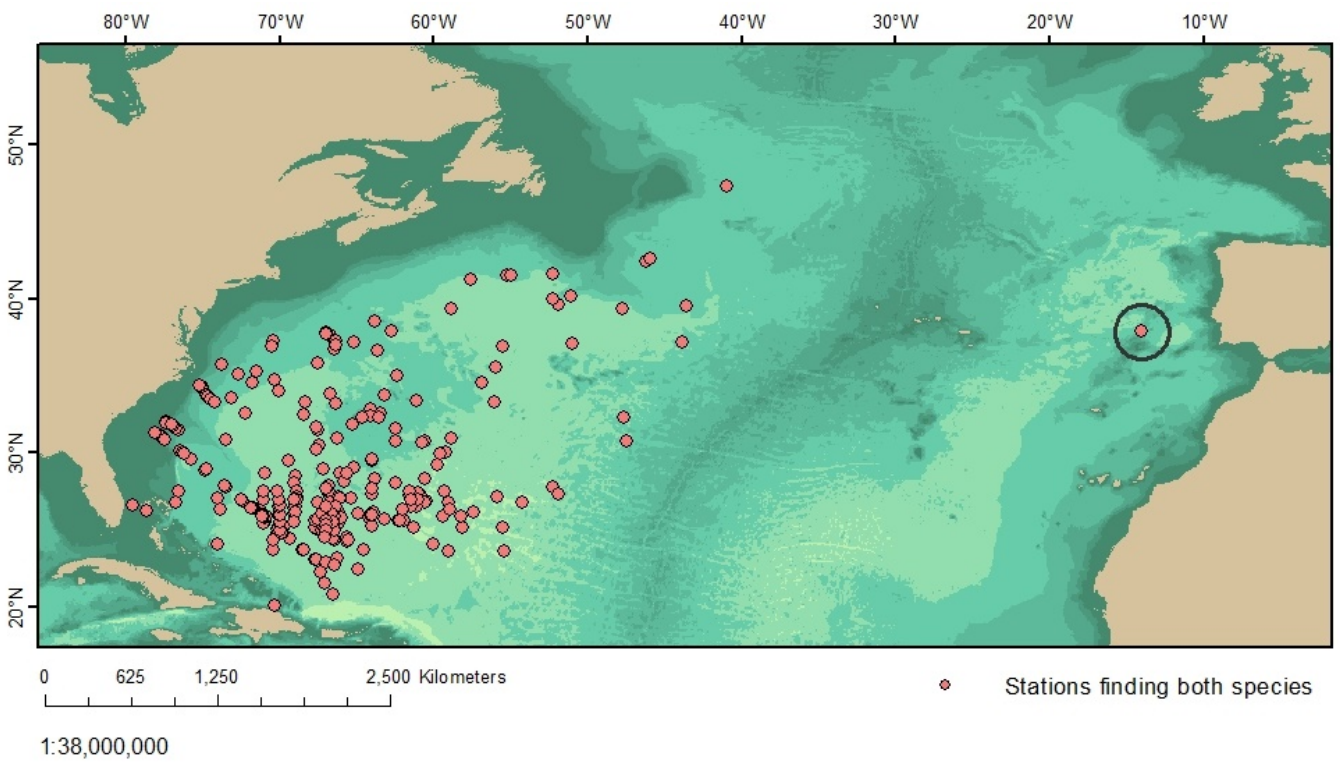

Figure 16. Locations of species overlap. Both American and European eel species of leptocephali were found present at 300 geographic locations with the greatest concentration in the North American basin in the Sargasso Sea. The spread extends from the north side of the Dominican Republic to a station in the Newfoundland Basin. One outlying station in the western North Atlantic basin also found both species off the coast of Portugal (circled).

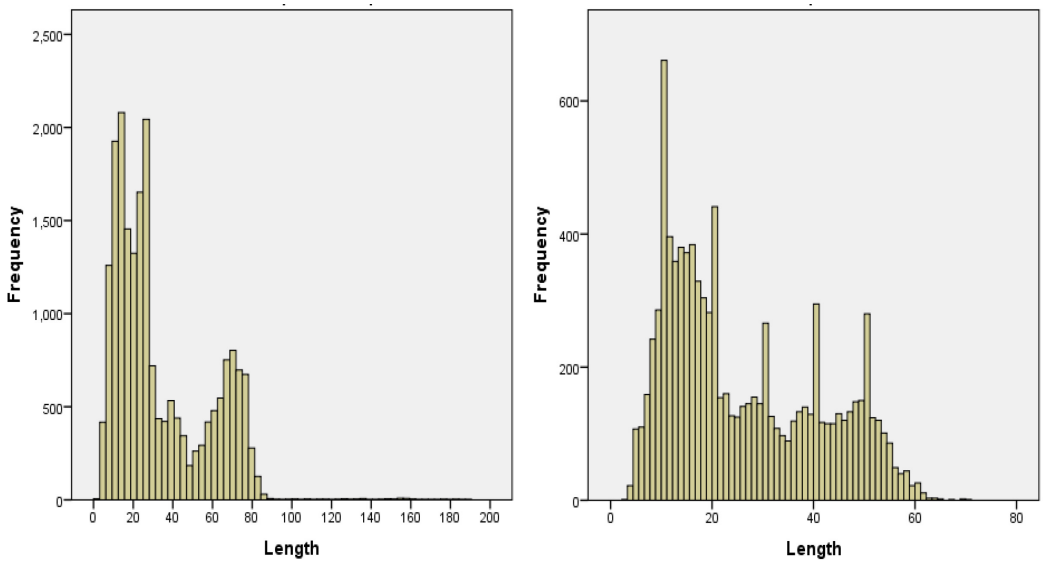

Figure 17. Histograms of sampled larval lengths. The histograms of European eel (left) and American eel leptocephali (right) at the scale of the North Atlantic Ocean.

of 26.0 mm (*SD* = 14.95 mm) and a median of 21 mm. *A. anguilla* leptocephali ranged in length from 3 to 190 mm with a mean length of 33.9 mm (*SD* = 24.3 mm) and a median of 25.0 mm. A group of 114 observations of larvae < 90 mm from five locations in the Mediterranean Sea contributed to the wide spread of the European eel mean lengths, while the American eel length distributions showed less of a spread and smaller deviation. An ANOVA test found a significant difference ($p = < .001$) between the mean lengths of the two species and their logs.

Smaller larvae of both species concentrated in the area of the Sargasso Sea with larger sizes radiating outwards (Figure 18; Figure 19). Larger sizes of *A. rostrata* leptocephali radiated east and north along the continental shelf of North America and

with the Gulf Stream. *A. anguilla* in the southern latitudes of the eastern Atlantic Ocean were relatively smaller than those at more northern latitudes. Few leptocephali larger than 40 mm were found north of 40° N in the eastern Atlantic basin. The increasing size gradients showed leptocephali recruiting to the European continent were larger than those of both species off the North American continent.

Geographical Centers and Directional Trends

Leptocephali of each species were grouped into size categories (≤ 5 mm, ≤ 10 mm, > 10 ≤ 20 mm, > 20 ≤ 30 mm, > 30 ≤ 40 mm, and > 40 ≤ 50 mm) and analyzed to determine geographic centers, directional trends, and standard distances (Table 2, Table 3). Figure 20 shows the directional trends and geographic centers the of ≤ 5 mm larval distributions. Geographic statistical tendencies for all size groups are compiled in Appendix G. The distributions of both species experienced a five-fold expansion in the area of their standard distances at particular points in their development, greatly increasing the size of distributions for *A. rostrata* in the > 20 ≤ 30 mm size group and *A. anguilla* in the > 30 ≤ 40 mm size group. The standard distance areas (km^2) of the directional ellipses of *A. anguilla* of all size groups were greater than those of *A. rostrata.*

The deviational ellipses indicate the directional trends by measuring compactness around the short and long axes of distributions and calculating the rotation of their deviational ellipses. Weighting locations by counts of larvae observations influenced the shape and direction of the directional ellipses, compared to weighting locations by larvae presence or absence only. This influence of weighting stations by numbers of larvae counted was most striking with the > 20 ≤ 30 mm group of *A. rostrat*a (Figure 21).

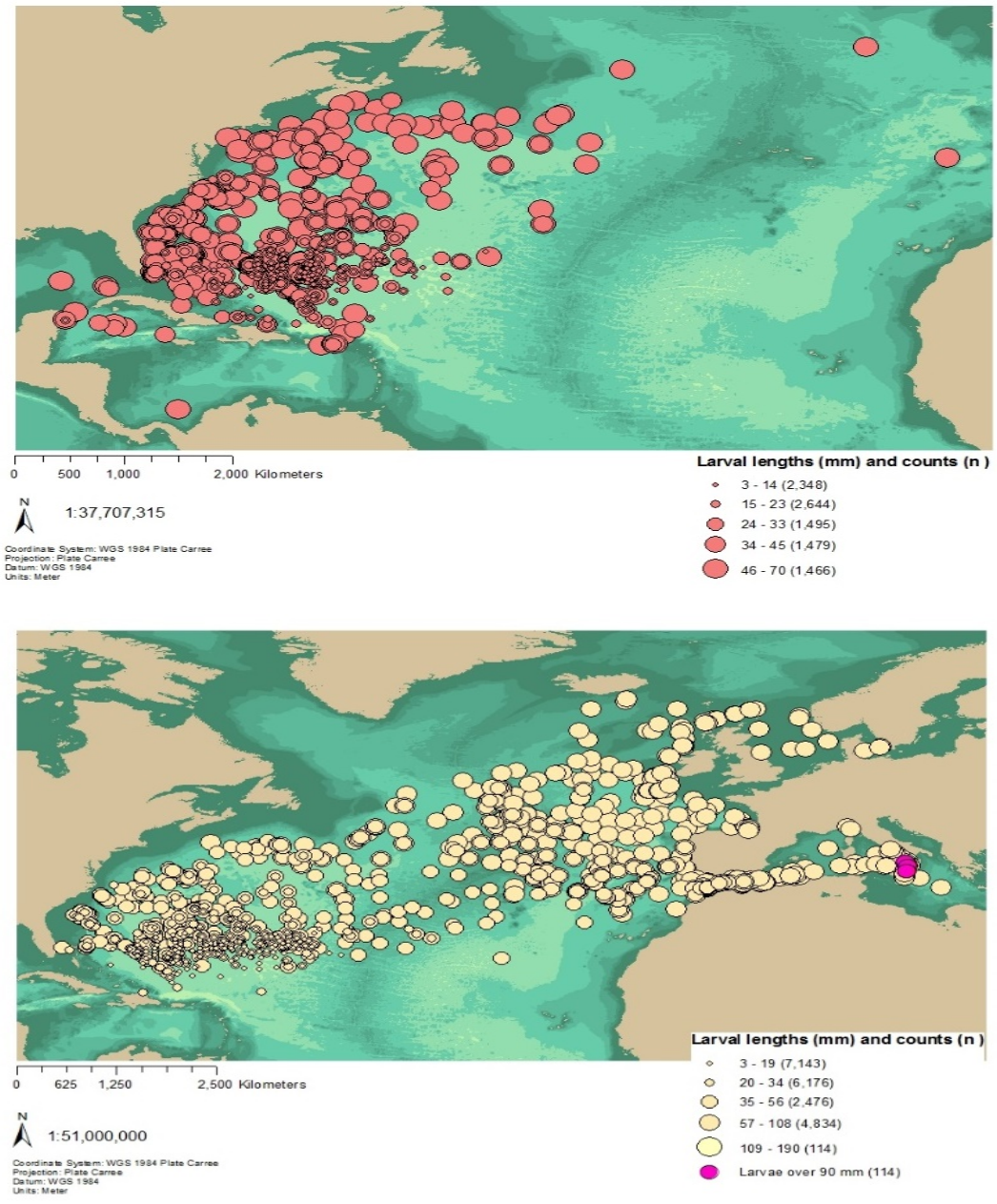

Figure 18. Graduated length distributions. The geographic distribution and counts of *A. rostrata* (top) and *A. anguilla* (bottom). Observations of 114 *A. anguillae* larvae > 90 mm at five stations in the Mediterranean Sea are highlighted (pink).

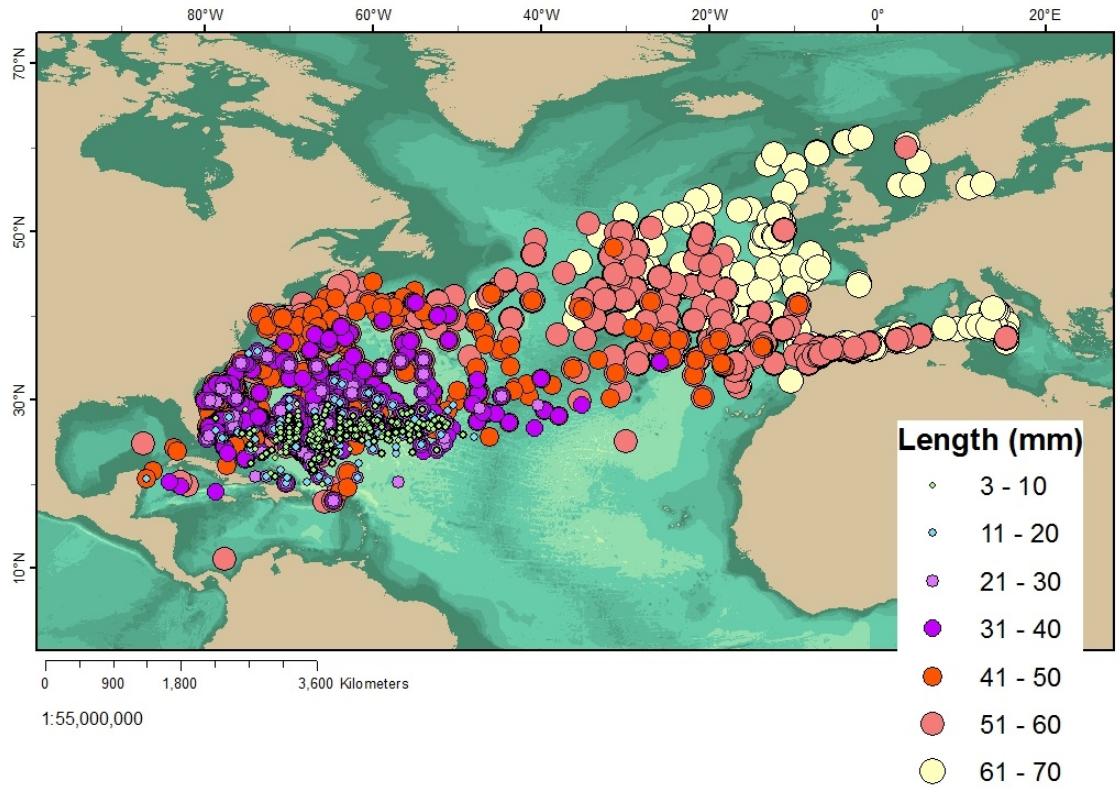

Figure 19. Geographic distributions of larval lengths. Size groups of larvae (≤ 3, 11 ≤ 20 mm, 21 ≤ 30 mm, 31 ≤ 40 mm, 41 ≤ 50 mm, 51 ≤ 60 mm, 61 ≤ 70 mm, and > 70 mm) are color coded and graduated. Smallest larvae are concentrated in the area of the Sargasso Sea. The increased lengths of leptocephali of the European continent contrast with the generally smaller sizes of those recruiting in North America. Among larvae on the eastern half of the Atlantic, smaller larvae extent eastwards in southern latitudes, compared to larger sizes off Europe.

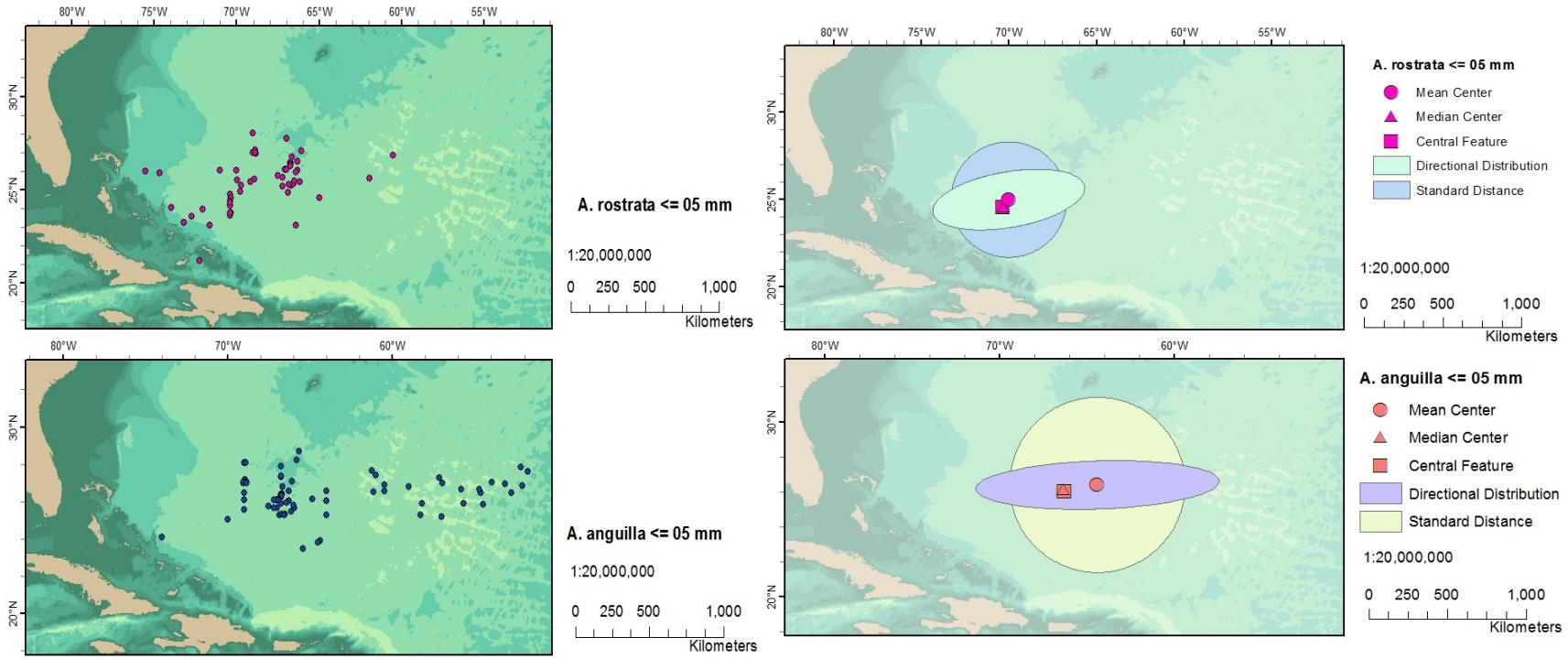

Figure 20. Geographic distribution and central tendencies (larvae ≤ 5 mm). Geographic distribution (left) and central tendencies (right) of ≤ 5 mm size *A. rostrata* (above) and *A. anguilla* (below).

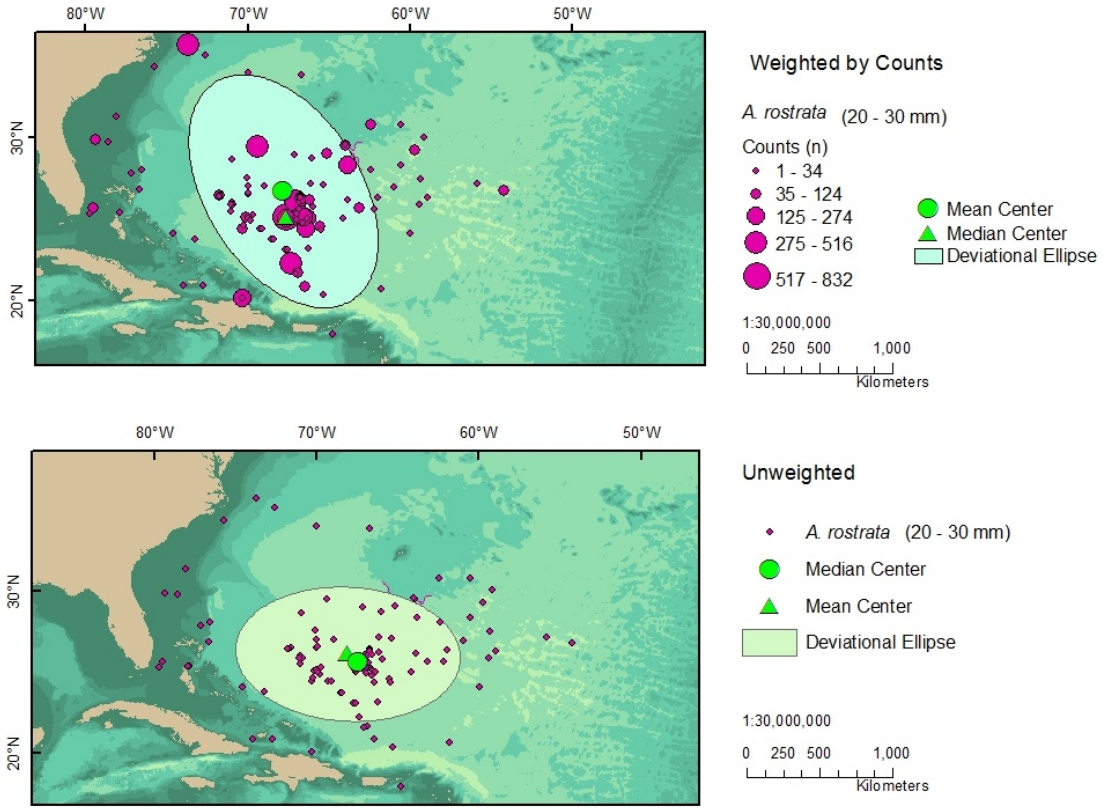

Figure 21. Weighted and unweighted deviational ellipses of *A. rostrata* (20–30 mm). The directional tendencies as shown by the deviational ellipses (1 *SD*) of *A. rostrata* in the < 20 ≤ 30 mm size group when weighted by counts (above) and unweighted (below). The degree of rotation for the weighted ellipse was 148° (from "noon) and that of the unweighted ellipse was 93.3°. Stations finding the size group of larvae are graduated by counts (above) and ungraduated (below).

Table 2. Central tendencies of *A. rostrata* by size groupings.

Length (mm)	Rotation (° from noon)	short axis 1 *SD* (km)	long axis 1 *SD* (km)	Mean Latitude	Mean Longitude	Area (km^2)
≤ 5	80	177	489	24.99	-70.03	272,288
≤ 10	83	190	455	25.27	-68.25	272,034
> 10 ≤ 20	84	213	334	25.16	-67.12	223,615
> 20 ≤ 30	148	882	532	26.70	-67.83	1,473,263
> 30 ≤ 40	92	886	672	27.56	-69.55	1,870,040
> 40 ≤ 50	68	635	924	30.33	-72.78	1,843,506

The directional trends (rotational degrees from noon) and standard distance (km^2) area of directional ellipses for different size groups of *A. rostrata*. Analysis was weighted by counts of larvae found at the sampling locations.

Table 3. Central tendencies of *A. anguilla* by size groupings.

Length (mm)	Rotation (° from noon)	short axis 1 *SD* (km)	long axis 1 *SD* (km)	Mean Latitude	Mean Longitude	Area (km^2)
≤ 5	88	153	773	26.37	-64.41	372,239
≤ 10	86	148	879	26.47	-62.44	407,867
> 10 ≤ 20	84	211	827	27.12	-59.65	548,184
> 20 ≤ 30	96	562	257	28.31	-59.37	454,070
> 30 ≤ 40	86	568	1,293	30.45	-60.07	2,306,016
> 40 ≤ 50	89	560	1,976	32.43	-54.34	3,478,313

The directional trends (rotational degrees from noon) and standard distance (km^2) area of directional ellipses for different size groups of *A. anguilla*. Analysis was weighted by counts of larvae found at the sampling locations.

The large count of *A. rostrata* leptocephali at certain stations tilted the directional trend of the overall group 64° to the northeast with a distinctive change from that of other size groups. When locations were weighted equally by presence only, the rotation showed greater consistency with other size groups. Weighting the larval distribution by counts shifted its mean center northwards by 123 km and median center by 119 km, while increasing the standard distance of the long axis by 101 km. and the short axis by 72 km. This influence of weighting on the measurements of central positions (mean, median, and central feature) is also evident with the ≤ 5 mm size group of *A. rostrata* and *A. anguilla* (Figure 22). Weighting the stations by counts of larvae observations shifted the *A. rostrata* distribution mean center by 128 km, the median center by 167 km, and the central feature by 164 km towards the southeast.

Mid-Size Larval Scale

An initial study area was constructed around a minimum boundary area convex polygon defined by the extent of all larvae ≤ 30 mm. This convex polygon was enclosed in a rectangular shape with a 200 km buffer to compensate for edge effect and on the premise that larvae smaller than 30 mm also may occur beyond what had been observed in the sampling data (Figure 23). The resulting study area was 5580 km long and 2300 km wide and covered a total area of 13,257,400 km^2. The study area contained 1429 sampling stations. Of these, 882 "positive" stations recorded a total of 24,190 larvae samples, while 547 "null" stations made no observations. American eels were found at 602 stations and European eels at 561 of the 1429 sampling locations. *A. rostrata* larvae (n = 2901) ranged in size from 3 to 63 mm (M = 20.9 mm, SD =14.2 mm), and

A. anguilla (n = 3400) from 3 to 59 mm (M = 21.9 mm, SD = 10.2 mm). Both species were found co-occurring at 281 locations. The combined lengths of both species within the study area ranged from 3 to 63 mm and had a mean of 22.4 mm (SD = 12.0 mm). Lengths appeared skewed but approached normal when log transformed (Figure 24).

Nearest Neighbors and Distance Increment Analyses

Nearest neighbor distances between sampling locations were averaged and compared with what would be expected in a random distribution (Table 4). The observed average distance between all sampling locations and their nearest neighbor was 22.7 km, smaller than the expected average of 48.2 km. The corresponding z-score of -38.17 and p-value (< .001) indicated non-random spatial clustering of sampling in the study area. Positive and null stations were tested separately and demonstrated similar degrees of clustering with one another (z-scores of -28.84 and -29.29 respectively) with low probability of randomness (p-values < .001). The species distributions were also highly clustered. Both American eels (z- = -27.56) and European eels (z- = -23.13) showed unlikely probabilities of random distribution (p-values < .001). Weighting the analysis with larval counts or attributes, as opposed to giving equal weight for presence only, inflated the observed nearest neighbor value for each feature by counting a location as its own neighbor, resulting in even lower z-scores and so an indication of greater clustering.

Hot Spot and Clustering

Testing of larval length measurements with the Local Anselin Moran's I Clusters and Outliers tool found significant clusters of smaller sized *A. rostrata* and *A. anguilla*

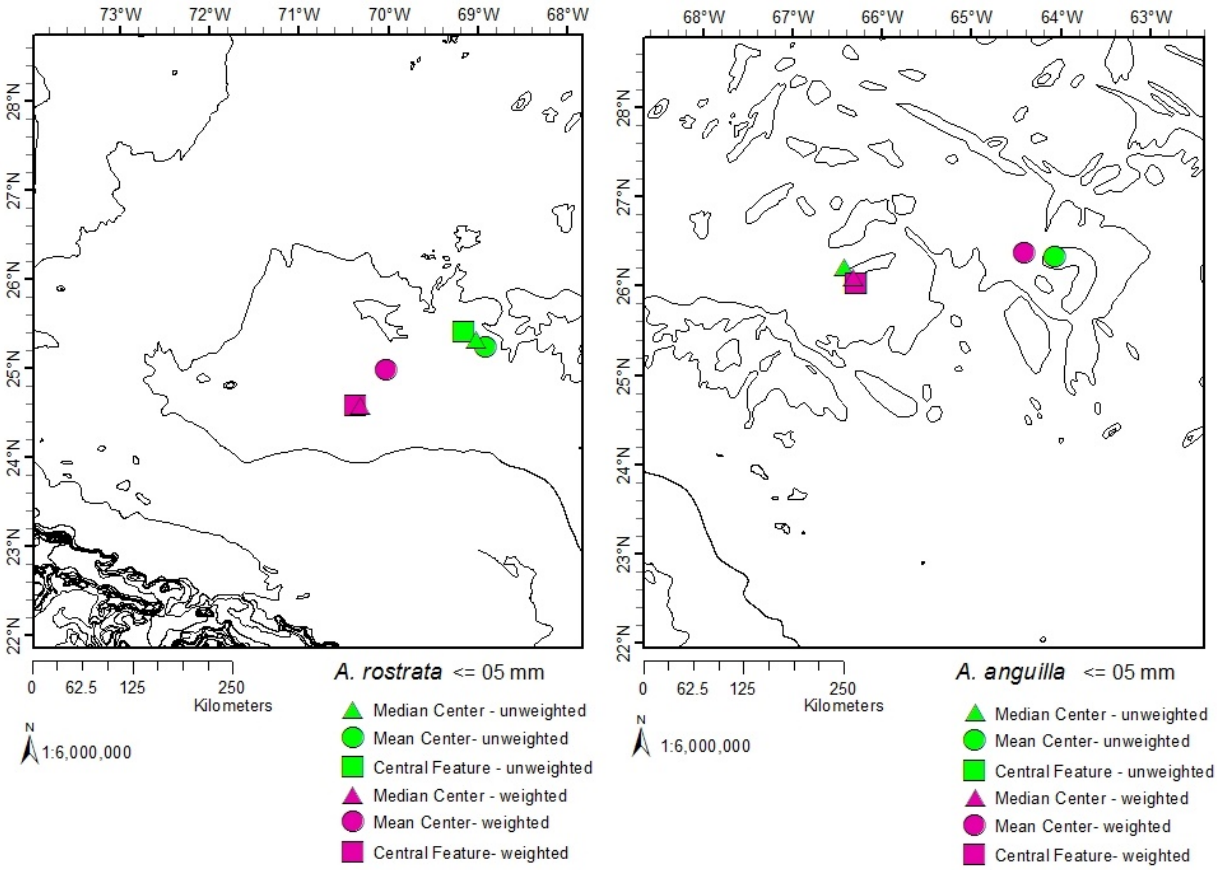

Figure 22. Comparison of weighted and unweighted geographic centers. The central measurements of ≤ 5 mm size groups of *A. rostrata* (left) and *A. anguilla* (right) when weighted by counts (magenta) and unweighted (green).

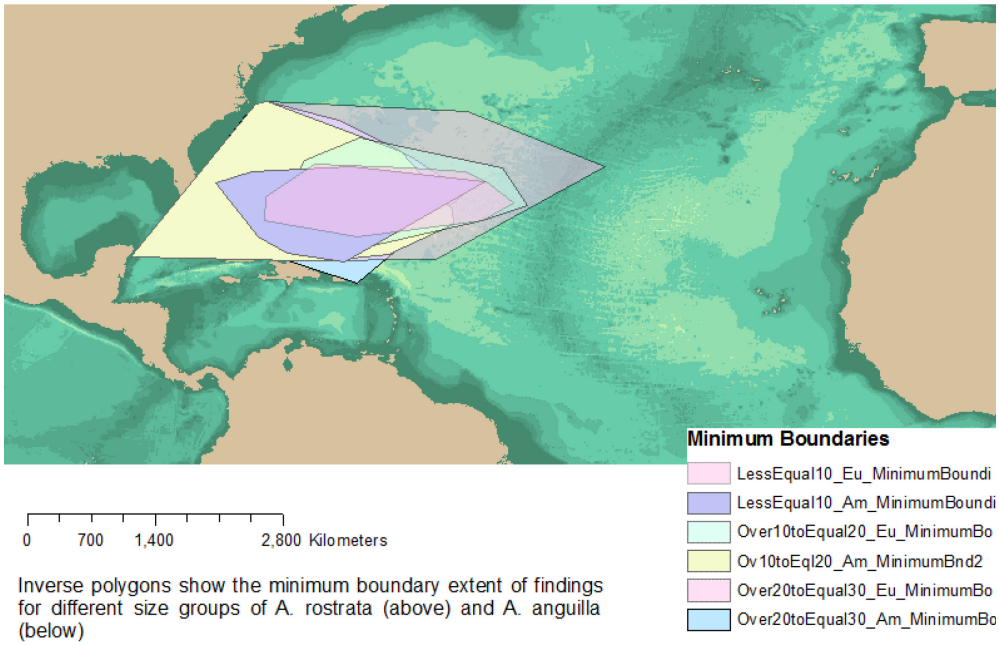

Figure 23. Minimum boundary areas. The minimum boundary extent convex polygons of 10 mm increments larvae sizes up to 30 mm were used to create Study Area 1.

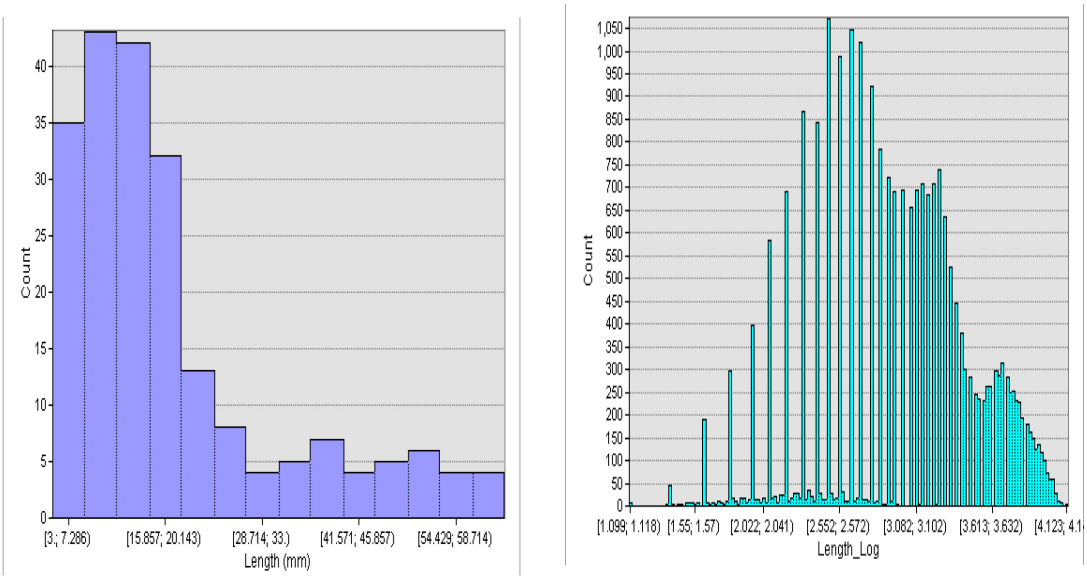

Figure 24. Length histograms (Study Area 1). Untransformed (left) and log (ln) transformed (right) larval length distributions in the study area based on the extent of ≤ 30 mm larvae.

Table 4. Average nearest neighbor analysis (Study Area 1).

Feature	Area (km^2)	Observed (km)	Expected (km)	NNI	*z*-score	*p*-value
All Stations	13,257,399	22.7	48.2	0.47	-38.17	< .001
Null Station	13,257,399	26.9	77.8	0.35	-29.29	< .001
Positive Station	13,257,399	30.2	61.3	0.49	-28.84	< .001
A. rostrata	13,257,399	30.6	74.2	0.41	-27.56	< .001
A. anguilla	13,257,399	37.6	76.9	0.49	-23.13	< .001
Weighted larvae counts	13,257,399	0.4	11.3	0.04	-296.02	< .001
Length Incidents (Am)	13,257,399	2.6	33.8	0.08	-95.23	< .001
Length Incidents (Eu)	13,257,399	2.0	31.2	0.06	-104.47	< .001

Average nearest neighbors for Study Area 1 for all stations, null and positive stations, and the two Atlantic species. These analyses showed a non-random distribution within the 13,257,399 km^2 area. Negative *z*-scores (an indication of clustering) were even greater when geographic locations were weighted by larval counts or length frequencies as these resulted in station locations being counted as their own neighbors.

larvae south of Bermuda in the central part of the study area (Figure 25). Significant clusters of larger larvae extended from the Sargasso Sea to mid-latitudes. These clusters of larger larvae formed around the periphery of smaller larvae and extended west and north towards the continental shelf and Gulf Stream, north of Bermuda, and moving away from the North American continent to the northeast.

Small Larval Scale

A second and smaller study area was created to examine the area of newly hatched larvae at a closer scale. This second area was formed by creating convex polygons around the minimum area occupied by larvae ≤ 10 mm in length and then fit within a rectangle and buffered by a distance of 250 km (Figure 26). The resulting rectangle encompassed an area of 5,823,306 km^2 and contained 1116 stations sampled between years 1862 and 2007 (Figure 27). The distribution included 668 positive stations and 448 null stations.

Larval lengths within the boundaries of this area ranged from 3 to 60 mm with a mean length of 20.7 mm (*SD* = 10.9 mm). Measured lengths of American eel (*n* = 8,185) ranged from 3 to 60 mm with a mean of 23.2 mm (*SD* = 13.3 mm). Lengths of European eels (n = 13,815) ranged from 3 to 55 mm with a mean length of 19.2 mm (*SD* = 8.8 mm). Length distributions and their transformed logs (ln) are shown in Figure 28.

The nearest neighbor index for the distribution of sampling stations, null and positive stations, *A. rostrata* and *A. anguilla*, and the ≤ 10 mm size groups of both species all indicated significant spatial clustering ($p < .001$) within this study area (Table 5). *A. rostrata* ($z = -22.77$) showed greater clustering than *A. anguilla* ($z = -17.32$).

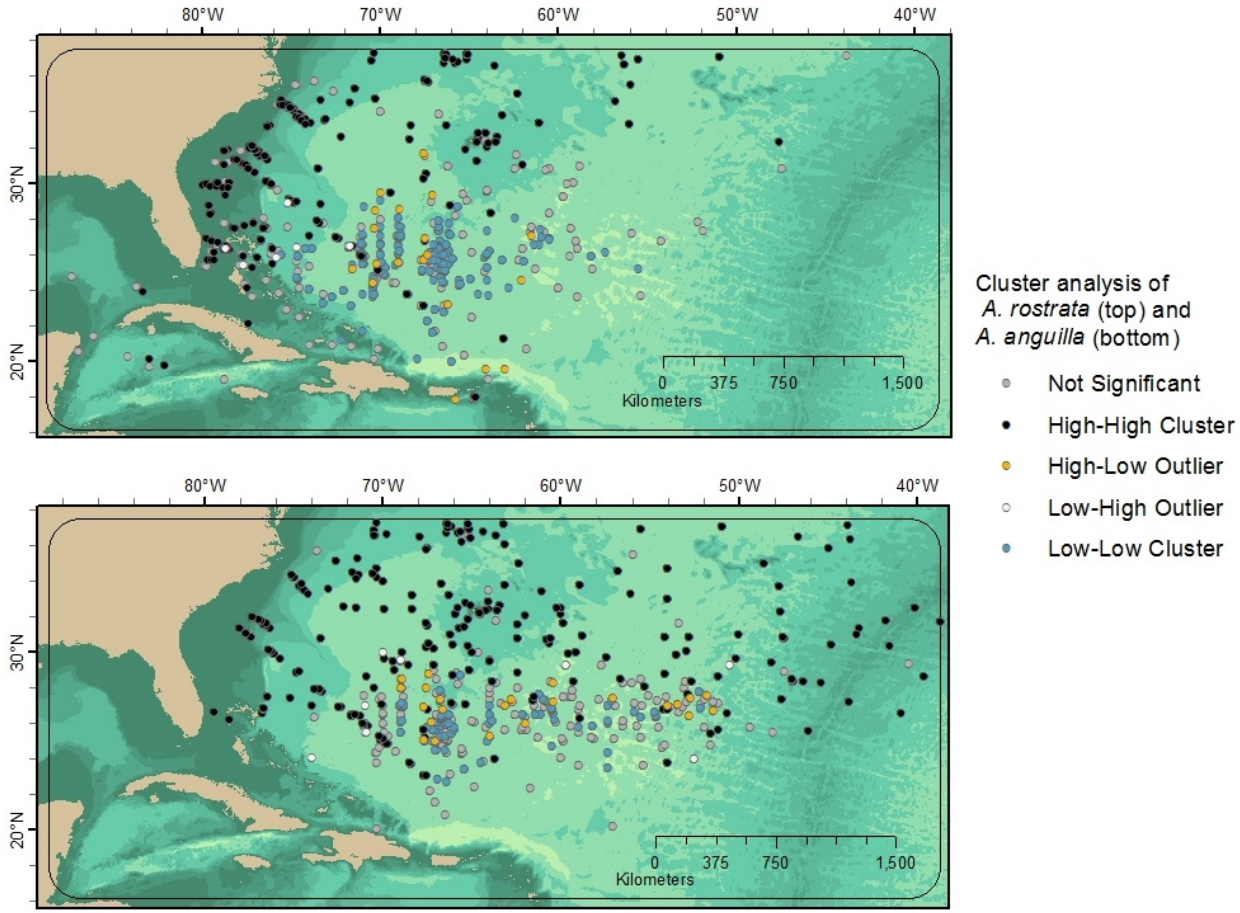

Figure 25. Clustering and outliers by species (Study Area 1). Clusters and outliers of *A. rostrata* (top) and *A. anguilla* (bottom) with clusters of larger larvae (black) and smaller larvae (blue). Large sized outliers in clusters of small larvae ("high-low") are yellow and small sized outliers in clusters of large sizes ("low-high") are white. Insignificant clusters are in gray.

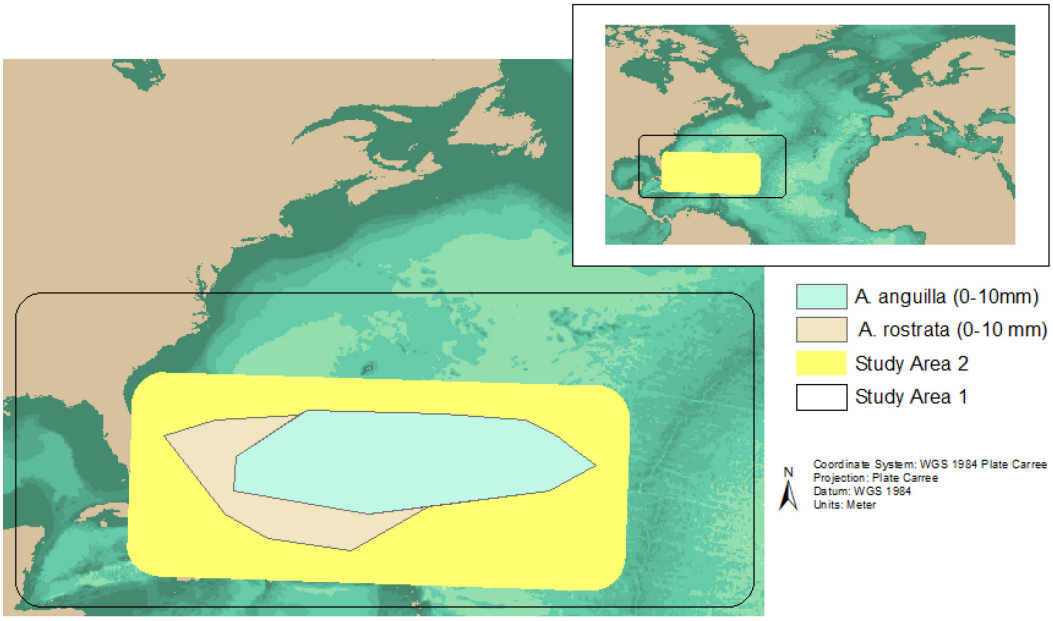

Figure 26. Study Area 2. The second study area was formed by creating a 250 km buffer around two convex polygons representing the minimum boundary area of small *A. rostrata* and *A. anguilla* leptocephali (≤ 10 mm).

This difference between species was not evident in distributions of small larvae (≤ 10 mm), where *A. rostrata* (*z*-score =-15.28) and *A. anguilla* (*z* =-16.40) showed more similar levels of clustering.

The results of the multidistance spatial autocorrelation of larval distribution reconfirmed that of the larger area (Table 6). Patterns of spatial dependency for *A. anguilla* were best discerned at a distance of 420 km for the European eel and 1000 km for American eel (Figure 29). Stations with overlapping species spatial dependency patterns peaked at a distance of 880 km.

The Ripley's K test showed that small (≤ 10 mm) *A. rostrata* larvae exhibited

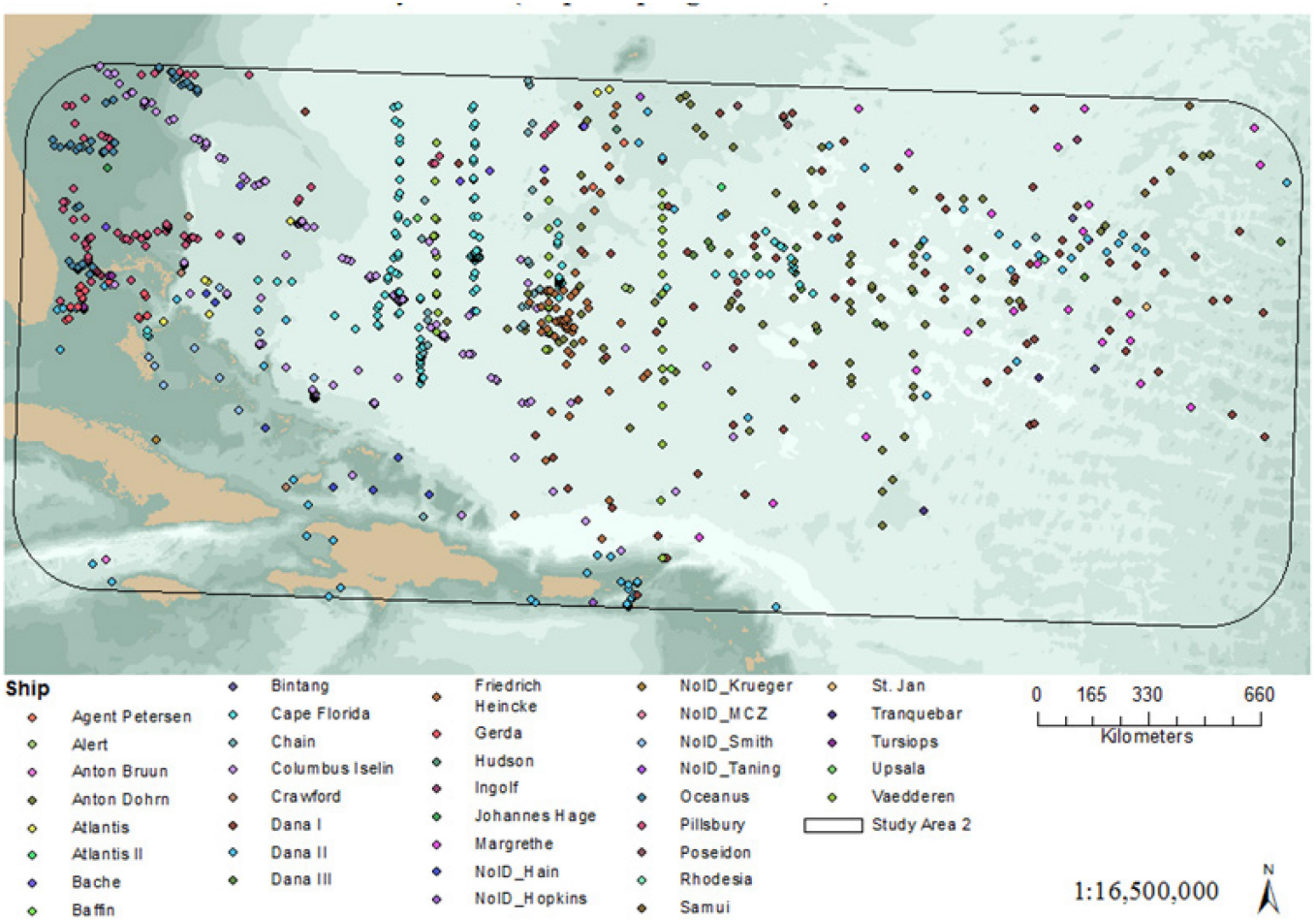

Figure 27. Ships and their sampling locations in Study Area 2. There were 1116 ship sampling stations in the second study area.

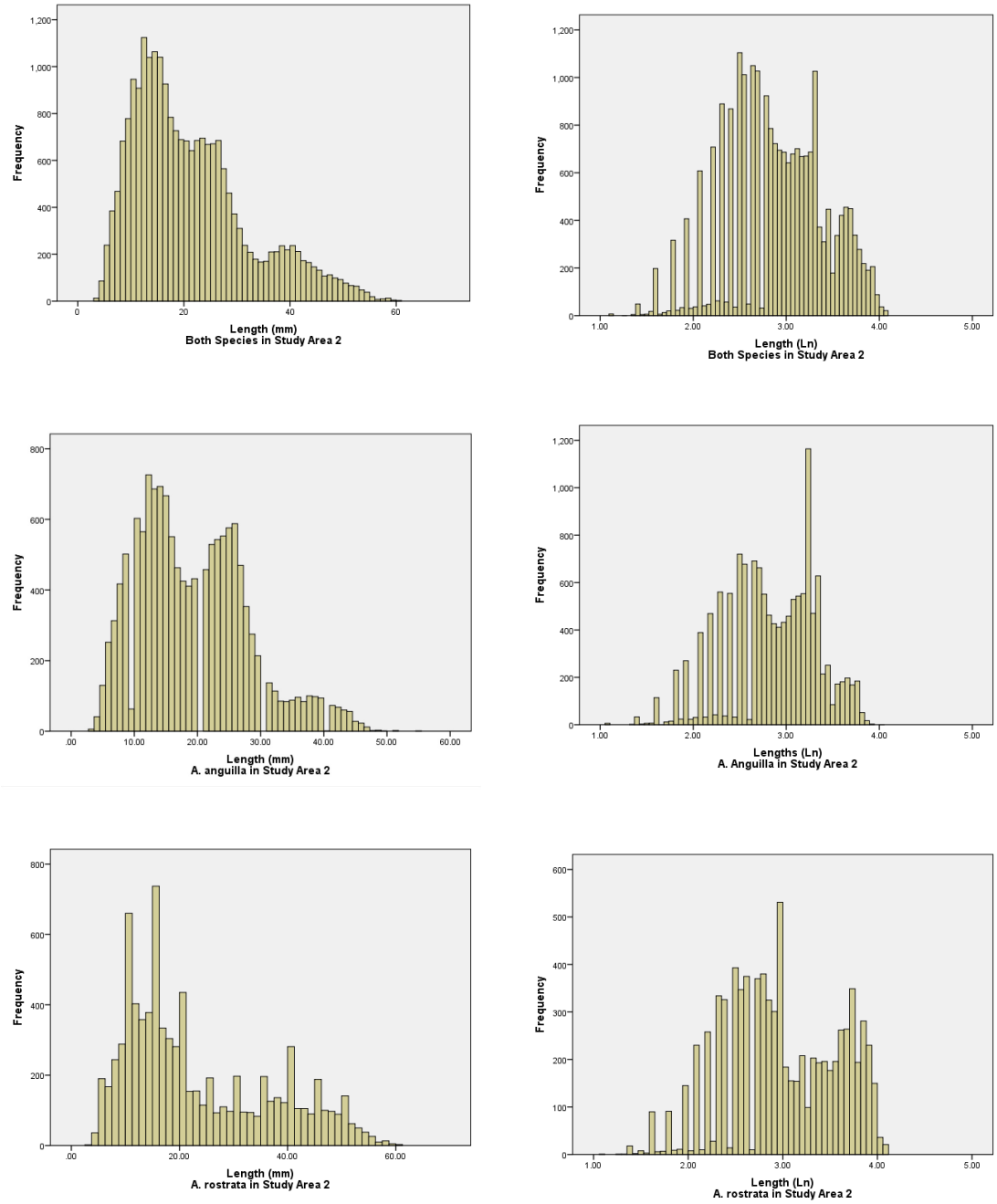

Figure 28. Length distributions and their logs (ln) (Study Area 2). Histograms of the length (mm) distributions (right) and their natural logs (left) for both species (top), *A. anguilla* (middle) and *A. rostrata* (below). The study area was defined by a 200 km buffered around the minimum extent of larvae ≤ 10 mm.

Table 5. Average nearest neighbor analysis (Study Area 2).

Feature	Area (km^2)	Observed (km)	Expected (km)	NNI	*z*-score	*p*-value
All Stations	5,823,306	19.3	36.1	0.53	-29.84	< .001
Null Station	5,823,306	23.9	57.0	0.42	-23.53	< .001
Positive Station	5,823,306	26.1	46.7	0.56	-21.77	< .001
A. rostrata	5,823,306	25.2	54.2	0.47	-22.77	< .001
A. anguilla	5,823,306	33.0	60.0	0.55	-17.32	< .001
≤ 10 mm (*A. rostrata*)	5,823,306	37.1	85.5	0.43	-15.28	< .001
≤ 10 mm (*A. anguilla*)	5,823,306	34.1	82.7	0.41	-16.40	< .001
≤ 10 mm (both species)	5,823,306	33.1	73.0	0.45	-17.27	< .001
Length Incidents (Am)	5,823,306	11.7	23.9	0.07	-89.76	< .001
Length Incidents (Eu)	5,823,306	1.4	22.5	0.06	-96.04	< .001

Average nearest neighbor analysis for Study Area 2 (5,823,306 km^2) indicated highly probable clustering (< .001) for parameters: all, null and positive stations the two Atlantic species, ≤ 10 mm size groups, and when weighted by length frequencies.

Table 6. Multi-distance spatial autocorrelation analysis (Study Area 2).

Feature	Attribute Tested	Start distance (km)	Increments (km)	Peak variance (km)	*z*-score	*p*-value
A. rostrata	length	300	20	560	554.33	< .001
A. rostrata	length	300	20	800	554.33	< .001
A. rostrata	length	500	200	1000	563.4	< .001
A. anguilla	length	300	200	420	203.3	< .001
A. anguilla	length	5	20	445	201.8	< .001
Overlap Stations*	length (min)	30	50	880	54.42	< .001
Overlap Stations*	length	30	50	1030	55.53	< .001

* removing 2 outliers)

The above table shows inputs for the multi-distance spatial autocorrelation analysis. Inputs were features and attributes tested, starting distance and increments. Results are the peak variance, *z*-score and *p*-values.

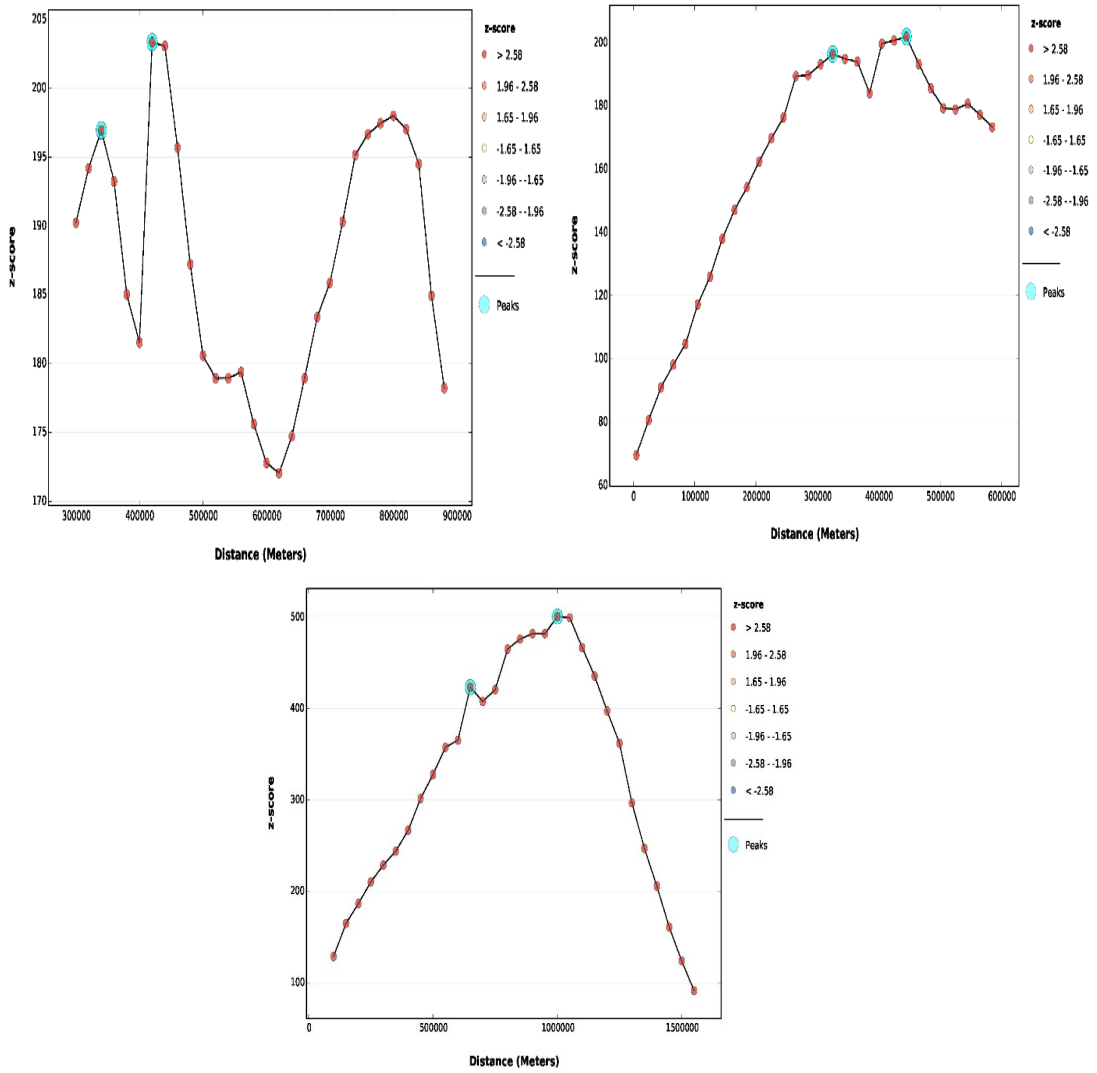

Figure 29. Spatial autocorrelation of *A. anguilla* and *A. rostrata* by distance. Graph shows probabilities of clustering or dispersal based on peak *z*-scores (blue circles) at incremental distances (m). Spatial dependency peaked for *A. anguilla* (top left and top right) at 420 km. The first peak of 34 km had no neighbors at that distance, invalidating that result. The comparison of analyses for *A. anguilla* shows the importance of scale in spatial analyses. *A. rostrata* (below) peaked at 650 km and 1,000 km, but because features at distances below 650 km had no nearest neighbor that first result was unreliable.

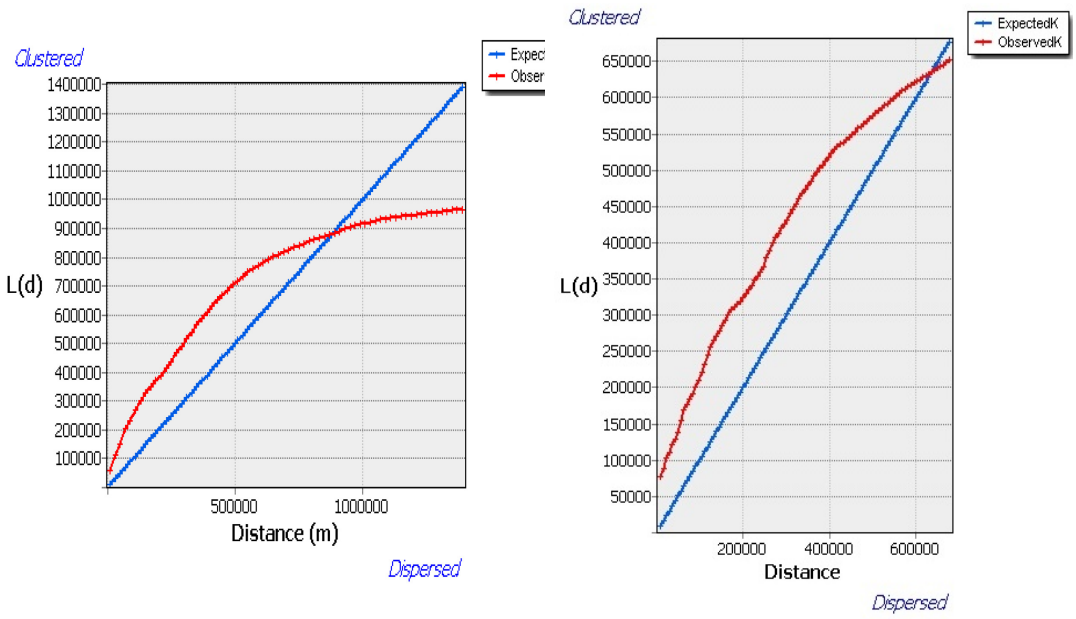

Figure 30. Ripley's K function test for small (≤ 10 mm) larvae.Observed patterns of spatial distribution (red line) at a range of distances (m) are shown for *A. rostrata* (left) and *A. anguilla* (right). The observed pattern is clustered if it has a higher L(d) value than the expected random distribution (blue line) and dispersed when they have a lower L(d) value. The L(d) value, or K-function, calculates expected dispersal of a number of features in a function with distance.

peak clustering at a scale of 400 km and transitioned into a dispersal pattern at 890 km (Figure 30). Clustering of small (≤ 10 mm) *A. anguilla* peaked at 307 km and transitioned into dispersal at a scale of 676 km. Significant peaks at smaller scales were unreliable because nearest neighbors could not be found for features at those scales.

An initial analysis of the spatial distribution of locations where both species overlapped did not at first succeed due to the influence of spatial outliers. ArcGIS recommends consideration of outliers when building a weighted table matrix or running tools that are sensitive to distance, like the incremental spatial autocorrelation tool. Outliers here are defined as features whose nearest neighbor is greater than three standard

distances of the average nearest neighbor distance. To identify outliers, distances were measured between individual points and nearest neighbors using the ArcGIS Near tool and then compared to the average. The locations with overlapping species had a considerably higher nearest neighbor standard distance (202 km) than the average of 67 km. Two stations with both species were found to be outliers, one at 15.72 and the other 3.8 standard distances from its nearest neighbors. Once these outliers were removed, stations with both species showed a peak of spatial dependency at 880 km.

The local clustering pattern analyses of small larvae (≤ 10 mm) produced the same results as in the larger study area since both study areas contained the entire population. A hot spot Getis-Ord Gi* clustering analysis of larvae ≤ 10 mm using only positive stations was compared to an analysis that included both positive and null stations. The second analysis weighted stations with aggregated counts at positive locations and counted null stations as zero. The addition of the null stations increased the coverage of the analysis and did not contradict, but supported the results of the analysis using only positive stations (Figure 31). The results of the positive and null station cluster analysis for the ≤ 10 mm larvae were transformed into an interpolated raster chloropleth image showing predicted density values for both species of ≤ 10 mm larvae (Figure 32).

Central Tendencies and Bathymetric Reference Points

As previous analyses showed small larvae (≤ 10 mm) clustering south of Bermuda and over the Bermuda Rise, this area was examined more closely (Figure 33).
The literature search found two Deep Sea Drilling Project (DSDP) drill points (sites 417 and 418) in the vicinity of larval clustering. These drill sites provided useful reference

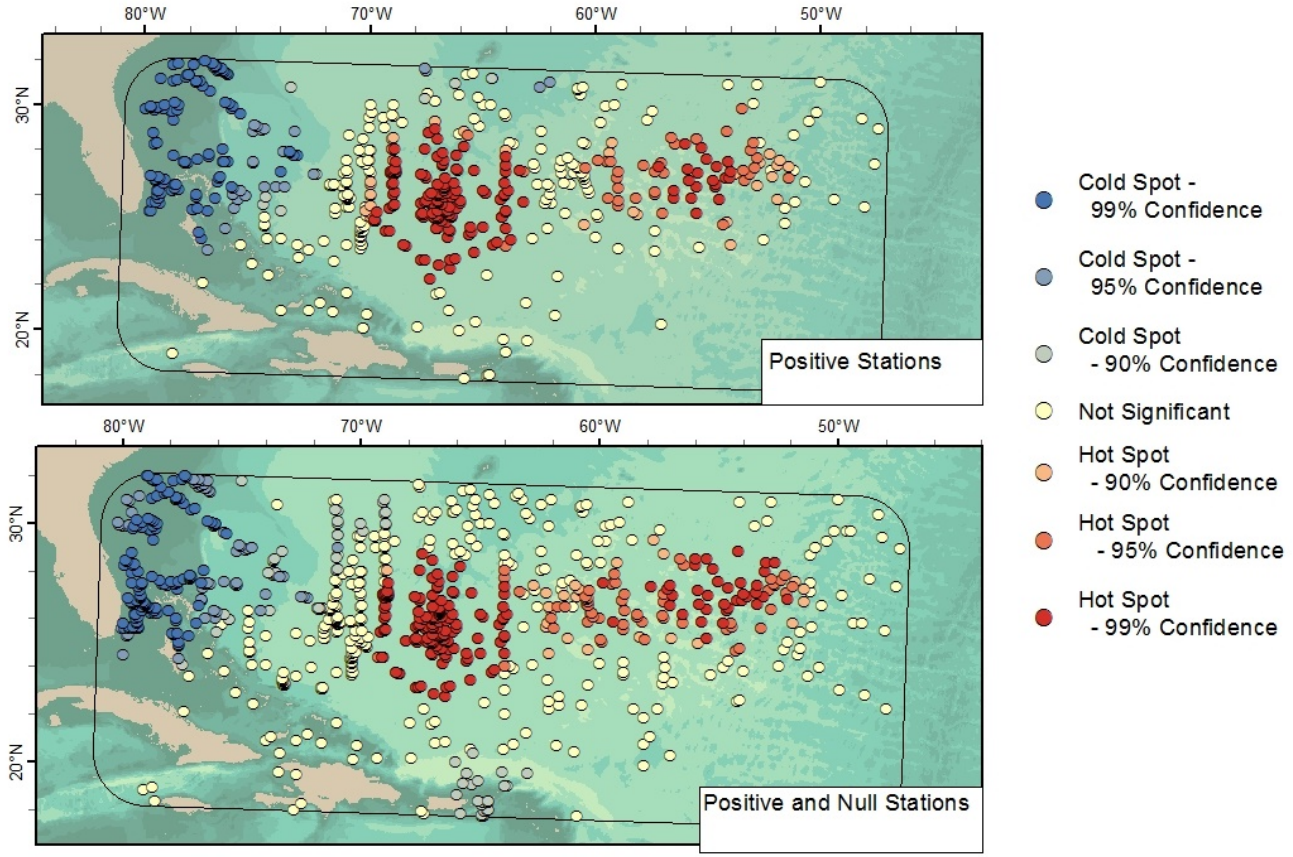

Figure 31. Comparison of ≤ 10 mm larval clusters using only positive vs. positive and null station data. The maps show 90%, 95% and 99% confidence intervals for clusters of high counts (red) and low counts (blue) of the ≤ 10 mm larvae. Top uses only observed larvae counts. The bottom map adds null data for greater coverage. Their results were consistent and with only slight differences.

F

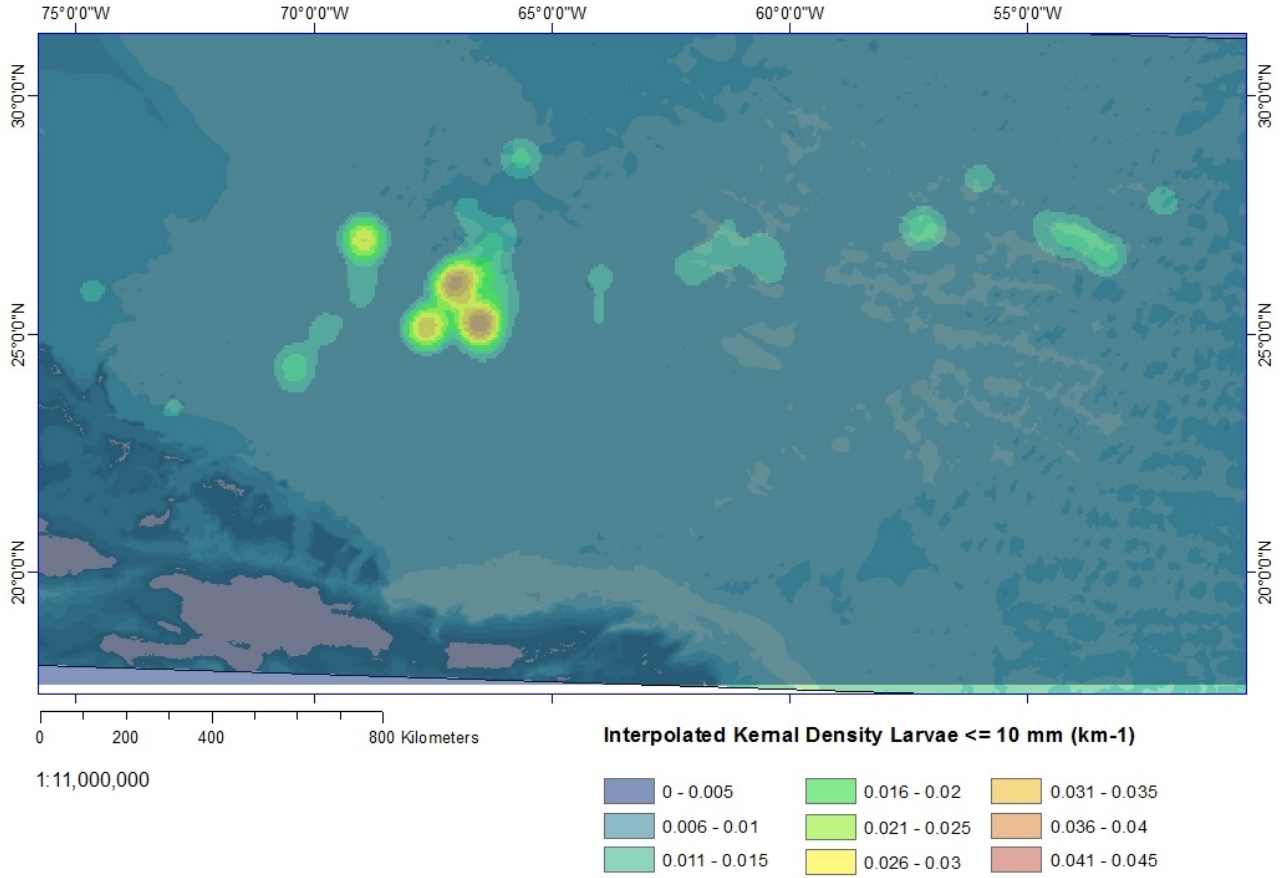

Figure 32. Interpolated kernel density Map for larvae ≤ 10 mm. The larvae densities for the study area were interpolated into a raster map showing predicted densities based on aggregated counts of the larvae in the ≤ 10 mm size group. Null stations and positive stations not finding larvae of that size where counted as zero. Density numbers are relative and not considered accurate.

points for the geographic measured centers of the small larvae (≤ 10 mm). The DSDP geological drilling sites were located on the southern end of the southwest Bermuda Rise and on the northern edge of the Vema gap (Swift, Bolmer, & Stephen, 1989). Their location had been purposefully sited on the M0 magnetic anomaly, a dated magnetic iscochron that extends on a northeast axis from the Antilles Outer Ridge, through the middle of the Vema Gap, and up the axis of the Bermuda Pedestal (Swift et al., 1989), as shown in Figure 34. The central measurements of *A. anguilla*, *A. rostrata*, and stations with both species are shown in Figure 35. The mean and median geographic centers and central feature of ≤ 10 mm size *A. rostrata* were all located within 16 km of one another, approximately 115 km to the northeast of the DSDP sites. The median and central feature of *A. anguilla* (≤ 10 mm) observations coincided within 26 km of each another, approximately 130 km from those of *A. rostrata* and 245 km east of the two DSDP sites. The mean center of the ≤ 10 mm *A. anguilla* was approximately 248 km farther east of the median, reflecting a larger spread compared to the ≤ 10 mm *A. rostrata*. The geographic median of stations finding an overlap of both species (≤ 10 mm) lay midway between the median of *A. rostrata* (≤ 10 mm), 59 km to the northwest, and the median of *A. anguilla* (≤ 10 mm), 81 km to the east. The central measurements of small *A. rostrata*, *A. anguilla*, and stations where they overlapped were located along a narrow latitudinal range that was 65 km wide, just over one arc minute between 25°37' N and 26°12" N. A greater longitudinal distance separated the means and medians of the two species and measured 390 km (from 67°15'W to 63°42'W) and 134 km respectively.

Depth

Bathymetric depth values were extracted from the GEBCO 2014 30-second arc grid to explore a possible spatial relationship with sampling locations. Depths in the study area descended to 7,123 meters with a minimum recorded depth of 2 m, not counting four unresolved data points above sea level (Figure 36). The mean depth of the sampling locations was 4342 m (*SD* = 1907 m). Shallow waters were along the southeast continental shelf of the United States and the Greater Antilles. Deeper depths occurred on the eastern side of the study area.

Depths at larval observation points were tested for spatial autocorrelation and spatial randomness (Figure 37). Significant clusters of *A. rostrata* at shallow depths followed the continental shelf from the northeast and south along the Greater Antilles. Significant clusters of *A. anguilla* in shallow depths occurred in the northeast corner of the study area along the continental shelf, north of the latitude of the southern tip of Florida (approximately 25° N). Deep water clusters of *A. rostrata* larvae had a greater latitudinal distribution (1,121 km) than those of *A. anguilla* (500 km). The deep water clusters of *A. anguilla* extended farther east towards the Mid-Atlantic Ridge.

Slope

Slope was calculated from the GEBCO_2014 raster data points using the ESRI Slope tool and then extracted to sampling locations. A kernel density map of larvae ≤ 10 mm was combined to that with points graduated by standard distance of slope (Figure 38). The result showed that slopes where small larvae concentrated were

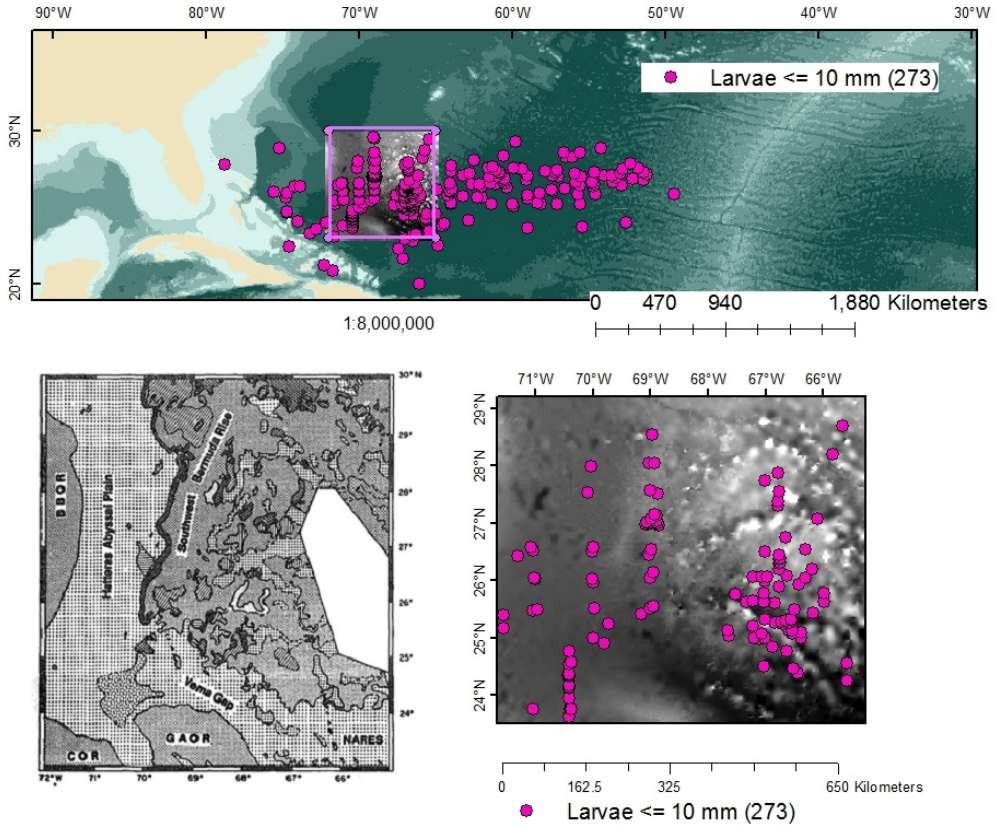

Figure 33. Vema Gap, southwest Bermuda Rise and Hatteras Abyssal Plain. Vema Gap, southwest Bermuda Rise and Hatteras Abyssal Plain (bottom left) from Driscoll & Laine (1976). The bottom right image is a closeup of the square in the top figure and shows the bottom of the Bermuda Rise, the Hatteras Abyssal Plain and entrance to the Vema Gap. The top image shows the distributions of small larvae (≤ 10 mm).

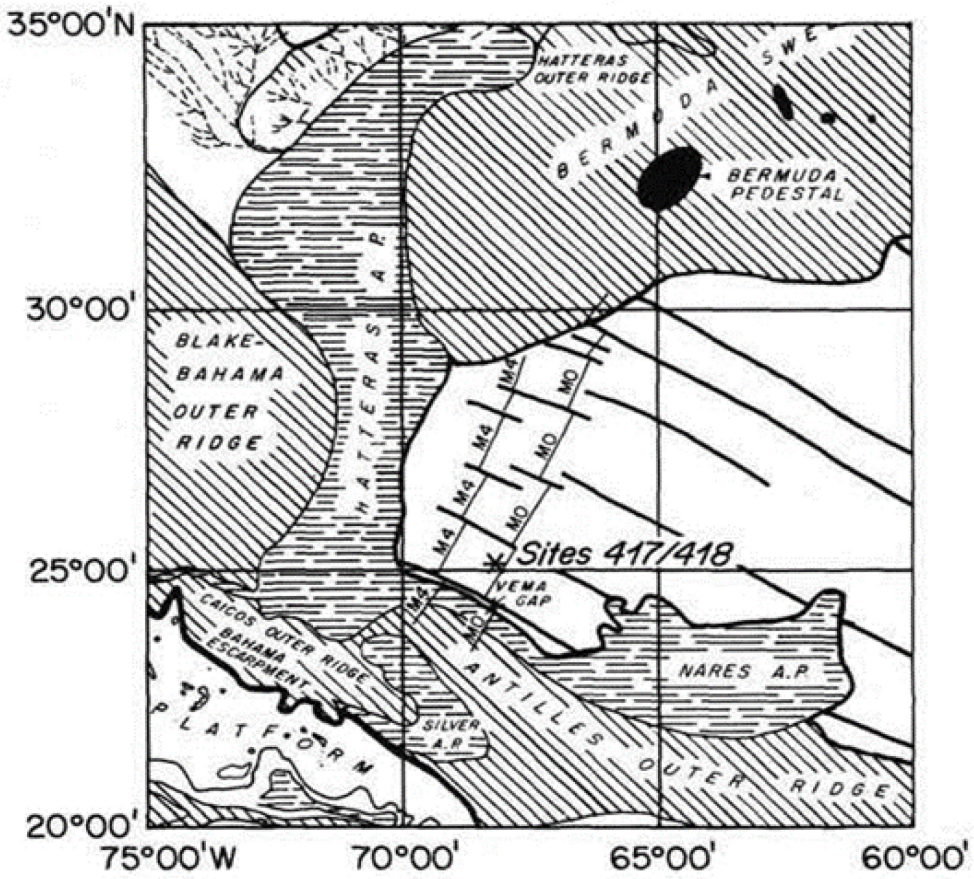

Figure 34. Deep Sea Drill Program (DSDP) Sites 417 and 418. Drill points 417 and 418 lie on the line of magnetic anomaly M0 on the edge of the Vema Gap. Other bathymetric features shown include the Hatteras and Nares Abyssal Pain, the Antilles Outer Ridge, Blake-Bahama Outer Ridge, Caicos Outer ridge and fracture zones. From: Emery and Uchupki in Senske & Stephen (1988).

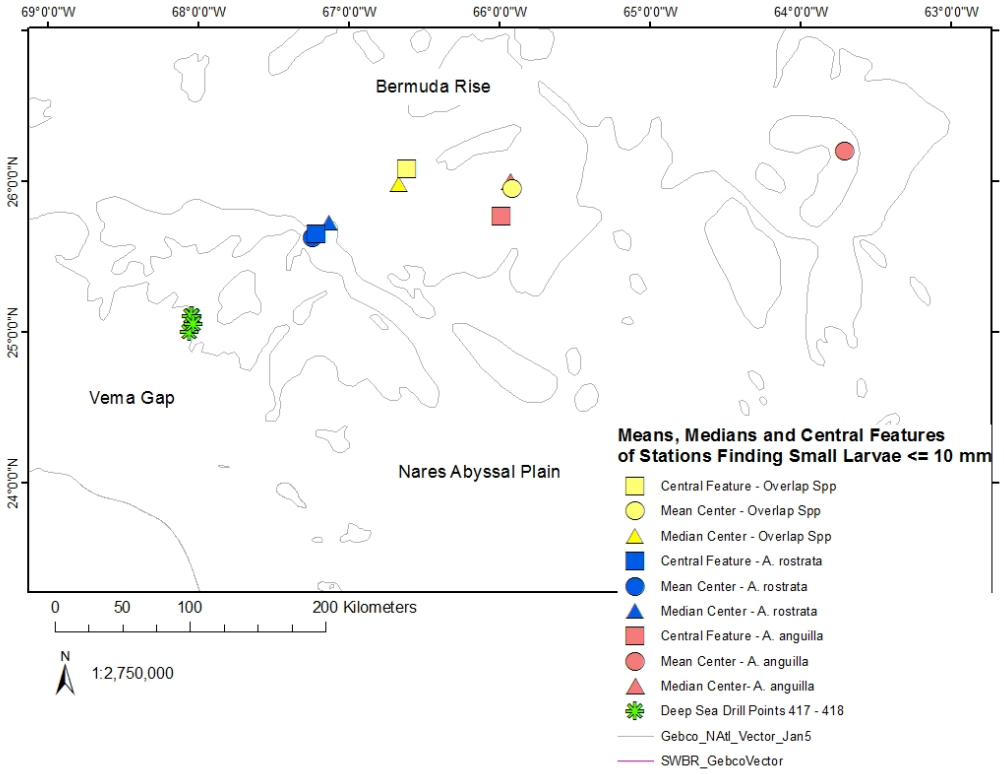

Figure 35. Geographic centers of ≤ 10 mm larvae and DSDP sites. The mean centers (circles), median centers (triangle) and central features (square) of *A. rostrata* (blue), *A. anguilla* (red) and stations where they have been found overlapping (yellow). The features are seen in reference to the DSDP drill sites (green asterisk). The geographic means occur across a narrow latitudinal range of 65 km between 25°37' N and 26°12" N and across a longitudinal range of 130 km between the medians of the two species.

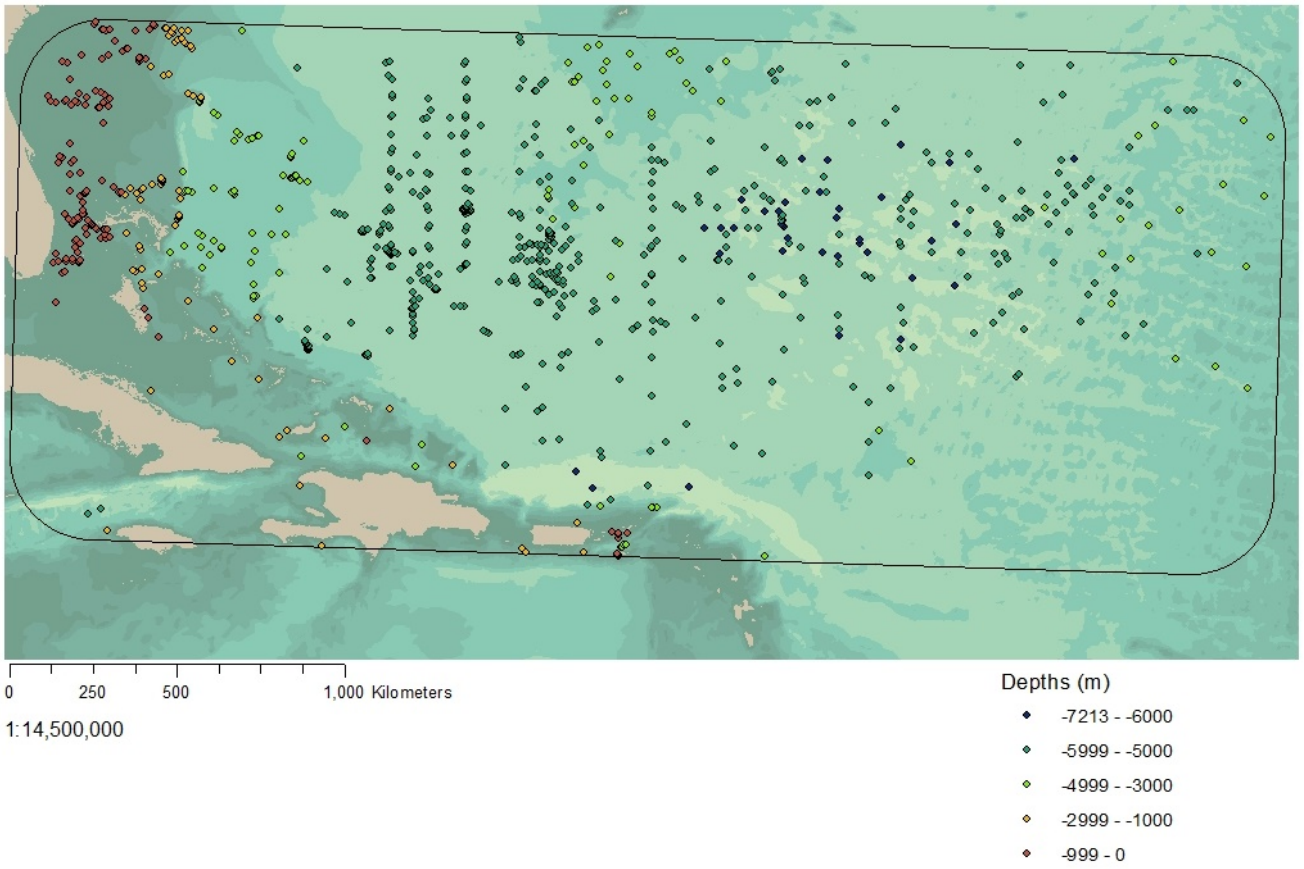

Figure 36. Bathymetric depths at sampling stations (Study Area 2).Depths at sampling stations are shown in a color scale marking 1000 m increments of depth, with red being sea-level to -999 m (red) and dark blue marking depths below 6,000 m to a maximum depth of 7,123 m. (dark blue).

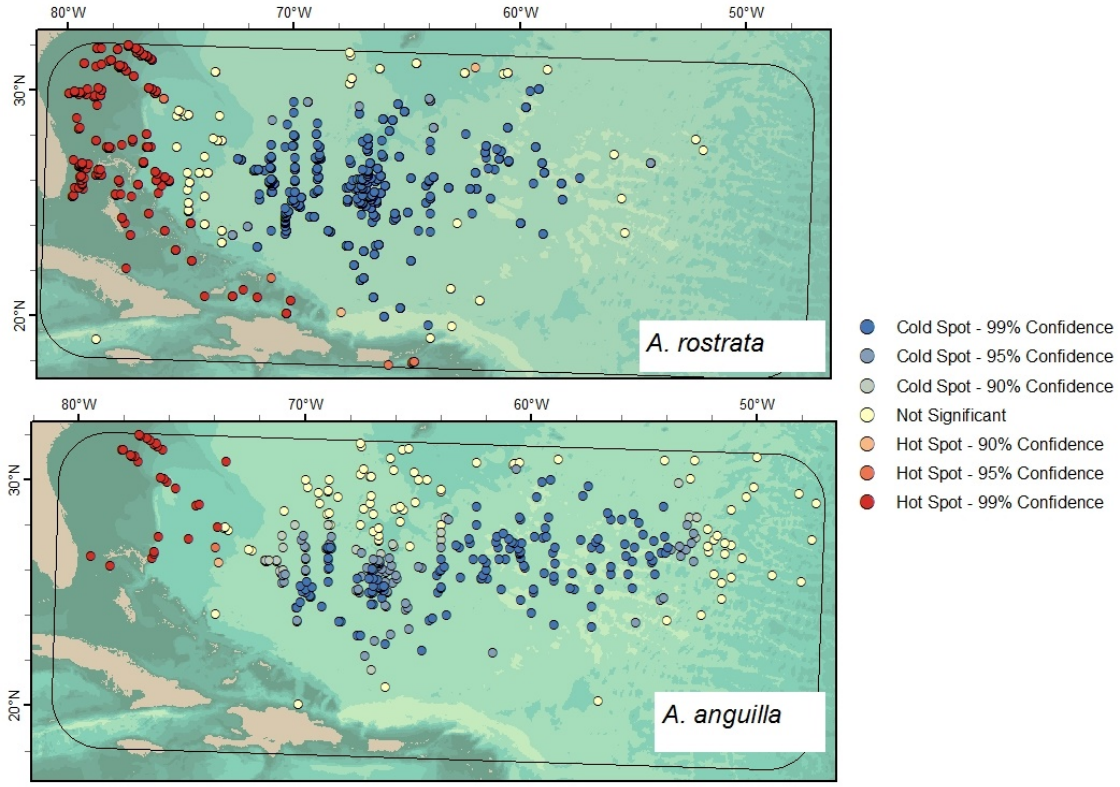

Figure 37. Hot spot analysis of larvae and depth. Confidence levels of larvae forming significant clusters in shallower than average (deepening shades of red) and deeper than average water (deepening shades of blue). Clusters that were non-significant to depth are shown in yellow.

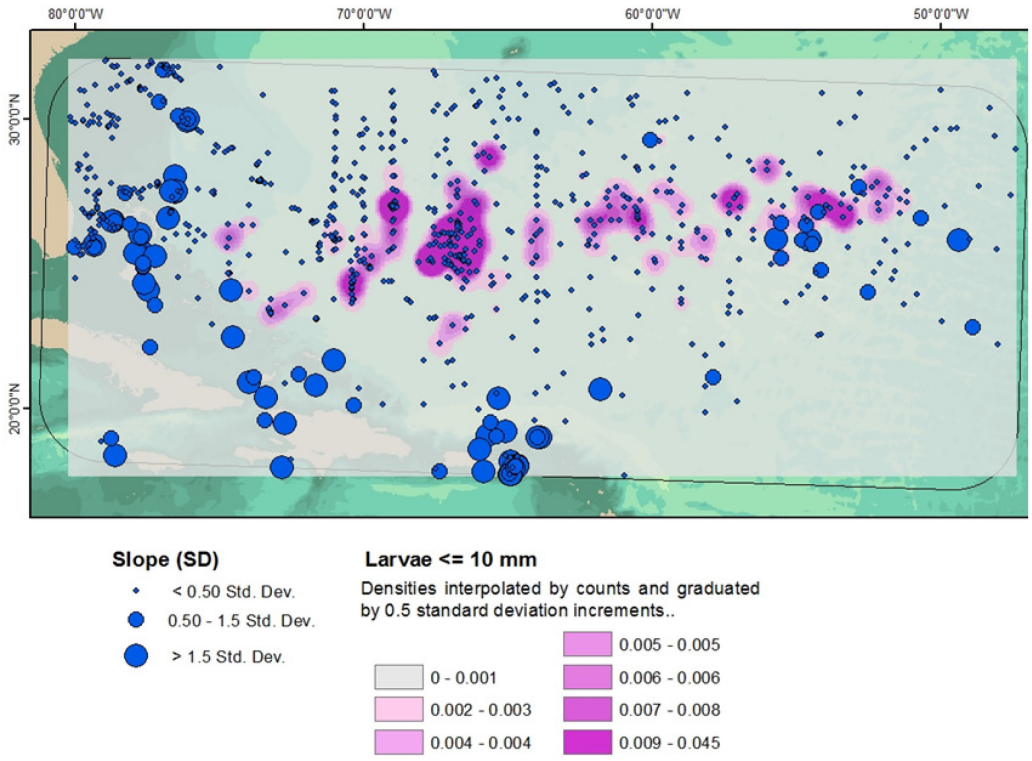

Figure 38. Slope and ≤ 10 mm larvae densities. Slope values were extracted to sampling locations and are shown here (blue) in relation to predicted densities of small larvae (≤ 10 mm) interpolated from their counts and hot spot analysis (pink).

generally insignificant, within one half a standard deviation of the sampling mean slope of 0.94° (*SD* = 2.45°). Across the entire study area, which also contained land, the maximum slope was 42.3° and the minimum was a fraction over 0° (*M* = 1.15°, *SD* = 2.3°).

Geomagnetic Intensity

After downloading the EMAG2 grid of geomagnetic anomalies of the Earth's crust (Figure 39), values of magnetic intensity were extracted at the points of larvae sampling locations (Figure 40). The distribution of crustal geomagnetic intensities were then analyzed with the Anselin Local Moran's I and Getis-Ord Gi* tools for non-random local patterns in relation to the locations of larvae ≤ 10 mm in length. The results were influenced by what spatial concept was chosen for the analysis. Both an inverse distance and a fixed band spatial conceptualization were used. With an inverse band concept all features exert an influence on one another that diminishes with distance, whereas the fixed band concept (recommended by ESRI for clustering analyses) only considers the influence of features within a "moving widow" based on a specified distance. The inverse distance spatial conceptualization analysis returned insignificant confidence levels for spatial patterns of *A. rostrata*, except for two small clusters (low intensity, and high-low outlier) off the coast of the Bahamas (Figure 41). Small clusters of *A. anguilla* around high geomagnetic intensities were scattered on a vertical axis south of Bermuda, while small clusters of low intensity were scattered throughout the small larval distribution, but without any visibly overriding pattern.

Using the fixed distance band concept for the hot spot and local clustering

analyses required inputs from the nearest neighbor average, Ripley K-function, and multi-distance spatial autocorrelation analyses in order to determine what size of moving window to apply. An additional analysis calculated the distance that would the features being analyzed give a number of 8 neighbors. The 8 neighbor distance for all larvae ≤ 10 mm ranged from 2.6 to 1572 km and averaged 109 km. These figures were used to create a spatial weight matrix for clustering analysis. The matrix applied a fixed distance band of 200 km to analyze local clustering of small larvae weighted by geomagnetic intensities of their location. The fixed distance analysis found larvae clustered significantly around higher than average magnetic intensities that ranged between -97.4 and 123.5 nT (M = 34.7 nT, SD = 45.4 nT). These clusters around high magnetic intensities occurred along a north–south axis (410 km long and 220 km wide) and approximately 500 km south–southwest of Bermuda (Figure 42). Small larvae (≤ 10 mm) also clustered significantly over lower than average magnetic intensities (from -129 to 30.6 nT; M = -35.5, SD = 38.7). These lower intensity clusters formed to the west of the high intensity clusters over an approximate 600 km latitudinal and 400 km longitudinal range. Smaller sized larvae (≤ 10 mm) appeared to cluster most prominently around above average high geomagnetic intensities than over lower than average intensities (Figure 42).

A Getis-Ord Gi* hot spot analysis of all larvae within the second study area, using a fixed distance spatial conception, found significant clusters (99% confidence level) of larval length distributions weighted by geomagnetic intensities in the central area of the Sargasso Sea (Figure 43). Both species showed a high confidence (99%) of clustering over higher than average magnetic intensities over the Bermuda Rise. Outside of this

highly visible cluster around the Bermuda Rise, larval patterns for *A. rostrata* were generally non-significant except for a few stations in the northeast corner of the study area and some low intensity clusters off the Greater Antilles. *A. anguilla* larvae showed a more varied contrast of highly significant (CI = 99%) clustering around high intensities southwest of Bermuda and low intensity clusters radiating to the west and northwest and to the east.

Separate Getis-Ord Gi* hot spot analyses found that small larvae (≤ 10 mm) of both species formed a hot spot over high geomagnetic intensities around the Bermuda Rise (Figure 44). While small *A. rostrata* larvae clustering was limited to the high intensities around the Bermuda Rise, small *A. anguilla* (≤ 10 mm) also formed a cluster around an area of lower than average intensities approximately 250 km farther to the east.

Magnetic Gradient

Magnetic intensities were converted from the EMAG2 grid into gradients using the ESRI Slope tool. Gradients were then extracted to sampling locations as degrees. Neither the Getis-Ord GI* or Local Moran's I spatial pattern analyses demonstrated significant local clustering of small larvae along either steep or low magnetic gradients. However, as is shown in Figure 45, high densities of ≤ 10 mm larvae were on either side of a high gradient band running through their midst. Although small *A. anguilla* (≤ 10 mm) were observed on either side of the high gradient band, newly hatched (≤ 5 mm) *A. anguilla* were found almost exclusively to its east (Figure 46). Newly hatched *A. rostrata* (≤ 5 mm) occurred on either side of the high magnetic gradient band, although the mean and median centers of their geographic distributions were positioned

just to its west. Central measurements (mean, median, central feature) of newly hatched ≤5 mm larvae were found on either side of from 150 to 190 km wide band. However, no sampling data were available from inside the magnetic gradient band itself.

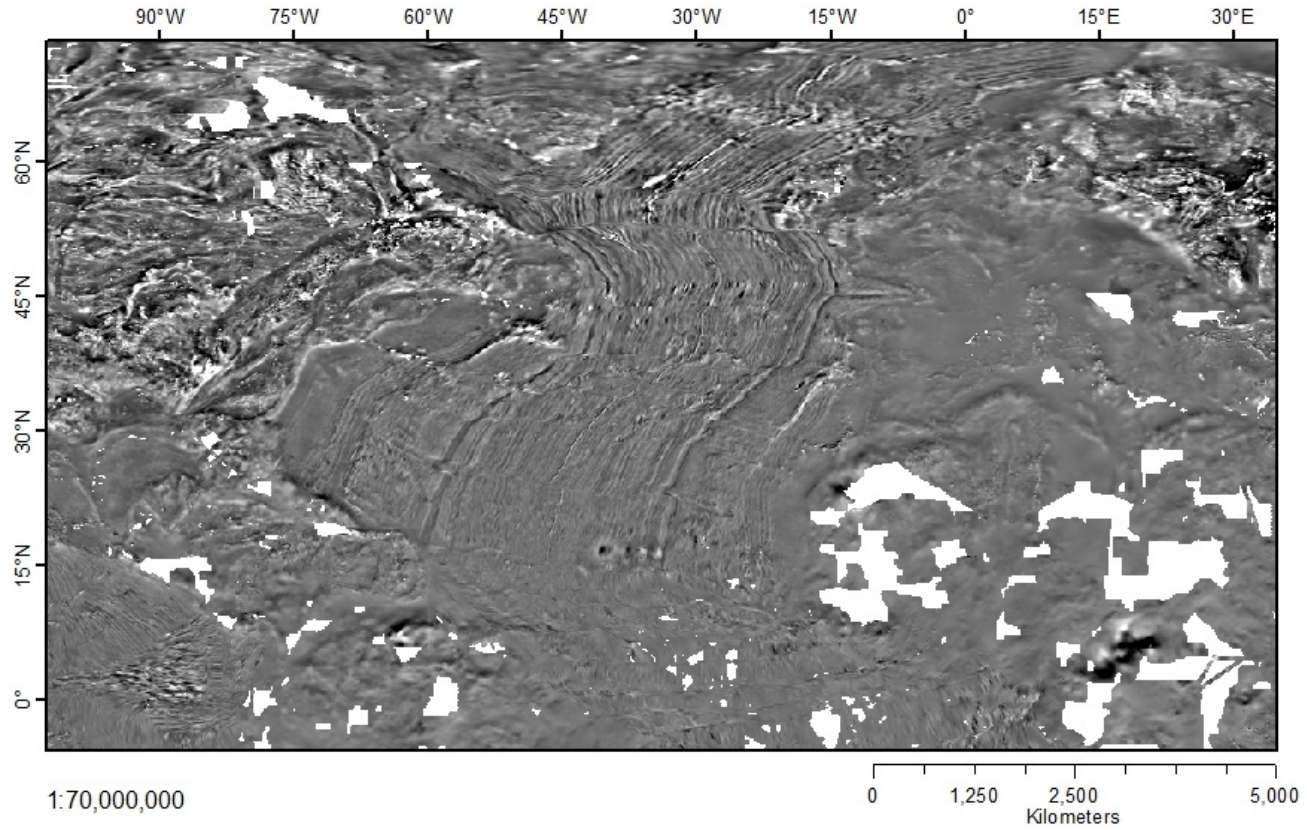

Figure 39. Magnetic anomalies in the North Atlantic Ocean. Magnetic anomalies of the North Atlantic Ocean from the EMAG 2-arc minute magnetic anomaly grid.

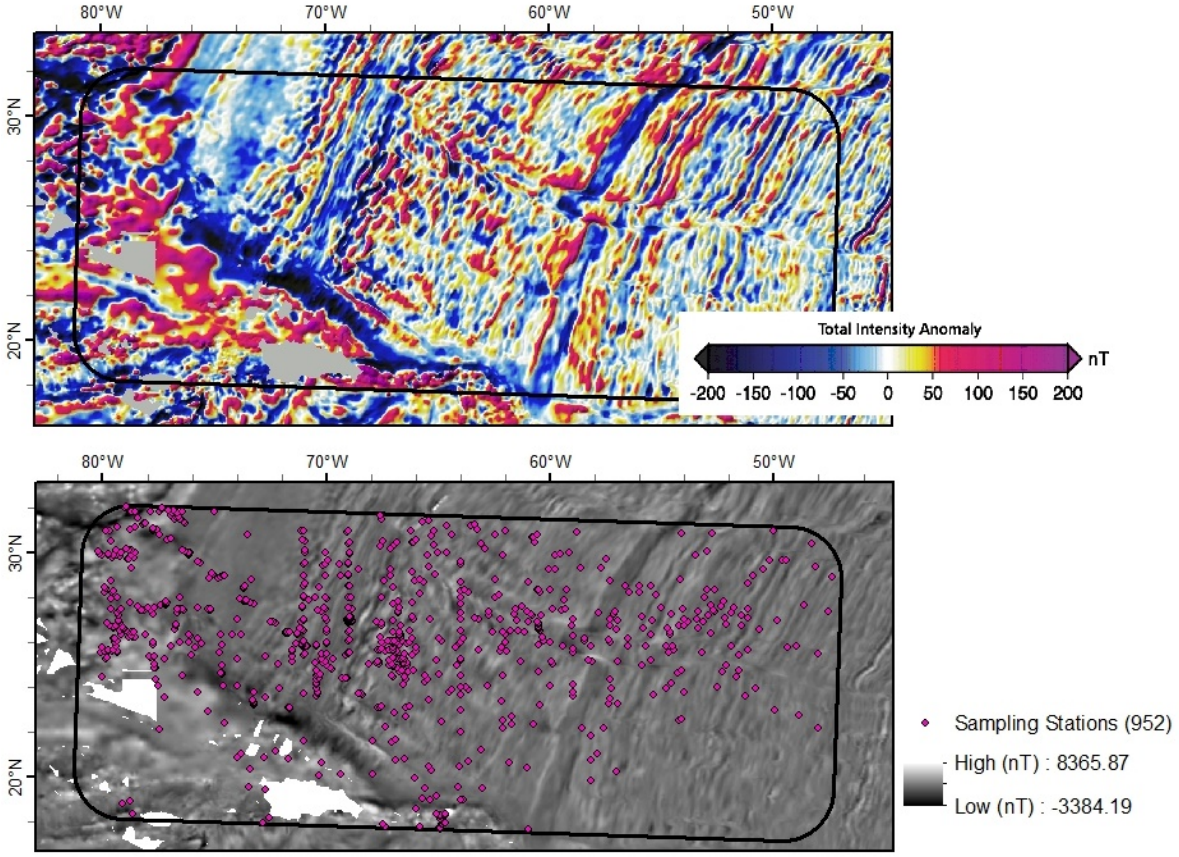

Figure 40. Magnetic anomalies and sampling locations (Study Area 2). The intensities (nT) of the crustal magnetic anomalies in color show the striped patterns and variation on the ocean floor (above). The distribution of sampling locations are visualized across a gray scale crustal magnetic anomaly map (below).

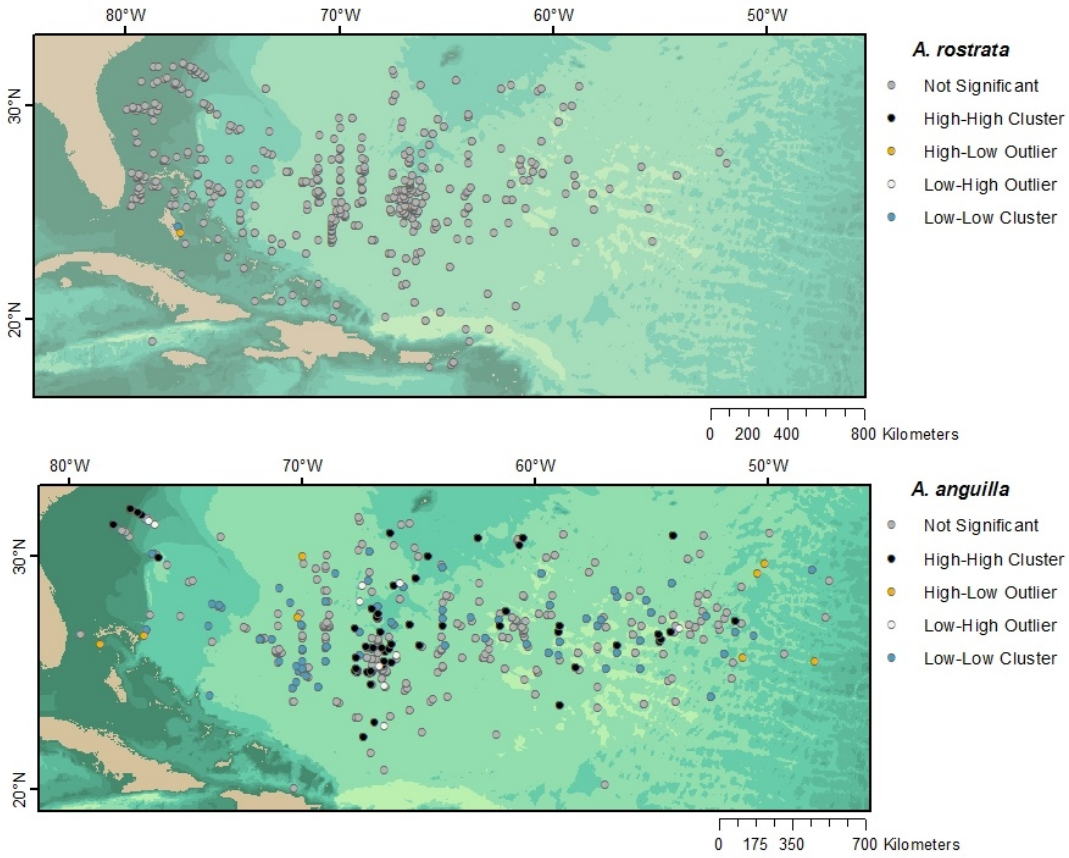

Figure 41. Clustering over geomagnetic intensities (Inverse Distance Spatial Conceptualization). Results of Anselin Local Moran's I clustering and outlier analysis showing larval clusters over higher than average magnetic intensities (black), lower than average magnetic intensities (blue), high intensity outliers near low intensity clusters ("high-low" in yellow), and low intensity outliers near high intensity clusters ("low-high" in white). Insignificant clusters are shown in gray. This model tested the larval distribution with an inverse distance spatial conceptualization.

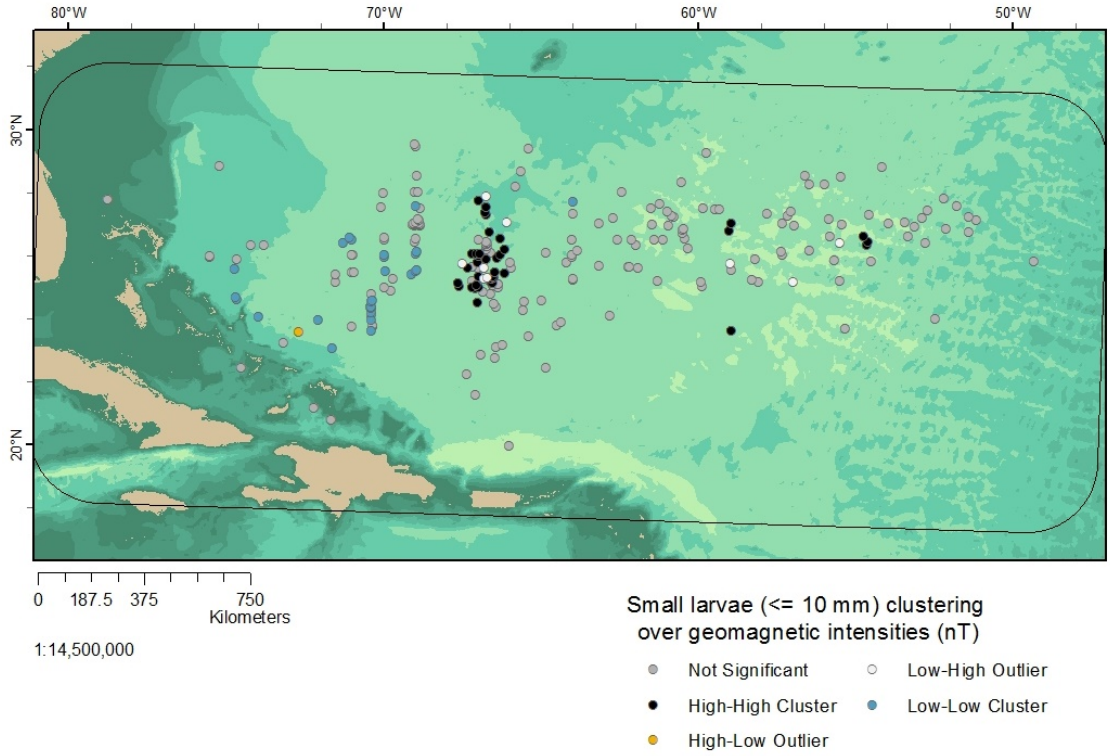

Figure 42. Geomagnetic intensities at locations of small larvae ≤ 10 mm (Fixed Band Spatial Conceptualization). Clustering of small larvae (both species) over higher than average magnetic intensities (black), lower than average magnetic intensities (blue), high intensity outliers near low intensity clusters ("high-low" in yellow), and low intensity outliers near high intensity clusters ("low-high" in white). Insignificant clusters are shown in gray. Numerous high intensity clusters occurred 500 km to the south–southwest of Bermuda. Clustering over lower than average intensities occurred to the west. This model applied a fixed band spatial conceptualization.

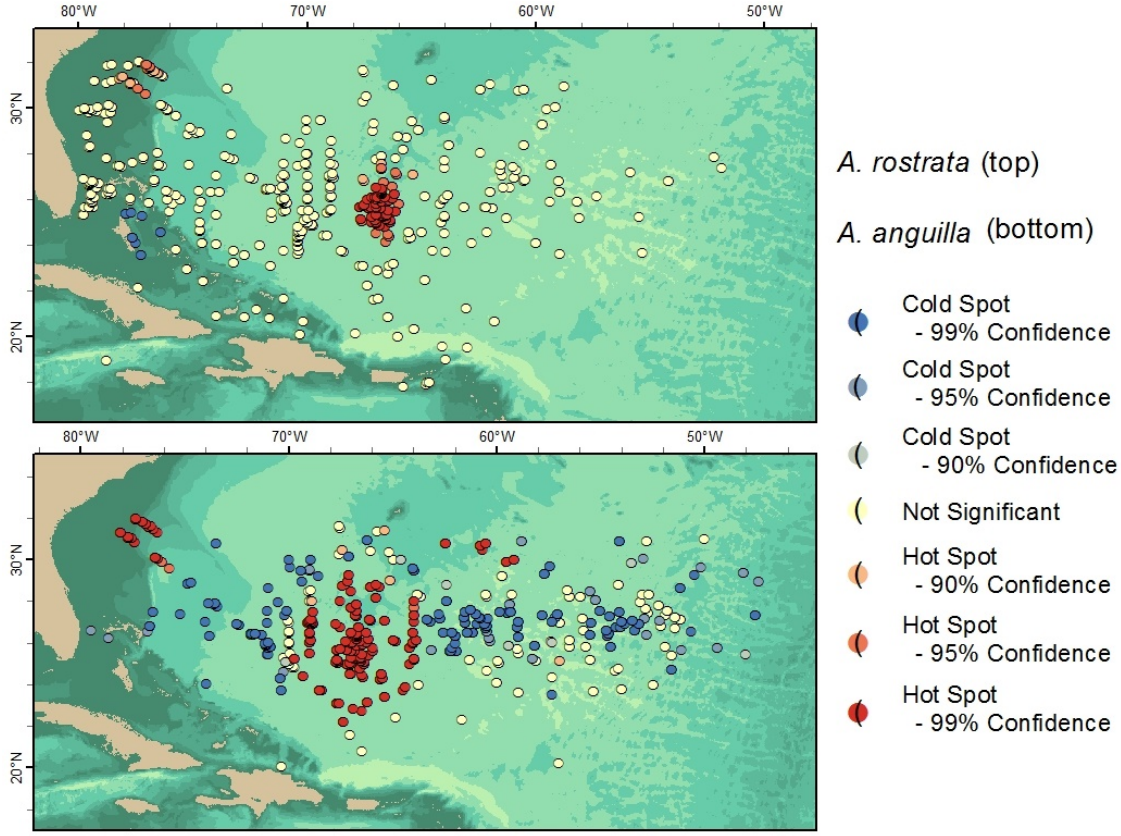

Figure 43. Hot spots of larvae clustered around crustal geomagnetic intensities. The map shows confidence intervals for the non-randomness of larvae (all sizes in the study area) clustering around above average (deepening shades of red) and below average (deepening shades of blue) for all larvae in the second study area. This model applied a fixed band spatial conceptualization.

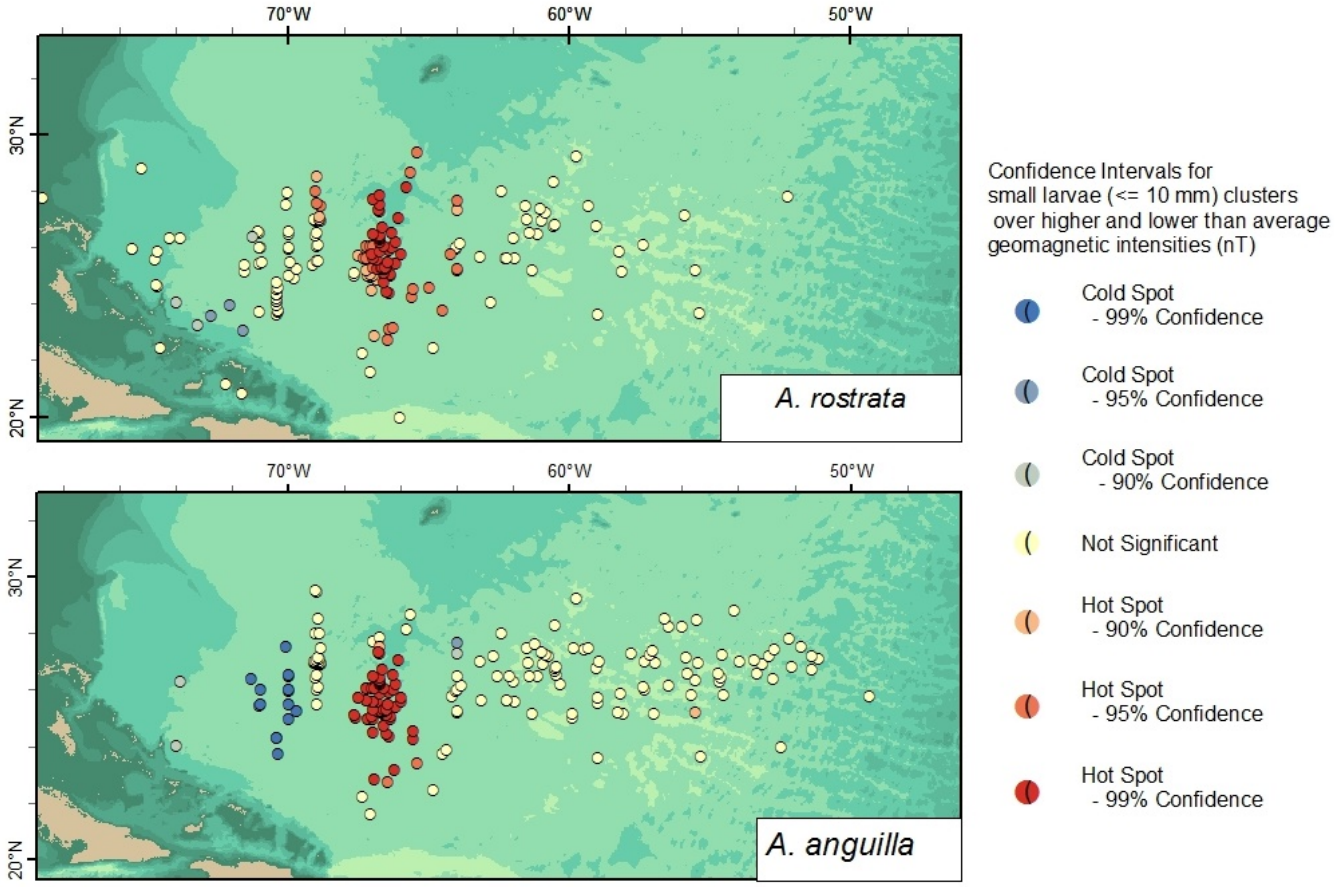

Figure 44. Hot spots of small larvae (≤ 10 mm) over geomagnetic intensities (nT). The map shows confidence intervals for non-random larval clustering around above average (deepening shades of red) and below average (deepening shades of blue) for all larvae in the second study area. This model applied a fixed band spatial conceptualization.

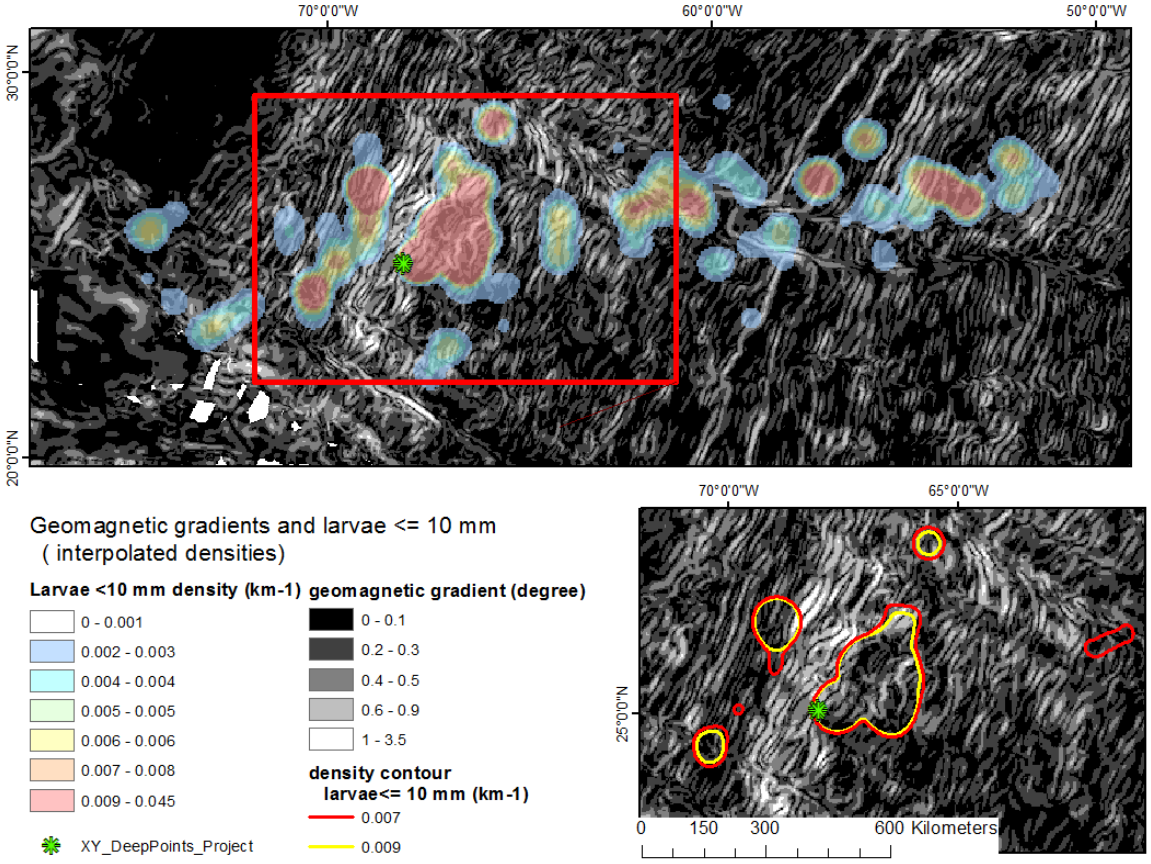

Figure 45. Interpolated densities of small larvae counts over magnetic gradients. High densities of small larvae (≤ 10 mm) of both species) are shaded in red over a map of magnetic gradients (top). Steeper gradients (°) are white and level towards black. The insert shows two density areas separated by a steep gradient band near the DSDP sites (green asterisk).

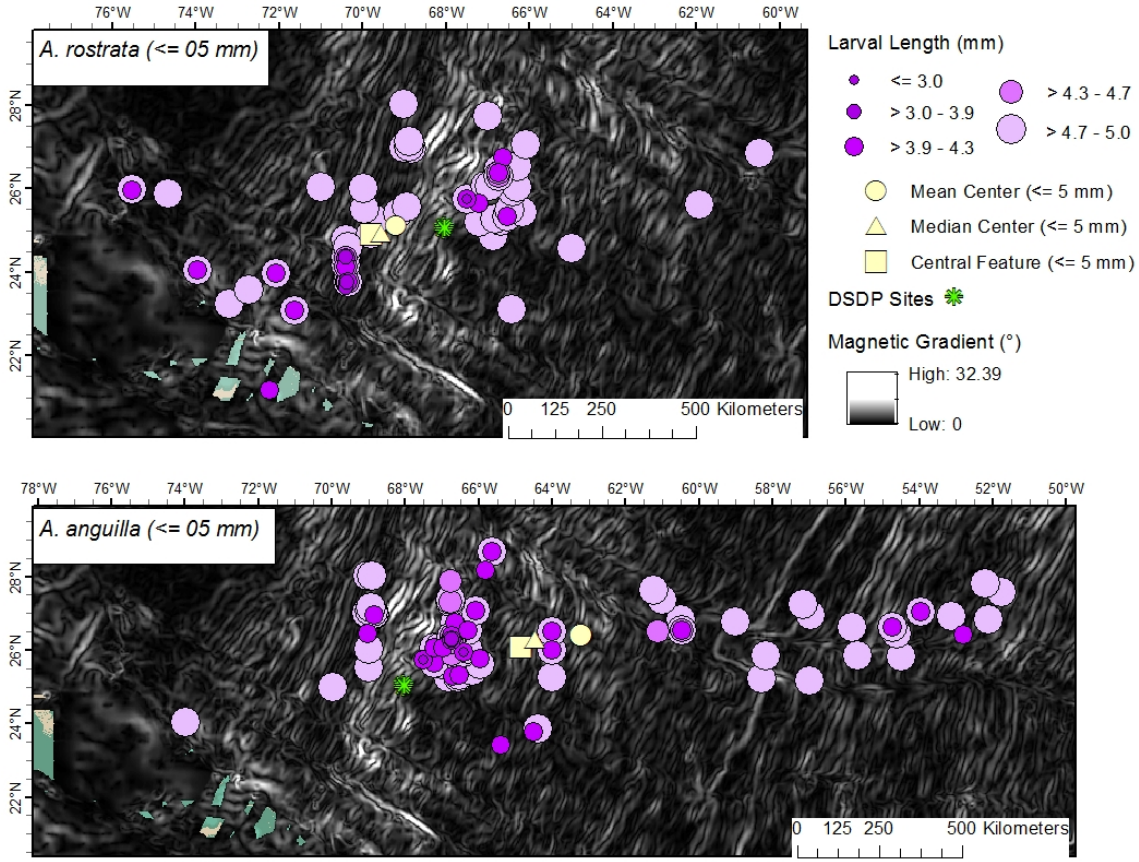

Figure 46. Newly hatched larvae (≤ 5 mm) adjacent to a high magnetic gradient. Larval sizes are graduated in size. Mean center (circle), median center (triangle) and central features (square) are shown for *A. rostrata* (top) and *A. anguilla* (bottom). Steeper magnetic gradients (°) are shown in white.

Chapter IV

Discussion

In the context of declining populations of freshwater eels in Europe and North America and inspired by observations of Japanese eel spawning near seamounts, this study explored the hypothesis of a possible spatial relationship between the spawning grounds of Atlantic eels and surrounding geophysical features in the Sargasso Sea. The research aimed to shed light on geophysical and spatial factors that would provide new insights on eel spawning and migration and inform both eel conservation and that of the Sargasso Sea. Analyzing aggregated samples of small larvae recorded between 1863 and 2007, the results found that the highest density of small larvae (≤ 10 mm) observations occurred in clusters over higher than average geomagnetic intensities. These small larval clusters and densities formed above over the axis of the southwest Bermuda Rise where it terminates at the Vema Gap. An underwater channel with a steep gradient, the Vema Gap directs the Antarctic Abyssal Bottom Current flow between the Nares and the Hatteras Abyssal Plains. Larvae were not found in significant clusters around depth, slope or magnetic gradients. However, a high magnetic gradient running through this landscape emerged as an area of interest on account of its position separating the central distributions of newly hatched larvae of the two species.

In addition to the geophysical explorations, the spatial analyses measured and displayed directional trends and standard deviations of larvae at various size increments. These analyses highlighte stages of larval dispersal and suggest areas for conservation

and research focus. The sampling distribution of null and positive stations supported previous assessments that additional sampling is needed to determine an eastern limit for *A. anguilla* leptocephali and verify the existence of an alternative and more direct eastern larval migration route from the Sargasso Sea to southern Europe (Boëtius & Harding, 1985; Schoth, 1982). However, it should be noted that the distribution of the historical aggregated sampling data was found non-random in all study areas. The non-random sampling distribution likely confounded natural distributions with sampling bias. As well, weighting stations with counts of larvae observations, as opposed to by presence only, influenced resulting directional ellipses of larval distributions. Conservationists and researchers conducting spatial analyses will need to consider the independence of their data when deciding how to weight their data.

This analysis was based on the spatial patterns of aggregated anguillid observations and their spatial relationship to depth, slope, geomagnetic intensities and gradients. Larvae observations from the ICES Egg and Larvae data set (McCleave, 2011) were supplemented with null catch data from original sources. To get a big picture of historic sampling trends, data were first analyzed on the scale of the North Atlantic Ocean, including its entrance into the North Sea and to the middle of the Mediterranean Ocean. Data were then divided into study areas. The first study area was based on the buffered extent of mid-sized larvae up to 30 mm in length. The second study area was based on the extent of smaller larvae up to 10 mm. As before, non-random sampling patterns likely confounded natural distributions with sampling preferences; however despite limitations of the data, the results succeeded in identifying a specific region for future investigation.

The following discusses the distribution of the larvae in relation to the landscape and geophysical attributes of depth, slope, magnetic intensities and their gradients, followed by a discussion on the spatial analyses of larval and sampling distributions and their implications for research and conservation.

Geophysical Characteristics

The favorable conditions for successful eel reproduction in the Sargasso Sea are attributed to dynamic and seasonal temperature gradients in the latitudes of the subtropical convergence zone. Geophysical features may play a further role in helping migrating eels navigate and aggregate in the Sargasso Sea, and thereby contribute to the fit of factors predicting their spawning locations. Japanese eel spawning in the proximity of the Mariana Seamounts in the North Pacific has led to the formulation of a "Seamount Hypothesis". This hypothesis postulates that nearby seamounts provide some kind of a cue that orients migrating Japanese eels into spawning aggregations, although this association remains uncertain (Aoyama et al., 2014; Fricke & Tsukamoto, 1998; Tsukamoto et al., 2003).

Using larval counts from the ICES data set (McCleave, 2011), this study found the highest interpolated densities of smaller larvae (≤ 10 mm) in the vicinity of the southwest Bermuda Rise, a topographically uneven region marked by abyssal knolls and hills (Bush, 1976). The geographic means, medians, and central features of the observations of newly hatched eel larvae of the two species and their overlapping stations were centered above or adjacent to this southern part of the Bermuda swell. This end of the Bermuda Rise separates the Hatteras Abyssal Plain to the west from the Nares

Abyssal Plain to its east. The Vema Gap at its southern end connects these two abyssal plains. The Antarctic Abyssal Bottom Current flows from the Nares Abyssal Plain through the more than 5000 m deep Vema Gap and into the Hatteras Abyssal Plain. The effect of local turbulence and upward forcing of abyssal bottom currents on other hydrographic phenomena such as eddies, overlying currents and ocean layers are not well known, nor its abyssal ecosystem well understood, but present factors of possible ecological interest. Two drill points from the Deep Sea Drill Program, sites 417 and 418 are located on the edge of the Vema Gap and provide a useful geographic reference in an otherwise largely unreferenced bathymetric landscape. The DSDP sites are located on the edge of the M0 magnetic anomaly, which travels the axis of the Bermuda Rise. The geographic medians of *A. rostrata* and *A. anguilla*, and the locations where the species have been found to overlap are positioned in a northeasterly direction 123 km, 260 km, and 180 km respectively from these drill points.

The depth analyses for this study found statistically significant clustering of larvae over both shallower and deeper than average depths. The larvae that clustered around shallower than average depths were in areas closer to the continental shelf and the Greater Antilles. The *A. rostrata* that clustered in shallower than average waters were likely either recruiting to coastal waters, or else entering the Gulf Stream for northward migration. *A. rostrata* and *A. anguilla* formed significant clusters in deeper than average depths. Small larvae clustered in deep water at depths over 4000 m, but with no discernable pattern. The deep water clusters of larvae were broadly spread out and generally uninformative other than to support a conclusion that larvae farther out at sea cluster at deeper depths than those near land. These results would support the argument

that the ocean floor in the Sargasso Sea is too remote to affect the distribution of migrating and spawning adult eels, or without influence for some other reason. However, the inclusion of land and near shore areas in the study area may also have increased the range of depths to a point that obscured smaller and more relevant variations in the deep sea area of interest. Additionally, bathymetric data is based on smoothing and interpolation of data from incompletely surveyed areas. For these reasons, the grids used in this analysis may omit existing features in the landscape or smoothed out their variation through interpolation.

The bathymetric slopes ranged from a minimum slope of just above 0° up to a maximum slope of 42°. Larval clusters were largely insignificant to higher and lower than average slope values and did not demonstrate a spatial pattern in relation to distributions of small larvae. Migrating eels may simply be indifferent to bathymetric slope, or the bathymetry in the Sargasso Sea may lack sufficient variation to influence behavior. However, as with the depth analyses, the inclusion of land in the study area may have introduced too large a scale and obscured variation in the deeper water area of greatest interest. Alternatively, incomplete surveys and smoothing of bathymetric data also may have reduced variation affecting the analysis of slope at deeper depths.

While the analysis did not find a spatial relationship between larvae observations and bathymetric features of depth and slope, it did find significant spatial distributions of small and newly hatched larvae around higher and lower than average geomagnetic intensities. Small larvae (≤ 10 mm) of both species aggregated in significant clusters around high magnetic intensities over the southwest Bermuda Rise. Small *A. anguilla* (≤ 10 mm) also clustered over lower than average intensities west of the Bermuda Rise,

along a north–south axis close to 70°24" W. The Anselin Local Moran's I test for spatial autocorrelation found larvae clustered over higher than average intensities that ranged from -97 to 124 nT and lower than average intensities ranging from -129 to 31 nT.

This clustering of small eel larvae (≤ 10 mm) around higher and lower than average geomagnetic intensities indicates some kind of spatial relationship between the magnetic anomalies and eel spawning and migratory behavior. The nature of this spatial relationship may be coincidental to the aggregation of eels in the thermal gradients and other favorable conditions of the subtropical convergence zone frontal system. However, as evidence of the geomagnetic sense and navigational skills of many migrating animals continues to build (Lohmann et al., 2007), the clustering over magnetic intensities discovered in this study warrants further investigation and verification.

Much of the research on geomagnetism and ocean migration has resolved around salmon (Putnam, 2014) and sea turtles (Lohmann, Lohmann, et al., 2008; Putman et al., 2011). The remarkable homing ability of salmon and sea turtles has given rise to the hypothesis that they and other migrating species may be born or inherit a magnetic imprint that enables their return to a specific location after many years and over long distances (Lohmann, Putman, & Lohmann, 2008; Putman et al., 2014). The consideration of a magnetic sense or imprinting has been speculatively raised with eels (Tsukamoto, 2009) and supported by studies on the ability of eels to sense and respond to magnetic cues. Juvenile yellow and maturing silver eels, for example, have been shown to slow their swimming significantly when near electromagnetic fields emitted by underwater power cables (Westerberg & Lagenfelt, 2008). Eels also have shown preferences in how they orient to manipulated changes in magnetic polarities (Durif et al., 2013). This

magnetic sensory ability is apparently acquired as early as the glass eel phase suggesting magnetic imprinting could take place at the larval level (Nishi & Kawamura, 2005). Yet the levels of intensity (12,000 to190,000 nT) that caused a heartbeat response in the glass eels (Nishi & Kawamura, 2005) was greater by orders of magnitude to the EMAG2 magnetic anomaly values at which this study found the small larvae clustered (from -129 to 124 nT).

Magnetic intensities decrease at a cubic rate through water and so presumably an eel with a magnetic sense would perceive the magnetic intensity of the ocean floor more intensely at depth. The EMAG2 magnetic anomaly grid measures magnetic intensity at the ocean surface at a 4 km altitude resolution. As the ocean floor is the source of magnetism, the intensities of the anomalies would intensify in deeper water and closer to the ocean floor. Migrating adult eels have been found swimming at depths exceeding 1000 m during the day in open ocean (Aarestrup et al., 2009). If eels can sense the magnetism of the ocean floor, they should also sense it more strongly in in deeper water. Predator avoidance, greater swimming efficiency, and temperature regulation for warmth or to delay sexual maturity have all been suggested as possible reasons for the eel swimming at deep depths during its spawning migration. The increasing intensity of the crustal magnetic field with proximity to the ocean floor could be an additional factor for the depth preference of a migrating eel if it were to provide an advantage in orientation. The biological and ecological influence of crustal geomagnetism as it travels through the ocean's vertical water column does not appear well studied. An initial literature search on magnetism in the vertical water column returned articles relating to the use of magnometers for finding locations of sunken planes, ships and other ferrous objects, but

not to its possible biological importance.

While the magnetic intensity of the ocean floor may intensify with depth, it represents only a fraction of the Earth's core field. The internal core field constitutes 90% of Earth's total magnetic field and its intensity is approximately 400 times greater than that of the lithospheric, or crustal, magnetic field (Thébault & Mandea-Alexandrescu, 2007). It is the main core field that determines polarity, presumably key for navigation. The Earth's magnetic pole, however, varies between years (Thébault & Mandea-Alexandrescu, 2007) and so polar direction would change during the interim between an eel's larval and spawning migrations. This secular interannual variance of the Earth's core field could limit its effectiveness as a navigational aid for an eel relying on a magnetic imprint as some kind of homing device. Unlike the core field, however, the magnetic field of the lithosphere remains stable over the life of an eel by retaining the polarities that were extant during the time of its crustal formation. Due to complexities in distinguishing crustal from core field magnetism, magnetic anomalies are modeled as high or low based on a comparison of observed to expected total field intensities. The constancy of the anomalies of the ocean floor are retained over millennia and form the basis of modern knowledge on tectonics and geological history (Thébault & Mandea-Alexandrescu, 2007). Because of their stability the magnetic anomalies in the ocean floor could hypothetically represent an important component of the geomagnetic field for eel navigation despite being of lesser intensity than the core field.

This study also investigated the possibility of a spatial relationship between larval distributions and magnetic gradients, which reflect the rate of change in magnetic intensity across the ocean floor. The results of the analysis showed larval clusters were

insignificant in relation to magnetic gradients. Nonetheless, an area of interest emerged from the analysis in the form of a high magnetic gradient band positioned between the geographical centers of newly hatched (≤ 5 mm) American and European eel larvae. This high magnetic gradient band ran in a north–south direction through the area with the highest density of small larvae (≤ 10 mm). The band coincided with M0 magnetic anomaly as indicated by location of the two DSDP drill sites on its eastern edge. Newly hatched (≤ 5 mm) *A. anguilla* were found almost exclusively to the east of the high magnetic gradient. *A. rostrata* (≤ 5 mm) were present on both sides of the gradient, but with its mean and median centers positioned to its west. Unfortunately, no sampling had taken place inside the high gradient band, and field work is required to see if these larval distributions reflect a natural pattern. This position identifies an area for future sampling to see if the high magnetic gradient band might be associated with differences in the spatial relationships between the two eel species, for example functioning as an imperfect barrier separating the two species of newly hatched larvae. Under this hypothesis, migrating *A. anguilla* silver eels that had not already spawned earlier to the east would aggregate along the band as it deterred or slowed their further movement westward. Of course, migrating adult eels may pass over even higher magnetic gradients during their migration without deterrence, and recruiting anguillid leptocephali as well must likely confront and cross over areas of high magnetic gradients as they approach land. However, these are questions for further investigation and invite further lines of inquiry, such as whether magnetic fields might play a role in triggering the metamorphosis of leptocephali into glass eels as they approach the continental shelf.

Spatial Patterns

Protecting larvae of critical species is among the objectives identified for pelagic marine reserves, yet greater knowledge of larval dispersal patterns is needed to fulfill that objective (Sale et al., 2005). This is true not only for anguillid leptocephali, but also for other marine species that inhabit or migrate to the Sargasso Sea (Miller et al., 2009). In addition to exploring spatial associations between small larvae and their geophysical environment, this study measured the spatial distributions of larvae at 10 mm increments of growth. While this exercise in many respects resembled and reconfirmed work of previous researchers, as shown by Schmidt's ellipse (1923) in Figure 1, McCleave's polygon (1993) in Figure 7, and Miller et al.'s (2014) ellipse in Figure 8, it also adds value by measuring the central tendencies, standard distances and deviations of the larval spatial distributions. By inferring the extent of 68% of a normally distributed population, the use of a standard distance provides additional tools for eel research and conservation. As an example, this study found that a single standard deviational ellipse for the ≤ 5 mm *A. rostrata* larvae extended from 74° W to 65° W over a range of nine degrees. This standard deviational ellipse for the newly hatched ≤ 5 mm larvae was about six degrees of longitude smaller than the full extent of the ≤ 6 mm larval distribution, which was (75° W–60° W) as found by Miller et al. (2014). This difference in longitudinal extent may be due to the 1 mm larger size of larvae in the example of Miller et al. (2014), but also in part to the fact that this study used the standard distance measurement for the ≤ 5 mm larval distribution. A close match between the western extent of a standard deviational ellipse of the distribution and one showing its full range of the distribution

would indicate that the limit for the distribution is also close to the center of its spread.

The analysis of positive and null stations revealed a non-random distribution at all the scales studied. The similar degree of non-randomness in the distribution of null and positive stations suggests that larvae observations were likely not independent of the sampling pattern. Historically research has tended to discard null tows from data and analyses. Null catch data augmented the number of stations by 29%, allowing for a greater assessment of the sampling distribution. The null data used in this study represents an estimated two-thirds to what could be added from existing sources, promising opportunities to further expand on this line of research. The addition of null data to the analyses in this study did not contradict previous research but added to the understanding of the underlying sampling distributions.

A preponderance of the sampling took place in the region of the Sargasso Sea. This sampling preference likely reflects the keen desire of Schmidt and subsequent researchers to solve mysteries relating to eel spawning migration and origins. The most frequently observed larvae in this study were 12 mm in length. This size frequency could as well reflect the research interest in Atlantic eel spawning and origins. However, the greater number of smaller larvae observations could also mean that the greatest densities and abundances of leptocephali naturally occur during early stages of development, before wider dispersal and mortalities. Early densities of larvae may attenuate during later stages of dispersal and migration.

At the scale of the North Atlantic Ocean, the European eel represented close to two-thirds of the species distribution based on number of larvae observations. The greater number of European eels at this scale possibly reflects the early interest of European

researchers, beginning with Schmidt, in tracking the origin of European eel, as the years in the 1920s were included among peak periods of sampling. However, in the smaller scales of the two study groups, defined by the extents of larvae ≤ 30 mm and ≤ 10 mm, the two species were more evenly distributed. It appears that there is a more even natural distribution of species within the range of larvae that are ≤ 30 mm.

The results in this study confirmed the accepted findings of previous research that European eels are on average larger than American eels (Miller et al., 2014; Schmidt, 1923; Tesch, 2003). At the North Atlantic scale, larvae over 90 mm from three locations in the Mediterranean Sea added to the spread in the mean sizes of the European eel leptocephali. Possibly these larger larvae from the Mediterranean were already metamorphosing into glass eels, but even with removal of these outliers the European eel maintained a larger size difference. At the scale defined by the extent of ≤ 30 mm larvae, the difference in maximum size of *A. rostrata* (63 mm) and *A. anguilla* (59 mm) became less pronounced.

Local clustering analyses found significant clusters of smaller larvae in the Sargasso Sea. Clusters of smaller than average *A. anguilla* were narrower and had a longer longitudinal shape than those of *A. rostrata,* which had a wider north–south spread. These pattern of small larval distributions reconfirmed the overall trends found in previous eel research (McCleave, 1993; Miller et al., 2014; Schmidt, 1923) and also indicated where these patterns showed greatest statistical significance. Smaller *A. anguilla* leptocephali aggregated in the central study area below Bermuda, with isolated clusters of larger larvae radiating outwards to the east, northeast, north of Bermuda and west presumably along or towards the Gulf Stream, i.e., in more or less all

directions except to the south. By contrast, clusters of larger *A. rostrata* were largely absent directly east of the concentration of small larvae where both species mixed together below Bermuda. The larger sizes of larvae found along continental shelves and near shore areas was not either surprising. The larger larvae over the continental shelves and near coastal areas were presumably larvae in migration along the Gulf Stream or advancing towards recruitment on the North American or European continent.

As has already been shown in previous research, this study found that European eel larvae migrating to southern Europe are larger than those recruiting to more northern latitudes. The potential for eastward jets and frontal counter currents combined with the unexplained cline of smaller sizes recruiting to southern Europe in the Sargasso Sea supports the hypothesis of a more direct and eastward distribution, migration, and possible spawning by *A. anguilla* (McCleave, 1993; Munk et al., 2010). The pattern of null and positive stations combine to show unsampled areas that support conclusions of Boëtius and Harding (1985b) and Schoth and Tesch (1982) that more sampling is needed before establishing an eastern or southeastern limit to the breeding grounds of *A. anguilla* or ruling out the possibility of a more directly east larval migratory route from the Sargasso Sea to southern Europe (Kettle et al., 2011; McCleave, 1993).

The directional trends, based on a one standard distance deviational ellipse, showed that at their early stages of growth both species maintained fairly stable distributions. At a certain size increment each experienced a five-fold expansion in distribution. *A. rostrata* experienced this expansion at a smaller size category (20–30 mm) than *A. anguilla* (30–40 mm). The shape of their deviational ellipses corroborate the ellipses drawn by Schmidt (1922), but show a thinner and more elongated

shape due to their representing only one standard deviation of the larval distribution. The dramatic expansion in the standard distance of their distributions suggests a critical stage in Atlantic eel larval development and migration. The slower larval growth rate, longer migration, and larger average size of *A. anguilla* compared to that of *A. rostrata* may leptocephali may explain why it would experience this expansion phenomenon at a larger size. The two species may follow parallel stages of development but attain that stage at a different size range due to different growth rates and migration loops. Further analyses of their deviational ellipses in conjunction with ocean currents may provide insights into these and other questions about larval migration, such as those relating to the motility and directional ability of leptocephali

Weighting the data with counts influenced larval directional trend analyses. The influence of weighting was particularly evident with the directional trends of the $< 20 \leq 30$ mm size group of *A. rostrata*. When stations were weighted by larvae counts, the deviational ellipse of this size group of *A. rostrata* rotated 64° to the northeast compared to when their locations were weighted equally by presence only. Geographic centers also changed with weighting. The weighted mean center of newly hatched *A. rostrata* (≤ 5 mm) larvae shifted 128 km to the southwest from a purely spatial analysis based purely on presence at stations. The decision on whether or not to weight the data for modeling eel distributions will depend on how one evaluates the independence of the data. Admittedly, the aggregated data of cruises from different time periods and with individual sampling objectives did not conform into an ideal or reliable sampling scheme. The non-random pattern of sampling locations and similar degree of clustering by positive and null stations requires that their analyses be treated with a grain

of salt. Yet despite limitations, these analyses succeed in pointing out gaps and potential trends for future research.

Larval dispersal has been identified as an area where greater knowledge is needed for the planning of pelagic conservation areas (Sale et al., 2005). As this study shows, the standard distances and central measurements of the anguillids varied by species and stage of larval development. Leptocephali of any size are extremely fragile and newly hatched leptocephali are buoyant but lack motility (Tesch, 1977). Because newly hatched pre-leptocephali maintain their egg globule as a food source, the smallest leptocephali may be comparatively less vulnerable than one-or two-week old larvae as they transition to external food sources, gain motility and begin to vertically migrate (Miller, 2009). The fivefold expansion in the standard deviations of mid-sized *A. rostrata* ($< 20 \leq 30$ mm) and *A. anguilla* ($< 30 \leq 40$ mm) leptocephali may therefore mark a transition following a potentially more vulnerable stage of development in the $< 10 \leq 30$ mm size bracket before the larvae begin to disperse more widely.

The large areas of ocean that would be required to protect larvae of critical species have raised arguments against the practicality of such an objective when planning conservation areas. The wide dispersal of Anguillid leptocephali, which undergo one of the greatest larval migrations known, would be no exception in this regard. By contrast, protection of aggregating spawning adult eels, rather than dispersing leptocephali, may represent a more attainable goal in the Sargasso Sea. As single breeding populations, Atlantic eels congregating in the Sargasso Sea in a weakened state after a long migration represent a vulnerable stage for reproduction and species survival. A more precise identification of the geographic centers and directional tendencies of eel spawning

distributions is essential for establishing areas of protection from oil pollution from shipping, destructive fishing, potential commercial harvesting of *Sargassum*, deep sea mining or cable laying.

Dynamic characteristics in the ocean environment pose unique considerations for eel conservation in the Sargasso Sea. The non-stationary seasonal frontal system associated with anguillid reproduction may make eel conservation a moving target whose boundaries require frequent adjustment. While the geography of eel spawning may be largely guided by shifting dynamics, this study suggests the southwest Bermuda Rise as an area of interest for further research and of potential conservation value. The "grape bunch" of young larvae observations along this axis of the Bermuda Rise may represent a constant or tendency that figures as a low hanging fruit for future eel research and conservation. Further field research will clarify the potential role of geomagnetic intensities and gradients as a factor in eel reproduction and animal migration, while the surrounding landscape offers opportunities for study as an ecosystem of abyssal connectivity and boundary mixing within the deep and upper layers of the Sargasso Sea.

List of References

Aarestrup, K., Økland, F., Hansen, M. M., Righton, D., Gargan, P., Castonguay, M., . . . McKinley, R. S. (2009). Oceanic spawning migration of the European eel (*Anguilla anguilla*). *Science, 325*(5948), 1660. doi:10.1126/science.1178120

Albert, V., Jónsson, B., & Bernatchez, L. (2006). Natural hybrids in Atlantic eels (*Anguilla anguilla*, *A. rostrata*): Evidence for successful reproduction and fluctuating abundance in space and time. *Molecular Ecology, 15*(7), 1903–1916. doi:10.1111/j.1365-294X.2006.02917.x

Als, T. D., Hansen, M. M., Maes, G. E., Castonguay, M., Riemann, L., Aarestrup, K. I. M., . . . Bernatchez, L. (2011). All roads lead to home: Panmixia of European eel in the Sargasso Sea. *Molecular Ecology*, *20*(7), 1333–1346. doi:10.1111/j.1365–294X.2011.05011.x

Amante, C., & Eakins, B. W. (2009). ETOPO1 1 arc-minute global relief model: Procedures, data sources and analysis. *NOAA Technical Memorandum NESDIS NGDC–24.* National Geophysical Data Center, NOAA. doi:10.7289/V5C8276M

Aoyama, J. (2009). Life history and evolution of migration in catadromous eels (Genus *Anguilla*). *Aqua-BioScience Monographs, 2*(1), 1–42. doi:10.5047/absm.2009.00201.0001

Aoyama, J., Nishida, M., & Tsukamoto, K. (2001). Molecular phylogeny and evolution of the freshwater eel, Genus *Anguilla*. *Molecular Phylogenetics and Evolution, 20*(3), 450–459. doi:10.1006/mpev.2001.0959

Aoyama, J., & Tsukamoto, K. (1997). Evolution of the freshwater eels. *Naturwissenschaften*, 84(1), 17–21. doi:10.1007/s001140050340

Aoyama, J., Watanabe, S., Miller, M. J., Mochioka, N., Otake, T., Yoshinaga, T., & Tsukamoto, K. (2014). Spawning sites of the Japanese eel in relation to oceanographic structure and the West Mariana Ridge. *PLoS One, 9*(2), e88759. doi:10.1371/journal.pone.0088759

Ardron, J., Halpin, P., Roberts, J., Cleary, J., Moffitt, R., & Donnelly, B. (2011). Where is the Sargasso Sea? A report submitted to the Sargasso Sea Alliance. *Duke University Marine Geospatial Ecology Lab & Marine Conservation Institute. Sargasso Sea Alliance Science Report Series*, (2).

ASMFC. (2008). Addendum II to the Fishery Management Plan for American Eel. Atlantic States Marine Fisheries Commission. Retrieved 2015 from http://www.asmfc.org/uploads/file/amEelAddendum%20II.pdf

Backus, R. H., (1978). [Cruise report, R/V Oceanus (OC49)], Woods Hole Oceanic Institution Archives, Data Library and Archives.

Bayer, F. (1966). Dredging and trawling records of R/V John Elliot Pillsbury for 1964 and 1965. *Studies in Tropical Oceanography*, *4*(1), 82–105.

Begon, M., Townsend, C. R., & Harper, J. L. (2006). *Ecology: From individuals to ecosystems* (4th ed.). Malden, MA: Blackwell.

Béguer-Pon, M., Benchetrit, J., Castonguay, M., Aarestrup, K., Campana, S. E., Stokesbury, M. J. W., & Dodson, J. J. (2012). Shark predation on migrating adult American eels (*Anguilla rostrata*) in the Gulf of St. Lawrence. *PLoS One, 7*(10), e46830. doi:10.1371/journal.pone.0046830

Beguer-Pon, M., Castonguay, M., Shan, S., Benchetrit, J., & Dodson, J. J. (2015). Direct observations of American eels migrating across the continental shelf to the Sargasso Sea. *Nature Communications*, 6(8705), 9705. doi:10.1038/ncomms9705

Belkin, I. M., Cornillon, P. C., & Sherman, K. (2009). Fronts in Large Marine Ecosystems. *Progress in Oceanography, 81*(1–4), 223–236. doi:10.1016/j.pocean.2009.04.011

Belpaire, C. G. J., Goemans, G., Geeraerts, C., Quataert, P., Parmentier, K., Hagel, P., & De Boer, J. (2009). Decreasing eel stocks: Survival of the fattest? *Ecology of Freshwater Fish, 18*(2), 197–214. doi:10.1111/j.1600-0633.2008.00337.x

Boëtius, J. (1980). Atlantic *Anguilla*. A presentation of old and new data of total numbers of vertebrae with special reference to the occurrence of *Anguilla rostrata* in Europe. *Dana, 1*, 93–112. Retrieved 2015 from www.aqua.dtu.dk/english/-/media/Institutter/Aqua/Publikationer/Dana/dana_vol_1_pp_93_112.ashx?la=da

Boëtius, J., & Harding, E. F. (1985a). List of Atlantic and Mediterranean *Anguilla* leptocephali: Danish material up to 1966. *Dana*, *4*:163–249.

Boëtius, J., & Harding, E. F. (1985b). A re-examination of Johannes Schmidt's Atlantic eel investigations. *Dana, 4*, 129–162. Retrieved 2015 from www.aqua.dtu.dk/english/-/media/Institutter/Aqua/Publikationer/Dana/dana_vol_4_pp_129_162.ashx?la=da

Bonhommeau, S., Chassot, E., Planque, B., Rivot, E., Knap, A. H., & Le Pape, O. (2008). Impact of climate on eel populations of the Northern Hemisphere. *Marine Ecology Progress Series, 373*, 71–80. doi:10.3354/meps07696

Bonhommeau, S., Chassot, E., & Rivot, E. (2008). Fluctuations in European eel (*Anguilla anguilla*) recruitment resulting from environmental changes in the Sargasso Sea. *Fisheries Oceanography, 17*(1), 32–44. doi:10.1111/j.1365-2419.2007.00453.x

Burgerhout, E., Manabe, R., Brittijn, S., Aoyama, J., Tsukamoto, K., & van den Thillart,

G. E. (2011). Dramatic effect of pop-up satellite tags on eel swimming. *Naturwissenschaften, 98*(7), 631–634. doi:10.1007/s00114-011-0805-0

Busch, W. D. N., & Braun, D. P. (2014). A case for accelerated reestablishment of American eel in the Lake Ontario and Champlain watersheds. *Fisheries, 39*(7), 298–304. doi:10.1080/03632415.2014.923769

Bush, P. A. (1976). Bathymetry of the MODE-I region. *Deep Sea Research and Oceanographic Abstracts, 23*(12), 1105–1113. doi:10.1016/0011-7471 (76)90887-1

Butler, J. N., Morris, B. F., Cadwallader, J., & Stoner, A. W. (1983). *Studies of Sargassum and the Sargassum community*. Bermuda: Bermuda Biological Station for Research.

Campana, S., Joyce, W., & Fowler, M. (2010). Subtropical pupping ground for a cold-water shark. *Canadian Journal of Fisheries and Aquatic Sciences, 67*(5), 769–773. doi:10.1139/F10-020

Carr, J. W., & Whoriskey, F. G. (2008). Migration of silver American eels past a hydroelectric dam and through a coastal zone. *Fisheries Management and Ecology. 15*(5–6), 393–400. doi:10.1111/j.1365-2400.2008.00627.x

Casselman, J. M. (2003). Dynamics of resources of the American eel, *Anguilla rostrata*: Declining abundance in the 1990s. In K. Aida, K. Tsukamoto, & K. Yamauchi (Eds.), *Eel biology* (pp. 255–274). Springer Japan..

Castonguay, M., Dutil, J. D., & Desjardins, C. (1989). Distinction between American eels (*Anguilla rostrata*) of different geographic origins on the basis of their organochlorine contaminant levels. *Canadian Journal of Fisheries and Aquatic Sciences, 46*(5), 836-843. 10.1139/f89-105

Castonguay, M., Hodson, P. V., Couillard, C. M., Eckersley, M. J., Dutil, J. D., & Verreault, G. (1994). Why is recruitment of the American eel, *Anguilla rostrata*, declining in the St. Lawrence River and Gulf? *Canadian Journal of Fisheries and Aquatic Sciences, 51*(2), 479–488. doi:10.1139/f94-050

Castonguay, M., Hodson, P. V., Moriarty, C., Drinkwater, K. F., & Jessop, B. M. (1994). Is there a role of ocean environment in American and European eel decline? *Fisheries Oceanography, 3*(3), 197–203. doi:10.1111/j.1365-2419.1994. tb00097.x

Castonguay, M., & McCleave, J. D. (1987). Vertical distributions, diel and ontogenetic vertical migrations and net avoidance of leptocephali of *Anguilla* and other common species in the Sargasso Sea. *Journal of Plankton Research, 9*(1), 195.

Chow, S., Kurogi, H., Mochioka, N., Kaji, S., Okazaki, M., & Tsukamoto, K. (2008). Discovery of mature freshwater eels in the open ocean. *Fisheries Science, 75*(1),

257–259. 10.1007/s12562-008-0017-5

CITES. (n.d.). How CITES works. *Convention on International Trade in Endangered Species of Wild Fauna and Flora.* Retrieved 2015 http://www.cites.org/eng/disc/how.shtml

Clevestam, P. D., Ogonowski, M., Sjöberg, N. B., & Wickström, H. Too short to spawn? (2011). Implications of small body size and swimming distance on successful migration and maturation of the European eel *Anguilla anguilla*. *Journal of Fish Biology, 78*(4), 1073–1089. doi:10.1111/j.1095-8649.2011.02920.x

Cohen, K. M., Finney, S., & Gibbard, P. L. (2012). International Chronostratigraphic Chart: International Commission on Stratigraphy. doi: 10.1130/B30712.1

Congalton, R. G., & Green, K. (1992). The ABCs of GIS. *Journal of Forestry, 90*(11), 13–20.

Cornillon, P., Evans, D., & Large, W. (1986). Warm outbreaks of the Gulf Stream into the Sargasso Sea. *Journal of Geophysical Research, 91*(C5), 6583–6596. doi:10.1029/JC091iC05p06583

COSEWIC. (2006). *COSEWIC Assessment and status report on the American eel Anguilla rostrata in Canada*. Committee on the Status of Endangered Wildlife in Canada. Ottawa. x + 71 pp. Ottawa. Retrieved 2015 from http://www.sararegistry.gc.ca/virtual_sara/files/cosewic/sr_american_eel_e.pdf

COSEWIC. (2012). *COSEWIC Assessment and status report on the American eel Anguilla rostrata in Canada*. Committee on the Status of Endangered Wildlife in Canada. Ottawa. xii + 109pp. Retrieved 2015 from http://publications.gc.ca/collections/collection_2013/ec/CW69-14-458-2012-eng.pdf

Côté, C. L., Gagnaire, P.A., Bourret, V., Verreault, G., Castonguay, M., & Bernatchez, L. (2013). Population genetics of the American eel (*Anguilla rostrata*): FST = 0 and North Atlantic Oscillation effects on demographic fluctuations of a panmictic species. *Molecular Ecology, 22*(7), 1763–1776. doi:10.1111/mec.12142

Dale, A. (2010, March 4). Bermuda can take the lead in protecting the Sargasso Sea, Cox indicates in budget. *The Royal Gazette*. Hamilton, Bermuda. Retrieved 2015 from http://www.royalgazette.com/article/20100301/NEWS/303019977

Daverat, F., Limburg, K. E., Thibault, I., Shiao, J.C., Dodson, J. J., Caron, F., . . . Wickstrom, H. (2006). Phenotypic plasticity of habitat use by three temperate eel species, *Anguilla anguilla*, *A. japonica* and *A. rostrata*. *Marine Ecology Progress Series, 308*, 231–241. doi:10.3354/meps308231

Deacon, G. E. R. (1942). The Sargasso Sea. *The Geographical Journal, 99*(1), 16–28. doi:10.2307/1788092

Dekker, W. (2004a). Slipping through our hands: Population dynamics of the European eel. (Doctoral dissertation). University of Amsterdam (UvA). Retrieved from UvA-DARE, the institutional repository of the University of Amsterdam. http://hdl.handle.net/11245/1.226600

Dekker, W. (2004b). What caused the decline of the Lake IJsselmeer eel stock after 1960? *ICES Journal of Marine Science, 61*(3), 394–404. doi:10.1016/j.icesjms.2004.01.003

Driscoll, N. W., & Laine, E. P. (1996). Abyssal current influence on the southwest Bermuda Rise and surrounding region. *Marine Geology, 130*(3–4), 231–263. doi:http://dx.doi.org/10.1016/0025-3227(95)00133-6.

Durif, C. M. F., Browman, H. I., Phillips, J. B., Skiftesvik, A. B., Vøllestad, L. A., & Stockhausen, H. H. (2013). Magnetic compass orientation in the European eel. *PLoS One, 8*(3), e59212. doi:10.1371/journal.pone.0059212.

Durif, C. M. F., Dufour, S., & Elie, P. (2005). The silvering process of *Anguilla anguilla*: A new classification from the yellow resident to the silver migrating stage. *Journal of Fish Biology, 66*(4), 1025–1043. doi:10.1111/j.0022-1112.2005.00662.x.

Council Regulation (EC) 1100/2007. 18 September 2007. Establishing measures for the recovery of the stock of European eel. (2007). OJ L248/17.

EELREP. (2005). *Final report: Estimation of the reproduction capacity of European eel*. Retrieved 2010 from http://www.fishbiology.net/EELREP_final_report.pdf

Eigenmann, C. H., & Kennedy, C. (1902). The leptocephalus of the American eel and other American leptocephali. *Bulletin of the United States Fish Commission, 21*, 81–92. Retrieved 2015 from http://fisherybulletin.nmfs.noaa.gov/21-1/eigenmann3.pdf

Eldred, B. (1968). Larvae and glass eels of the American freshwater eel, *Anguilla rostrata* (Lesueur, 1817) in Florida waters. *Florida Board of Conservation: Marine Research Laboratory Leaflet Series 4* (1)9.

Eldred, B. (1971). First records of Anguilla rostrata larvae in the Gulf of Mexico and Yucatan Straits. *Florida Department of Natural Resources*: *Marine Research Laboratory, Leaflet Series 4* (1)19, 1–3.

ESRI. (2011). ArcGIS Desktop: Release 10.3. Redlands, CA: Environmental Systems Research Institute.

Facey, D. E., & van Den Avyle, M. J. (1987). *Species profiles: Life histories and environmental requirements of coastal fishes and invertebrates (North Atlantic)–American eel*. Biological Report 82 (11.74). U.S. Fish and Wildlife Service & U.S. Army Corp of Engineers. Retrieved 2015 from http://www.nwrc.usgs.gov/

wdb/pub/species_profiles/82_11-074.pdf

Fahay, M. P. (1978). *Biological and fisheries data on American eel, Anguilla rostrata (LeSueur)*: Sandy Hook Laboratory Technical Report (SHLTSR 17), Northeast Fisheries Center, National Marine Fisheries Service, National Oceanic and Atmospheric Administration. Retrieved 2015 from http://www.nefsc.noaa.gov/publications/series/shtsr/shltr17.pdf

Fricke, H., & Tsukamoto, K. (1998). Seamounts and the mystery of eel spawning. *Naturwissenschaften, 85*(6), 290. doi:10.1007/s001140050502

Friedland, K. D., Miller, M. J., & Knights, B. (2007). Oceanic changes in the Sargasso Sea and declines in recruitment of the European eel. *ICES Journal of Marine Science, 64*(3), 519–519. doi:10.1093/icesjms/fsm022

Gagnaire, P.A., Normandeau, E., Côté, C., Møller Hansen, M., & Bernatchez, L. (2012). The genetic consequences of spatially varying selection in the panmictic American eel (*Anguilla rostrata*). *Genetics, 190*(2), 725–736. doi:10.1534/genetics.111.134825

Gaines, A. G. (1977). *Cruise Report W-36: Scientific activities undertaken aboard R/V Westward, Woods Hole–San Juan, October 12-November 23, 1977*. Retrieved 2015 from Woods Hole, MA. https://darchive.mblwhoilibrary.org/handle/1912/4434

Grassi, G. B. (1896). The reproduction and metamorphosis of the common eel (*Anguilla vulgaris*). *Proceedings of the Royal Society of London, 60*, 260–271. doi:10.1098/rspl.1896.0045

Hanel, R., Stepputtis, D., Bonhommeau, S., Castonguay, M., Schaber, M., Wysujack, K., . . . Miller, M. J. (2014). Low larval abundance in the Sargasso Sea: New evidence about reduced recruitment of the Atlantic eels. *Naturwissenschaften, 101*(12), 1041–1054. doi:10.1007/s00114-014-1243-6

Haro, A. J. (1991). Thermal preferenda and behavior of Atlantic eels (genus *Anguilla*) in relation to their spawning migration. *Environmental Biology of Fishes, 31*(2), 171–184. doi:10.1007/BF00001018

Haro, A. J., Richkus, W., Whalen, K., Hoar, A., Busch, W.D., Lary, S., . . . Dixon, D. (2000). Population decline of the American eel: Implications for research and management. *Fisheries*, *25*(9), 7–16. doi:10.1577/1548-8446(2000)025<0007:PDOTAE>2.0.CO;2

Harris, P. T., & Whiteway, T. (2009). High seas marine protected areas: Benthic environmental conservation priorities from a GIS analysis of global ocean biophysical data. *Ocean & Coastal Management, 52*(1), 22–38. doi:10.1016/j.ocecoaman.2008.09.009

Heezen, B. C., Tharp, M., & Ewing, M. (1959). The floors of the oceans: I.The North Atlantic. Geol*ogical Society of America Special Papers, 65*, 1–126. doi:10.1130/SPE65-p1

Hitt, N. P., Eyler, S., & Wofford, J. E. B. (2012). Dam removal increases American eel abundance in distant headwater streams. *Transactions of the American Fisheries Society, 141*(5), 1171–1179. doi:10.1080/00028487.2012.675918

Howland, P. C., (1978). [Ship's Log, R/V Oceanus (OC49)]. Woods Hole Oceanic Institution, Data Library and Archives.

Huertas, M., Canario, A. V. M., & Hubbard, P. C. (2008). Chemical communication in the genus *Anguilla*: A minireview. *Behaviour, 145*(10), 1389–1407. doi:10.1163/156853908785765926

Hui, C. A. (1994). Lack of association between magnetic patterns and the distribution of free-ranging dolphins. *Journal of Mammalogy*, *75*(2), 399-405. doi:10.2307/1382559

ICES. (2008). Report of the ICES Advisory Committee. ICES Advice, 2008. Book 9, (205-212). Retrieved 2015 from http://www.ices.dk/sites/pub/Publication%20Reports/ICES%20Advice/2008/ICES%20ADVICE%202008%20Book%209.pdf

IOC, IHO, & BODC. (2008). *Centenary edition of the GEBCO digital atlas*. Retrieved from http://www.bodc.ac.uk/projects/international/gebco/

IPCC. (2007). The North Atlantic Oscillation and Northern Annular Mode. Section 3.6.4. In: *Climate change 2007: The physical science basis. Contribution of Working Group I to the Fourth Assessment Report of the Intergovernmental Panel on Climate Change*. Intergovernmental Panel on Climate Change. Retrieved 2015 from http://www.ipcc.ch/publications_and_data/ar4/wg1/en/ch3s3-6-4.html

ICUN (2015). *Anguilla anguilla* (European eel). *IUCN Red List of Threatened Species. Version 2015-3*. Retrieved 2015 from www.iucnredlist.org.

Jespersen, P., & Tåning. (1934). Introduction to the reports from the Carlsberg Foundation's oceanographic expeditions around the world 1928–30. The Carlsberg Foundation, Copenhagen. *Dana-Report, 1*, 1–77.

Johnson, G. L., & Vogt, P. R. (1971). Morphology of the Bermuda Rise. *Deep Sea Research and Oceanographic Abstracts, 18*(6), 605–617. doi:http://dx.doi.org/10.1016/0011-7471(71)90126-4

Kearns, T. A., & Breman, J. (2010). Bathymetry: The art and science of seafloor modeling for modern applications. In J. Bremen (Ed.), *Ocean Globe* (pp. 1–36). Redlands, CA: ESRI Press.

Kettle, A. J., Asbjørn Vøllestad, L., & Wibig, J. (2011). Where once the eel and the elephant were together: Decline of the European eel because of changing hydrology in southwest Europe and northwest Africa? *Fish and Fisheries, 12*(4), 380–411. doi:10.1111/j.1467-2979.2010.00400.x

Kettle, A. J., Bakker, D. C. E., & Haines, K. (2008). Impact of the North Atlantic Oscillation on the trans-Atlantic migrations of the European eel (*Anguilla anguilla*). *Journal of Geophysical Research: Biogeosciences, 113*(G3), doi:10.1029/2007JG000589

Kettle, A. J., & Haines, K. (2006). How does the European eel (*Anguilla anguilla*) retain its population structure during its larval migration across the North Atlantic Ocean? *Canadian Journal of Fisheries and Aquatic Sciences, 63*(1), 90–106. doi:10.1139/f05-198

Kettle, A. J., Heinrich, D., Barrett, J. H., Benecke, N., & Locker, A. (2008). Past distributions of the European freshwater eel from archaeological and palaeontological evidence. Quaternary Science Reviews, 27(13–14), 1309–1334. doi:10.1016/j.quascirev.2008.03.005

Kimura, S., & Tsukamoto, K. (2006). The salinity front in the North Equatorial Current: A landmark for the spawning migration of the Japanese eel (*Anguilla japonica*) related to the stock recruitment. *Deep Sea Research Part II: Topical Studies in Oceanography, 53*(3–4), 315–325. doi:http://dx.doi.org/10.1016/j.dsr2.2006.01.009

Kirk, R. S. (2003). The impact of Anguillicola crassus on European eels. *Fisheries Management and Ecology, 10*(6), 385–394. doi:10.1111/j.1365-2400.2003.00355.x

Kleckner, R. C., & McCleave, J. D. (1985). Spatial and temporal distribution of American eel larvae in relation to north Atlantic Ocean current systems. *Dana, 4*, 67–92. Retrieved 2015 from www.aqua.dtu.dk/english/-/media/Institutter/Aqua/Publikationer/Dana/dana_vol_4_pp_67_92.ashx?la=da

Kleckner, R. C., & McCleave, J. D. (1988). The northern limit of spawning by Atlantic eels (*Anguilla* spp.) in the Sargasso Sea in relation to thermal fronts and surface water masses. *Journal of Marine Research, 46*(3), 647. doi: 10.1357/002224088785113469

Kleckner, R. C., McCleave, J. D., & Wippelhauser, G. S. (1983). Spawning of American eel, *Anguilla rostrata*, relative to thermal fronts in the Sargasso Sea. *Environmental Biology of Fishes, 9*(3–4), 289–293. doi: 10.1007/BF00692377

Knights, B. (2003). A review of the possible impacts of long-term oceanic and climate changes and fishing mortality on recruitment of anguillid eels of the Northern Hemisphere. *Science of The Total Environment, 310*(1–3), 237–244. doi:10.1016/s0048-9697(02)00644-7

Krueger, W., & Oliveira, K. (1999). Evidence for environmental sex determination in the American eel, *Anguilla rostrata*. *Environmental Biology of Fishes, 55*(4), 381–389. doi:10.1023/A:1007575600789

Kuroki, M., Aoyama, J., Miller, M. J., Yoshinaga, T., Shinoda, A., Hagihara, S., & Tsukamoto, K. (2009). Sympatric spawning of *Anguilla marmorata* and *Anguilla japonica* in the western North Pacific Ocean. *Journal of Fish Biology, 74*(9), 1853–1865. doi:10.1111/j.1095-8649.2009.02299.x

Laffoley, D. d. a., Roe, H. S. J., Angel, M. V., Ardron, J., Bates, N. R., Boyd, I. L., . . . Vats, V. (2011). *The protection and management of the Sargasso Sea: The golden floating rainforest of the Atlantic Ocean. Summary Science and Supporting Evidence Case.* Sargasso Sea Alliance, 44 pp.

Lamson, H. M., Cairns, D. K., Shiao, J. C., Iizuka, Y., & Tzeng, W. N. (2009). American eel, *Anguilla rostrata*, growth in fresh and salt water: Implications for conservation and aquaculture [electronic resource]. *Fisheries Management and Ecology, 16*(4), 306–314. Retrieved from http://dx.doi.org/10.1111/j.1365-2400.2009.00677.x

Lecomte-Finiger, R. (2003). The genus *Anguilla* Schrank, 1798: Current state of knowledge and questions. *Reviews in Fish Biology and Fisheries, 13*(3), 265–279. doi: 10.1023/B:RFBF.0000033072.03829.6d

Lohmann, K. J. (2007). Sea Turtles: Navigating with magnetism. *Current Biology, 17*(3), R102-R104. doi:10.1016/j.cub.2007.01.023

Lohmann, K. J., Cain, S. D., Dodge, S. A., & Lohmann, C. M. F. (2001). Regional magnetic fields as navigational markers for sea turtles. *Science, 294*(5541), 364–366. doi:10.1126/science.1064557

Lohmann, K. J., Lohmann, C. M. F., Ehrhart, L. M., Bagley, D. A., & Swing, T. (2004). Animal behaviour: Geomagnetic map used in sea-turtle navigation. *Nature, 428*(6986), 909–910. doi:10.1038/428909a

Lohmann, K. J., Lohmann, C. M. F., Ehrhart, L. M., Bagley, D. A., Swing, T., Mast, R. B., . . . Hutchinson, A. H. (2008). A magnetic map sense in juvenile sea turtles. *Proceedings of the Twenty-fourth Annual Symposium on Sea Turtle Biology and Conservtion*, *NOAA Technical Memorandum, National Marine Fisheries Service, Southeast Fisheries Science Center*, (567), 61.. Retrieved 2015 from http://faculty.washington.edu/kikij/sites/all/themes/jackson/TM_567_Mast_etal_24.pdf

Lohmann, K. J., Lohmann, C. M. F., & Putman, N. F. (2007). Magnetic maps in animals: Nature's GPS. *Journal of Experimental Biology, 210*(21), 3697–3705. doi: 10.1242/jeb.001313

Lohmann, K. J., Putman, N. F., & Lohmann, C. M. F. (2008). Geomagnetic imprinting: A

unifying hypothesis of long-distance natal homing in salmon and sea turtles. *Proceedings of the National Academy of Sciences of the United States of America, 105*(49), 19096–19101. doi:10.1073/pnas.0801859105

Maguire, D. J., (1991). An overview and definition of GIS. In D. J. Maguire, M. F. Goodchild & D. W Rhind *Geographical information systems: Principles and applications*, *1.* London: London Scientific and Technical. 9–20. Retrieved 2015 from http://lidecc.cs.uns.edu.ar/~nbb/ccm/downloads/Literatura/OVERVIEW%20AND%20DEFINITION%20OF%20GIS.pdf

Mank, J. E., & Avise, J. C. (2003). Microsatellite variation and differentiation in North Atlantic eels. *Journal of Heredity, 94*(4), 310–314. doi:10.1093/jhered/esg062

Maus, S., Barckhausen, U., Berkenbosch, H., Bournas, N., Brozena, J., Childers, V., . . . Caratori Tontini, F. (2009). EMAG2: A 2-arc min resolution Earth Magnetic Anomaly Grid compiled from satellite, airborne, and marine magnetic measurements. *Geochemistry, Geophysics, Geosystems, 10*(8), [np]. doi:http://dx.doi.org/10.1029/2009GC002471

McCleave, J. D. (1983). [Station and haul data, R/V Cape Florida (CF8303)]. Unpublished raw data.

McCleave, J. D. (1983). [Station and haul data, R/V Cape Florida (CF8305)]. Unpublished raw data.

McCleave, J. D. (1984). [Station and haul data, R/V Columbus Iselin (CI8408)]. Unpublished raw data. (J. D McCleave, 1984)

McCleave, J. D. (1984). [Station and haul data, R/V Columbus Iselin (CI8410)]. Unpublished raw data.

McCleave, J. D. (1985) [Station and haul data, R/V Cape Florida (CF8503)]. Unpublished raw data.

McCleave, J. D. (1993). Physical and behavioural controls on the oceanic distribution and migration of leptocephali. *Journal of Fish Biology, 43*(sA), 243–273. doi:10.1111/j.1095-8649.1993.tb01191.x

McCleave, J. D. (2003). *Spawning areas of the Atlantic eels*.

McCleave, J. (2008). Contrasts between spawning times of Anguilla species estimated from larval sampling at sea and from otolith analysis of recruiting glass eels. *Marine Biology*, *155*(3), 249-262. doi:10.1007/s00227-008-1026-8

McCleave, J. D. (2011). Atlantic *Anguilla* surveys (1863 –2007). *ICES Egg & Larval Database*. Made available by the International Council of the Sea. Retrieved 2015 from http://eggsandlarvae.ices.dk

McCleave, J. D., Brickley, P. J., O'Brien, K. M., Kistner, D. A., Wong, M. W., Gallagher, M., & Watson, S. M. (1998). Do leptocephali of the european eel swim to reach continental waters? Status of the question. *Journal of the Marine Biological Association of the United Kingdom, 78*(1), 285. doi:10.1017/S0025315400040091

McCleave, J. D., & Kleckner, R. C. (1987). Distribution of leptocephali of the catadromous *Anguilla* species in the western Sargasso Sea in relation to water circulation and migration. *Bulletin of Marine Science, 41*(3), 789–806. Retrieved 2015 from http://www.ingentaconnect.com/content/umrsmas/bullmar/1987/00000041/00000003/art00002

McCleave, J. D., Kleckner, R. C., Castonguay, M., Dadswell, M. J., Klauda, R. J., Moffitt, C. M., . . . Cooper, J. E. (1987). Reproductive sympatry of American and European eels and implications for migration and taxonomy. *American Fisheries Society Symposium,1*, 286–297.

McCleave, J. D., & Kleckner,(1985). Oceanic migrations of Atlantic eels (*Anguilla* spp.): Adults and their offspring. In Chapter 3: *Fish migrations* (Legett, Ed.), In (Eds. Rankin, M. A.) *Contributions in Marine Science, 27*, 316–337. Retrieved 2015 in http://hdl.handle.net/2152/18035

McCleave, J. D., & Power, J. H. (1978). Influence of weak electric and magnetic fields on turning behavior in elvers of the American eel *Anguilla rostrata*. *Marine Biology, 46*(1), 29–34. doi:10.1007/BF00393817

Miller, M.J., Stepputtis, D., Bonhommeau, S., Castonguay, M., Schaber, M., Vobach, M., . . . Hanel, R. (2013). Comparisons of catches of large leptocephali using an IKMT and a large pelagic trawl in the Sargasso Sea. *Marine Biodiversity, 43*(4), 493–501. doi:10.1007/s12526-013-0170-7

Miller, M. J. (2009). Ecology of anguilliform leptocephali: Remarkable transparent fish larvae of the ocean surface layer. *Aqua-BioSci Monographs, 2*(4), 1–94. doi:10.5047/absm.2009.00204.0001

Miller, M. J., Bonhommeau, S., Munk, P., Castonguay, M., Hanel, R., & McCleave, J. D. (2014). A century of research on the larval distributions of the Atlantic eels: A re-examination of the data. *Biological Reviews*, n/a-n/a. doi:10.1111/brv.12144

Miller, M. J., Kimura, S., Friedland, K. D., Knights, B., Kim, H., Jellyman, D. J., & Tsukamoto, K. (2009). Review of ocean-atmospheric factors in the Atlantic and Pacific oceans influencing spawning and recruitment of anguillid eels. In *American Fisheries Society Symposium,* 69, 231-249. Retrieved 2015 from http://www.researchgate.net/profile/Michael_Miller30/publication/256543846_Review_of_ocean-atmospheric_factors_in_the_Atlantic_and_Pacific_oceans_influencing_spawning_and_recruitment_of_anguillid_eels/links/53d854160cf2e38c633172f4.pdf

Miller, M. J., & McCleave, J. D. (1994). Species assemblages of leptocephali in the Subtropical Convergence Zone of the Sargasso Sea. *Journal of Marine Research, 52*(4), 743. doi:10.1357/0022240943076948

Munk, P., Hansen, M. M., Maes, G. E., Nielsen, T. G., Castonguay, M., Riemann, L., . . . Bachler, M. (2010). Oceanic fronts in the Sargasso Sea control the early life and drift of Atlantic eels. *Proceedings of the Royal Society of London B: Biological Sciences, 277*(1700), 3593–3599. doi:10.1098/rspb.2010.0900

Nishi, T., & Kawamura, G. (2005). *Anguilla japonica* is already magnetosensitive at the glass eel phase. *Journal of Fish Biology, 67*(5), 1213–1224. doi:10.1111/j.1095-8649.2005.00817.x

Nishi, T., Kawamura, G., & Matsumoto, K. (2004). Magnetic sense in the Japanese eel, *Anguilla japonica*, as determined by conditioning and electrocardiography. *Journal of Experimental Biology, 207*(17), 2965–2970. doi:10.1242/jeb.01131

NOAA. (2014). Bathymetry. *Ocean Facts.* Retrieved 2015 from http://oceanservice.noaa.gov/facts/bathymetry.html

Nybakken, J. W., & Bertness, M. D. (2005). Marine biology: An ecological approach (6th ed.). San Francisco: Benjamin Cummings.

Ogden, J. C. (1970). Relative abundance, food habits, and age of the American eel, *Anguilla rostrata* (LeSueur), in certain New Jersey streams. *Transactions of the American Fisheries Society, 99*(1), 54–59. doi:10.1577/1548–8659(1970)99<54:RAFHAA>2.0.CO;2

Oliveira, K. (1999). Life history characteristics and strategies of the American eel, *Anguilla rostrata*. *Canadian Journal of Fisheries and Aquatic Sciences, 56*(5), 795–802. doi:10.1139/f99-001

Oliveira, K., & Hable, W. E. (2010). Artificial maturation, fertilization, and early development of the American eel (*Anguilla rostrata*). *Canadian Journal of Zoology, 88*(11), 1121–1128. doi:10.1139/Z10-081

OMNR. (2009). Species at Risk in Ontario (SARO) List. Retrieved 2015 from http://www.ontario.ca/page/american-eel

Palm, S., Dannewitz, J., Prestegaard, T., & Wickstrom, H. (2009). Panmixia in European eel revisited: No genetic difference between maturing adults from southern and northern Europe. *Heredity, 103*(1), 82–89. doi:10.1038/hdy.2009.51

Palstra, A., van Ginneken, V., Murk, A. J., & van den Thillart, G. (2006). Are dioxin-like contaminants responsible for the eel (*Anguilla anguilla*) drama? *Naturwissenschaften, 93*(3), 145–148. doi:10.1007/s00114-005-0080-z

Palstra, A., Heppener, D., van Ginneken, V., Székely, C., & van den Thillart, G. (2007).

Swimming performance of silver eels is severely impaired by the swim-bladder parasite Anguillicola crassus. *Journal of Experimental Marine Biology and Ecology, 352*(1), 244–256. doi:10.1016/j.jembe.2007.08.003

Palstra, A., van Ginneken, V., & van den Thillart, G. (2009). Effects of swimming on silvering and maturation of the European Eel, *Anguilla anguilla* L. In G. van den Thillart, S. Dufour, & J. C. Rankin (Eds.), *Spawning Migration of the European Eel*, *Fish & Fisheries Series, 30*, 229-251: Springer Netherlands. doi:10.1007/978-1-4020-9095-0_10

Parson, L., & Edwards, R. (2011). The geology of the Sargasso Sea Alliance study area, potential non-living marine resources and an overview of the current territorial claims and coastal states Interests. *Sargasso Sea Alliance Science Report Series* (8). 17 pp. Retrieved in 2015 from http://www.sargassoalliance.org/storage/documents/No8_Geology_HI.pdf

Pujolar, J., Maes, G., & Volckaert, F. (2006). Genetic patchiness among recruits in the European eel, *Anguilla anguilla*. *Marine Ecology Progress Series, 307*, 209–217. doi:10.3354/meps307209

Pushcharovskii, Y. M. (2004). Deep-sea basins of the Atlantic Ocean. *Russian Journal of Earth Sciences, 6*(2). Retrieved in 2015 from http://elpub.wdcb.ru/journals/rjes/v06/tje04146/tje04146.htm

Putman, N. F., Endres, C. S., Lohmann, C. M. F., & Lohmann, K. J. (2011). Longitude perception and bicoordinate magnetic maps in sea turtles. *Current Biology, 21*(6), 463–466. doi:http://dx.doi.org/10.1016/j.cub.2011.01.057

Putman, N. F., Scanlan, M. M., Billman, E. J., O'Neil, J. P., Couture, R. B., Quinn, T. P., . . . Noakes, D. L. G. (2014). An inherited magnetic map guides ocean navigation in juvenile Pacific salmon. *Current Biology, 24*(4), 446–450. doi:http://dx.doi.org/10.1016/j.cub.2014.01.017

Reul, N., & Chapron, B. (2013). Cross-frontal exchanges of salt detected by SMOS in the Gulf Stream. *2014*. Retrieved in 2015 from http://www.salinityremotesensing.ifremer.fr/news/cross-frontalexchangesofsaltdetectedbysmosinthegulfstream

Richardson, P. L. (1993). A census of eddies observed in North Atlantic SOFAR float data. *Progress in Oceanography, 31*(1), 1–50. doi: 10.1016/0079-6611(93)90022-6

Richardson, P. L., Strong, A. E., & Knauss, J. A. (1973). Gulf Stream eddies: Recent observations in the western Sargasso Sea. *Journal of Physical Oceanography, 3*(3), 297–301. doi:10.1175/1520-0485(1973)003<0297:GSEROI>2.0.CO;2

Riemann, L., Nielsen, T., Kragh, T., Richardson, K., Parner, H., Jakobsen, H., & Munk, P. (2011). Distribution and production of plankton communities in the subtropical convergence zone of the Sargasso Sea. I. Phytoplankton and bacterioplankton.

Marine Ecology Progress Series, 426, 57–70. doi:10.3354/meps09001

Righton, D., Aarestrup, K., Jellyman, D., Sébert, P., van den Thillart, G., & Tsukamoto, K. (2012). The *Anguilla* spp. migration problem: 40 million years of evolution and two millennia of speculation. *Journal of Fish Biology, 81*(2), 365–386. doi:10.1111/j.1095-8649.2012.03373.x

Roberts, J. J., Best, B. D., Dunn, D. C., Treml, E. A., & Halpin, P. N. (2010). Marine geospatial ecology tools: An integrated framework for ecological geoprocessing with ArcGIS, Python, R, MATLAB, and C++. *Environmental Modelling & Software, 25*(10), 1197–1207. doi:10.1016/j.envsoft.2010.03.029

Robinet, T., & Feunteun, E. (2002). Sublethal effects of exposure to chemical compounds: A cause for the decline in Atlantic eels? *Ecotoxicology, 11*(4), 265–277. doi:10.1023/A:1016352305382

Robins, C. R., Cohen, D. M., & Robins, C. H. (1979). The eels, *Anguilla* and *Histiobranchus*, photographed on the floor of the deep Atlantic in the Bahamas. *Bulletin of Marine Science, 29*(3), 401–405. Retrieved in 2015 from http://www.ingentaconnect.com/content/umrsmas/bullmar/1979/00000029/00000003/art00011

Sale, P. F., Cowen, R. K., Danilowicz, B. S., Jones, G. P., Kritzer, J. P., Lindeman, K. C., . . . Steneck, R. S. (2005). Critical science gaps impede use of no-take fishery reserves. *Trends in Ecology & Evolution, 20*(2), 74–80. doi: 10.1016/j.tree.2004.11.007.

Santillo D., Allsopp M., Walters A., Johnston P., & Perivier, H. (2006). Presence of perfluorinated chemicals in eels from 11 European countries. *Greenpeace Research Laboratories Technical Note, 07/2006*. Retrieved in 2015 from http://www.greenpeace.to/publications/perfluorinated-chemicals-eels.pdf

Schmidt, J. (1919). Stations in the Atlantic, etc. 1911–15 with two charts and introductory remarks. *Meddelelser fra Kommissionen for Havundersøgelser, Fiskeri 5* (7):1–29.

Schmidt, J. (1923). The breeding places of the eel. *Philosophical Transactions of the Royal Society of London. Series B, Containing Papers of a Biological Character(211),* 179-208. Retrieved from http://www.jstor.org/stable/92087

Schmidt, J. (1929). Introduction to the oceanographical reports including list of the stations and hydrographical observations The Danish "Dana" Expeditions 1920–22 in the North Atlantic and the Gulf of Panama. Leader: Professor Johs. Schmidt. *Oceanographical Reports Edited by the "Dana" Committee, 1*, 1–87. Copenhagen: Gyldendalske.

Schoth, M. (1982). Taxonomic studies on the 0-group eel larvae (*Anguilla* sp.) caught in the Sargasso Sea in 1979. *Helgoländer Meeresuntersuchungen, 35*(3), 279–287.

doi:10.1007/BF02006136

Schoth, M., & Tesch, F. W. (1982). Spatial distribution of 0-group eel larvae (*Anguilla* sp.) in the Sargasso Sea. *Helgoländer Meeresuntersuchungen, 35*(3), 309–320. doi:10.1007/BF02006139

Siegel, D. A., Kinlan, B. P., Gaylord, B., & Gaines, S. D. (2003). Lagrangian descriptions of marine larval dispersion. *Marine Ecology Progress Series, 260*, 83-96. doi:10.3354/meps260083

Smith, D. G. (1968). The occurrence of larvae of the American eel, *Anguilla rostrata*, in the Straits of Florida and nearby areas. *Bulletin of Marine Science* 18:280–293. Retrieved 2015 from http://www.ingentaconnect.com/content/umrsmas/bullmar/1968/00000018/00000002/art00002

Smith, M. W., & Saunders, J. W. (1955). The American eel in certain fresh waters of the Maritime Provinces of Canada. *Journal of the Fisheries Research Board of Canada, 12*(2), 238–269. doi:10.1139/f55-016

Souza, J. J., Poluhowich, J. J., & Guerra, R. J. (1988). Orientation responses of American eels, *Anguilla rostrata*, to varying magnetic fields. *Comparative Biochemistry and Physiology, 90*(1), 57–61. doi:10.1016/0300-9629(88)91005-5

Sparholt, H. (2007). [Station and Haul data, HMDS Vaedderren (Cruise 17, Galathea 3)]. Unpublished raw data.

Sverdrup, K. A., & Armbrust, E. V. (2008). *An Introduction to the World's Oceans* (9th ed.). New York, NY: McGraw-Hill.

Swift, S. A., Bolmer, S. T., & Stephen, R. A. (1989). *Site synthesis report of DSDP sites 417 and 418*. (No. WHOI-89-20). Woods Hole Oceanographic Institution. Accession number: ADA258461. Retrieved in 2015 from http://www.dtic.mil/cgi-bin/GetTRDoc?Location=U2&doc=GetTRDoc.pdf&AD=ADA258461

Tesch, F. W. (1977). *The eel : Biology and management of anguillid eels*. (P.H. Greenwood, Eng. Ed., J. Greenwood, Trans.);. London: Chapman and Hall.

Tesch, F. W., Thorpe, J.E. (Ed.), & White, R. J. (2003). *The eel* (5th Ed.). Oxford: Wiley-Blackwell.

Tesch, F. W., & Lelek, A. (1973). Directional behaviour of transplanted stationary and migratory forms of the eel, *Anguilla anguilla*, in a circular tank. *Netherlands Journal of Sea Research, 7*(0), 46–52. doi:10.1016/0077-7579(73)90031-8

Tesch, F. W., & Wegner, G. (1990). The distribution of small larvae of *Anguilla* sp. related to hydrographic conditions 1981 between Bermuda and Puerto Rico. *Internationale Revue der gesamten Hydrobiologie und Hydrographie, 75*(6), 845–858. doi:10.1002/iroh.19900750629

The Ring Group. (1981). Gulf Stream cold-core rings: Their physics, chemistry, and biology. *Science, 212*(4499), 1091–1100. doi:10.2307/1685370

Thébault, E., & Mandea-Alexandrescu, M. (2007). *The changing faces of the Earth's magnetic field: A glance at the magnetic lithospheric field, from local and regional scales to a planetary view*. Commission for the Geological Map of the World. Paris: Commission for the Geological Map of the World, 49 & CD-ROM.

Tomczak, M., & Godfrey, J. S. (2003). *Regional oceanography: An introduction* (pdf version 1.1 reprint of 1st ed. New York, NY: Elesvier Science.) Retrieved in 2015 from http://www.es.flinders.edu.au/~mattom/regoc/pdfversion.html

Tsukamoto, K. (2006). Oceanic biology: Spawning of eels near a seamount. *Nature, 439*(7079), 929–929. doi:10.1038/439929a

Tsukamoto, K. (2009). Oceanic migration and spawning of anguillid eels. *Journal of Fish Biology, 74*(9), 1833–1852. doi:10.1111/j.1095-8649.2009.02242.x

Tsukamoto, K., Aoyama, J., & Miller, M. J. (2002). Migration, speciation, and the evolution of diadromy in anguillid eels. *Canadian Journal of Fisheries and Aquatic Sciences, 59*(12), 1989–1998. doi:10.1139/f02-165

Tsukamoto, K., Chow, S., Otake, T., Kurogi, H., Mochioka, N., Miller, M. J., . . . Tanaka, H. (2011). Oceanic spawning ecology of freshwater eels in the western North Pacific. *Nature Communications, 2*, 179.

Tsukamoto, K., & Kuroki, M. (2014). *Eels and humans*. Tokyo: Springer Japan.

Tsukamoto, K., Otake, T., Mochioka, N., Lee, T.W., Fricke, H., Inagaki, T., . . . Suzuki, Y. (2003). Seamounts, new moon and eel spawning: The search for the spawning site of the Japanese eel. *Environmental Biology of Fishes, 66*(3), 221–229. doi:10.1023/a:1023926705906

Tsukamoto, K., Yamada, Y., Okamura, A., Kaneko, T., Tanaka, H., Miller, M. J., . . . Tanaka, S. (2009). Positive buoyancy in eel leptocephali: An adaptation for life in the ocean surface layer. *Marine Biology, 156*(5), 835–846. doi:10.1007/s00227-008-1123-8

Aoyama, J., Hissmann, K., Yoshinaga, T., Sasai, S., Uto, T., & Ueda, H. (1999). Swimming depth of migrating silver eels *Anguilla japonica* released at seamounts of the West Mariana Ridge, their estimated spawning sites. *Marine Ecology Progress Series, 186*, 265-269. doi:10.3354/meps186265

Ullman, D. S., Cornillon, P. C., & Shan, Z. (2007). On the characteristics of subtropical fronts in the North Atlantic. *Journal of Geophysical Research: Oceans, 112*(C1), C01010. doi:10.1029/2006JC003601

UNEP. (2008). Decision adopted by the conference of the parties to the Convention on

Biological Diversity at its ninth meeting: IX/20. Marine and coastal biodiversity, Agenda item 4.9. Bonn, 19–30 May 2008. Retrieved 2015 from http://www.cbd.int/doc/decisions/cop-09/cop-09-dec-20-en.pdf

USFWS. (2007). *12-Month Finding on a Petition To List the American eel as Threatened or Endangered*. 72 Federal Register. 4967–4997. Retrieved 2015 from http://edocket.access.gpo.gov/2007/pdf/07-429.pdf

USFWS. (2011). American eel may warrant protection under the Endangered Species Act. U.S. Fish and Wildlife Service, Northeast Region. Retrieved 2015 from http://www.fws.gov/northeast/news/2011/092811.html

van den Thillart, G., Palstra, A., & van Ginneken, V. (2009). Energy requirements of European eel for TransAtlantic spawning migration. In G. van den Thillart, S. Dufour, & J. C. Rankin (Eds.), *Spawning migration of the European eel (30*) 179–199: Springer Netherlands. doi: 10.1007/978-1-4020-9095-0_8

van Ginneken, V., Antonissen, E., Muller, U. K., Booms, R., Eding, E., Verreth, J., & van den Thillart, G. (2005). Eel migration to the Sargasso: Remarkably high swimming efficiency and low energy costs. *Journal of Experimental Biology, 208*(7), 1329–1335. doi:10.1242/jeb.01524

van Ginneken, V., Ballieux, B., Willemze, R., Coldenhoff, K., Lentjes, E., Antonissen, E., . . . van den Thillart, G. (2005). Hematology patterns of migrating European eels and the role of EVEX virus. *Comparative Biochemistry and Physiology Part C: Toxicology & Pharmacology, 140*(1), 97–102. doi:http://dx.doi.org/10.1016/j.cca.2005.01.011

van Ginneken, V., Bruijs, M., Murk, T., Palstra, A., & van den Thillart, G. (2009). The effect of PCBs on the spawning migration of European silver eel (*Anguilla anguilla* L.). In G. van den Thillart, S. Dufour, & J. C. Rankin (Eds.), *Spawning Migration of the European Eel (30*) 365–386: Springer Netherlands.

van Ginneken, V., Durif, C. M. F., Balm, S. P., Boot, R., Verstegen, M., Antonissen, E., & van Den Thillart, G. (2007). Silvering of European eel (*Anguilla anguilla* L.): Seasonal changes of morphological and metabolic parameters. *Animal Biology, 57*(1), 63–77. doi:doi:10.1163/157075607780002014

Vine, F. J., & Matthews, D. H. (1963). Magnetic anomalies over oceanic ridges. *Nature*, 199(4897), 947–949. doi:10.1038/199947a0

Vogt, P. R., & Jung, W.Y. (2007). Origin of the Bermuda volcanoes and the Bermuda Rise: History, observations, models, and puzzles. *Geological Society of America Special Papers, 430*, 553–591. doi:10.1130/2007.2430(27)

Volckaert, F., Maes, G., & Pujolar, M. (2005). Management implications of panmixia, introgression and a reduced reproductive potential the case of the European eel. *Theme session on integrating/implicating genetics into fisheries management.*

International Council for Exploration of the Sea. Retrieved 2015 from http://www.ices.dk/sites/pub/CM%20Doccuments/2005/T/T-2005.pdf

Wahlberg, M., Westerberg, H., Aarestrup, K., Feunteun, E., Gargan, P., & Righton, D. (2014). Evidence of marine mammal predation of the European eel (*Anguilla anguilla* L.) on its marine migration. *Deep Sea Research Part I: Oceanographic Research Papers, 86*(0), 32–38. doi:10.1016/j.dsr.2014.01.003

Walker, M. M., Kirschvink, J. L., Ahmed, G., & Dizon, A. E. (1992). Evidence that fin whales respond to the geomagnetic field during migration. *Journal of Experimental Biology, 171*(1), 67–78.

Westerberg, H., & Lagenfelt, I. (2008). Sub-sea power cables and the migration behaviour of the European eel. *Fisheries Management and Ecology, 15*(5–6), 369–375. doi:10.1016/j.dsr.2014.01.003

Wippelhauser, G. S., McCleave, J. D., & Kleckner, R. C. (1985). *Anguilla rostrata* leptocephali in the Sargasso Sea during February and March 1981. *Dana, 4*, 93. Retrieved 2015 from http://www.aqua.dtu.dk/English/Publications/Dana.aspx

Wirth, T., & Bernatchez, L. (2001). Genetic evidence against panmixia in the European eel. *Nature, 409*(6823), 1037. doi:10.1038/35059079

Wirth, T., & Bernatchez, L. (2003). Decline of North Atlantic eels: A fatal synergy? *Proceedings of the Royal Society of London B: Biological Sciences, 270*(1516), 681–688. doi:10.1098/rspb.2002.2301

Wysujack, K., Westerberg, H., Aarestrup, K., Trautner, J., Kurwie, T., Nagel, F., & Hanel, R. (2015). The migration behaviour of European silver eels (*Anguilla anguilla*) released in open ocean conditions. *Marine and Freshwater Research, 66*(2), 145–157. doi:http://dx.doi.org/10.1071/MF14023

Appendix A

Definition of Terms

For the purpose of this study reference to Atlantic eels refers collectively to both species of Anguillid eels found in the North Atlantic Ocean, the American eel (*Anguilla rostrata*) and the European eel (*Anguilla anguilla*). While the two species hatch and spawn in the marine environment, these and other members of the anguillid taxonomic family are commonly referred to in this report, as elsewhere, as ”freshwater eels”, distinguishing them from non-anguillid marine eels, i.e. those who live solely in a marine environment.

Other definitions:

Abyssal gap – a constricted and steeply slowing passage that connects two separated abyssal plains lying on different levels (Heezen et al., 1959).

Abyssal plain – a typically flat and vast submarine plain that extends from the steep continental slope in deep waters generally it depths below 4000 m (Sverdrup & Armbrust, 2008).

Bathymetry – the study of the features of the floor of an ocean or other water body, refers to the submarine topography formed by the depths, shapes and other variations of the ocean floor (NOAA, 2014).

Catadromous – A catadromous fish spends most of its life in inland or estuarine waters and then returns at the end of its life to spawn in the open ocean (Facey & van Den Avyle, 1987).

Diurnal or Diel Vertical Migration (DVM) – The daily migration of zooplankton and fish through the water column in response to daylight and nighttime darkness, typically changing depths from 100 to 400 meters. Potential reasons for DVM include avoidance of predators or solar radiation, or advantageous positions or resources at the different depths (Nybakken & Bertness, 2005).

Elver – A small pigmented, immature eel, metamorphosed from a glass eel stage, which travels inland, or resides in estuaries, before its maturation into a yellow eel (Facey & van Den Avyle, 1987).

GIS (Geographic Information Systems) – The organized capture, storage, management, retrieval, analysis and display of spatial data with the aid of computer hardware, software, geographic data and personnel. GIS, also known as geographic information sciences, helps people to visualize and understand spatial and geographical relationships (Maguire, Goodchiled, & Rhinds, 1991).

Glass eel – An early life-stage of the eels attained as it approaches the coastal regions, metamorphosing metamorphoses from the larval stage into an un-pigmented eel-like organism (USGS).

Group 0 larvae and fish –in their first year of life.

Hydrography – The study of the bathymetry, shoreline, tides, currents, waves and physical and chemical properties of the water (NOAA, 2014) (http://oceanservice.noaa.gov/facts/bathymetry.html).

Lagrangian models predict trajectory drift of particles in fluid environments (air or water) and may integrate account biological variables reflecting behavior or life cycles for ecological modeling (Siegel, Kinlan, Gaylord, & Gaines, 2003).

Leptocephali – flat, leaf-like eel larvae of freshwater and marine eels and other members of the Superorder (Facey & van Den Avyle, 1987; Miller, 2009).

Mid-Atlantic Ridge (MAR) – A submarine mountain range extending from Iceland into the Southern Atlantic Ocean, bisecting the Atlantic into its east and west basins. The Azores, Ascension and Tristan da Cunha islands are surface features of the ridge (Nybakken & Bertness, 2005).

North Atlantic Oscillation (NAO) – Fluctuations in atmospheric pressure between a subtropical high pressure system over the Azores and a low pressure system above Iceland. The NAO dominates climate in much of the Northern Hemisphere and influences temperature and currents in the North Atlantic (IPCC, 2007).

Panmictic – A population or species with little or no genetic differentiation due to random and unstructured mating (Als et al., 2011)

Population Viability Analysis (PVA) – Simulation models that predict how changes in the environment or other factors will affect a population in the long term. PVAs assist in conservation planning by showing potential outcomes of management decisions (Begon, Townsend, & Harper, 2006).

Silver eel – An adult eel that only reaches full maturity as it prepares for ocean migration (Facey & van Den Avyle, 1987).

Speciation – refers to the processes by which new species are formed, as for example when natural selection of a geographically isolated sub-population results in their genetic differentiation and subsequent reproductive isolation (Begon et al., 2006).

Subtropical Convergence Zone (STCZ) – A dynamic zone of steep thermal gradients where cold northern waters converge with warmer tropical waters, created by

the transition of Westerlies to the north and the easterly Trade Winds in the south and generally occurring between 22° N and 32° N. (Riemann et al., 2011; Ullman et al., 2007).

Yellow eel – A juvenile eel living in estuarine or inland waters (Facey & van Den Avyle, 1987).

Appendix B

Counts of Size Groups in Study Areas

Table B1. Counts of larvae observations per size group in study areas.

Species	0–7 mm (*n*)	0–10 mm (*n*)	10–20 mm (*n*)	20–30 mm (*n*)	30–40 mm (*n*)	40–50 mm (*n*)	50–60 mm (*n*)	> 60 mm (*n*)
N. Atlantic								
A. rostrata	385	1,243	3,403	1,477	1,218	1,322	737	35
A. anguilla	723	2,259	5,740	4,710	1,563	1026	1,082	4658
Study Area 1								
A. rostrata	385	1243	3403	1,477	1218	1200	529	3
A. anguilla	723	2259	5740	4,710	1499	851	58	0
Study Area 2								
A. rostrata	385	1243	3390	1196	1095	989	272	0
A. anguilla	723	2259	5687	4559	980	327	3	0

Appendix C

Sampling Year Frequencies

Table C1. Sampling year frequencies.

Year	n	% total	Year	n	% total
1922	197	9.1	1930	53	2.4
1984	188	8.7	2007	52	2.4
1964	176	8.1	1972	46	2.1
1979	156	7.2	1906	43	2.0
1921	146	6.7	1977	37	1.7
1983	137	6.3	1966	32	1.5
1981	112	5.2	1970	32	1.5
1978	86	4.0	1962	24	1.1
1920	81	3.7	1968	24	1.1
1913	79	3.6	1910	23	1.1
1985	78	3.6	1965	23	1.1
1931	57	2.6	1914	21	1.0
			1976	21	1.0

Appendix D

Null Data Sources

Backus, R. H. (1978). [*Cruise report, R/V Oceanus* (*OC49)*], Woods Hole Oceanic Institution Archives, Data Library and Archives.

Bayer, F. (1966). Dredging and trawling records of R/V John Elliot Pillsbury for 1964 and 1965. *Studies in Tropical Oceanography, 4*(1), 82–105.

Boëtius, J., & Harding, E. F. (1985). List of Atlantic and Mediterranean *Anguilla* leptocephali: Danish material up to 1966. *Dana, 4*,163–249.

Boëtius, J., & Harding, E. F. (1985). A re-examination of Johannes Schmidt's Atlantic eel investigations. *Dana, 4*, 129–162.

Eldred, B. (1968). Larvae and glass eels of the American freshwater eel, *Anguilla rostrata* (Lesueur, 1817) in Florida waters. *Florida Board of Conservation: Marine Research Laboratory Leaflet Series 4 part 1*, (9).

Eldred, B. (1971). First records of *Anguilla rostrata* larvae in the Gulf of Mexico and Yucatan Straits. *Florida Department of Natural Resources*: *Marine Research Laboratory Leaflet Series 4 part 1*(19), 1–3.

Howland, P. C., (1978). [Ship's Log, R/V Oceanus (OC49)]. Woods Hole Oceanic Institution, Data Library and Archives.

Jespersen, P., & Tåning. (1934). Introduction to the reports from the Carlsberg Foundation's oceanographic expeditions around the world 1928–30. The Carlsberg Foundation, Copenhagen. *Dana-Report, 1*, 1–77.

McCleave, J. D. (1983). [Station and Haul Data, R/V Cape Florida (CF8303)]. Unpublished raw data.

McCleave, J. D. (1983). [Station and Haul Data, R/V Cape Florida (CF8305)]. Unpublished raw data.

McCleave, J. D. (1984). [Station and Haul Data, R/V Columbus Iselin (CI8408)]. Unpublished raw data. (J. D McCleave, 1984)

McCleave, J. D. (1984). [Station and Haul Data, R/V Columbus Iselin (CI8410)]. Unpublished raw data.

McCleave, J. D. (1985) [Station and Haul Data, R/V Cape Florida (CF8503)]. Unpublished raw data.

Schmidt, J. (1919). Stations in the Atlantic, etc. 1911–15 with two charts and introductory remarks. *Meddelelser fra Kommissionen for Havundersøgelser, Fiskeri 5* (7):1–29.

Schmidt, J. (1929). Introduction to the oceanographical reports including list of the stations and hydrographical observations The Danish "Dana" Expeditions 1920–22 in the North Atlantic and the Gulf of Panama. Leader: Professor Johs. Schmidt. *Oceanographical Reports Edited by the "Dana" Committee, 1*, 1–87. Copenhagen: Gyldendalske.

Schoth, M., & Tesch, F. W. (1982). Spatial distribution of 0-group eel larvae (*Anguilla* sp.) in the Sargasso Sea. *Helgoländer Meeresuntersuchungen, 35*(3), 309–320.

Smith, D. G. (1968). The occurrence of larvae of the American eel, *Anguilla rostrata*, in the Straits of Florida and nearby areas. *Bulletin of Marine Science* 18:280–293.

Sparholt, H. (2007). [Station and Haul data, HMDS Vaedderren (Cruise 17, Galathea 3)] Unpublished raw data.

Appendix E

List of Ships

Table E1. Ships in the data set.

Ship	Stations	Start Date	End Date	Larvae (*n*)	Null Stations	Positive Stations	*A. anguilla* (*n*)	*A. rostrata* (*n*)	Stations finding both species
(Belloc)	5	1928-Apr-08	1928-Dec-08	116	0	5	0	116	0
(Hansen)	1	1911-Jul-04	1911-Jul-04	1	0	1	0	1	0
(Lango)	1	1930-Mar-05	1930-Mar-05	19	0	1	0	19	0
(Trombetta)	1	1911-Apr-25	1911-Apr-25	1	0	1	0	1	0
Agent Petersen	4	1912-Apr-19	1913-Jun-25	27	0	4	0	27	0
Alaminos	1	1968-Oct-31	1968-Oct-31	1	0	1	1	0	0
Albatross	2	1883-11-06	1883-11-06	2	0	2	2	0	0

Ship	Stations	Start Date	End Date	Larvae (*n*)	Null Stations	Positive Stations	*A. anguilla* (*n*)	*A. rostrata* (*n*)	Stations finding both species
Albatross IV	1	1972-Nov-03	1972-Nov-03	1	0	1	1	0	0
Alert	3	2007-Nov-04	2007-Dec-04	38	0	3	4	34	2
Algarve	1	1912-May-05	1912-May-05	1	0	1	0	1	0
Anton Bruun	4	1966-Oct-13	1966-Oct-16	4	0	4	4	0	0
Anton Dohrn	138	1966-Oct-17	1979-May-07	2961	90	48	1452	1509	24
Arkansas	2	1912-Apr-23	1912-Apr-24	2	0	2	0	2	0
Armauer Hansen	3	1922-Feb-06	1922-Nov-05	5	0	3	0	5	0
Atlantis	37	1931-Jul-14	1962-Sep-26	390	0	37	79	311	15
Atlantis II	54	1964-Sep-03	1973-Sep-05	420	0	54	84	336	12
Bache	14	1914-Jan-30	1914-Feb-28	42	0	14	11	31	3
Baffin	1	1966-Mar-27	1966-Mar-27	4	0	1	0	4	0
BEL	2	1975-Oct-28	1975-Oct-28	5	0	2	5	0	0

Ship	Stations	Start Date	End Date	Larvae (*n*)	Null Stations	Positive Stations	*A. anguilla* (*n*)	*A. rostrata* (*n*)	Stations finding both species
Bintang	4	1914-May-12	1915-Sep-07	33	0	4	0	33	0
Biologen	2	1958-Mar-23	1959-Jul-04	2	0	2	0	2	0
Blue Dolphin	2	1953-Aug-19	1953-Aug-26	39	0	2	39	0	0
Cape Florida	209	1983-Feb-13	1985-Mar-29	1615	95	114	604	1011	56
Cape Hatteras	2	2001-Aug-24	2001-Aug-24	4	0	2	4	0	0
Chain	94	1961-May-10	1972-Dec-07	824	0	94	544	280	11
Columbus Iselin	183	1981-Feb-14	1989-Feb-16	1226	80	103	960	266	48
Crawford	5	1961-Apr-05	1968-Nov-08	14	0	5	13	1	0
CRY	3	1905-May-27	1905-May-27	3	0	3	3	0	0
Dana I	132	1920-Mar-18	1921-May-12	7951	56	76	1807	6144	36
Dana II	375	1921-Sep-03	1934-Jul-05	7747	202	173	423	7324	9
Dana III	61	1938-Jun-21	1966-Dec-04	567	0	61	1	566	1

Ship	Stations	Start Date	End Date	Larvae (*n*)	Null Stations	Positive Stations	*A. anguilla* (*n*)	*A. rostrata* (*n*)	Stations finding both species
Edwin Link	1	2000-Jul-22	2000-Jul-22	1	0	1	1	0	0
Endeavor	5	1977-Feb-08	1977-Aug-14	17	0	5	8	9	3
Florida	1	1911-Jul-21	1911-Jul-21	1	0	1	0	1	0
Friedrich Heincke	62	1979-Feb-27	1981-May-08	2954	8	54	2127	827	31
Gerda	16	1962-Aug-27	1966-Apr-27	77	0	16	77	0	0
Hernan Cortez	1	1968-Jul-25	1968-Jul-25	1	0	1	1	0	0
Hudson	5	1965-Jan-01	1968-May-02	7	0	5	1	6	0
Ingolf	4	1911-Mar-22	1913-Jan-03	4	0	4	0	4	0
Johannes Hage	3	1862-06-16	1863-02-02	3	0	3	1	2	0
Johansen	2	1922-Feb-10	1922-Oct-14	2	0	2	0	2	0
Knorr	30	1974-Mar-16	1977-Oct-30	51	0	30	11	40	0
Margrethe	73	1913-Jul-16	1913-Dec-20	726	38	35	24	703	4

Ship	Stations	Start Date	End Date	Larvae (*n*)	Null Stations	Positive Stations	*A. anguilla* (*n*)	*A. rostrata* (*n*)	Stations finding both species
NoID_Bowman	5	1906-Jul-06	1911-Aug-23	13	0	5	0	13	0
NoID_Hain	13	1968-Mar-20	1978-Mar-20	34	0	13	34	0	0
NoID_Hopkins	1	1980-Nov-18	1980-Nov-18	1	0	1	1	0	0
NoID_Huntsman	33	1977-Aug-15	1989-Aug-11	46	0	33	20	26	0
NoID_Krueger	1	1976-Oct-06	1976-Oct-06	3	0	1	3	0	0
NoID_MCZ	5	1962-Sep-24	1968-Feb-05	72	0	5	8	64	3
NoID_Power	1	1978-Aug-09	1978-Aug-09	45	0	1	9	36	1
NoID_Smith	14	1962-Jun-19	1980-Sep-12	51	0	14	50	1	0
NoID_Taning	40	1929-May-10	1931-Sep-19	46	0	40	17	29	0
Oceanus	106	1970-Feb-23	1979-Nov-02	805	6	100	715	90	21
Panuliris I	1	1968-Jan-18	1968-Jan-18	1	0	1	0	1	0
Pennsylvania	4	1911-Oct-09	1913-Jun-10	11	0	4	2	9	0

Ship	Stations	Start Date	End Date	Larvae (*n*)	Null Stations	Positive Stations	*A. anguilla* (*n*)	*A. rostrata* (*n*)	Stations finding both species
Pillsbury	136	1964-Jul-24	1964-Aug-13	192	113	23	177	15	1
Poseidon	5	1993-Feb-21	1993-Mar-25	6	0	5	2	4	0
Prof Siedlecki	59	1984-Jul-25	1985-Apr-16	376	0	59	1	375	1
Rhodesia	1	1915-Jan-03	1915-Jan-03	1	0	1	0	1	0
Samui	6	1914-Mar-16	1914-Jun-13	26	0	6	0	26	0
San Pablo	2	1951-Feb-17	1951-Feb-21	9	0	2	0	9	0
Seward Johnson II	1	2001-Sep-23	2001-Sep-23	2	0	1	2	0	0
St. Croix	1	1911-Dec-08	1911-Dec-08	3	0	1	0	3	0
St. Jan	2	1911-Nov-29	1912-Jan-03	2	0	2	0	2	0
St. Thomas	1	1911-Dec-29	1911-Dec-29	1	0	1	0	1	0
Thor	94	1904-May-22	1910-Sep-17	891	0	94	0	891	0
Tranquebar	2	1915-Jun-22	1915-Sep-26	9	0	2	0	9	0

Ship	Stations	Start Date	End Date	Larvae (*n*)	Null Stations	Positive Stations	*A. anguilla* (*n*)	*A. rostrata* (*n*)	Stations finding both species
Tridens	3	1982-Nov-01	1982-Nov-01	25	0	3	0	25	0
Trident	13	1970-Aug-20	1970-Sep-07	15	0	13	0	15	0
Tursiops	4	1965-May-04	1965-Aug-01	4	0	4	4	0	0
Tydeman	11	1980-Apr-18	1981-Oct-05	53	0	11	0	53	0
Undaunted	2	1966-May-07	1966-May-08	2	0	2	0	2	0
Unifientified_Eldre d	1	1963-Aug-07	1963-Aug-07	2	0	1	2	0	0
Upsala	1	1895-03-16	1895-03-16	2	0	1	0	2	0
Vaedderen	49	2007-Mar-04	2007-Aug-04	271	9	40	108	163	18
VIAX	1	1905-May-24	1905-May-24	1	0	1	1	0	0
WIE(X)	4	1905-May-26	1905-May-26	10	0	4	10	0	0
(blank)									

Ship	Stations	Start Date	End Date	Larvae (*n*)	Null Stations	Positive Stations	*A. anguilla* (*n*)	*A. rostrata* (*n*)	Stations finding both species
Grand Total	2173		2007-Dec-04	30940	697	1476	9458	21483	300

Appendix F

Selected Cruise Tracklines

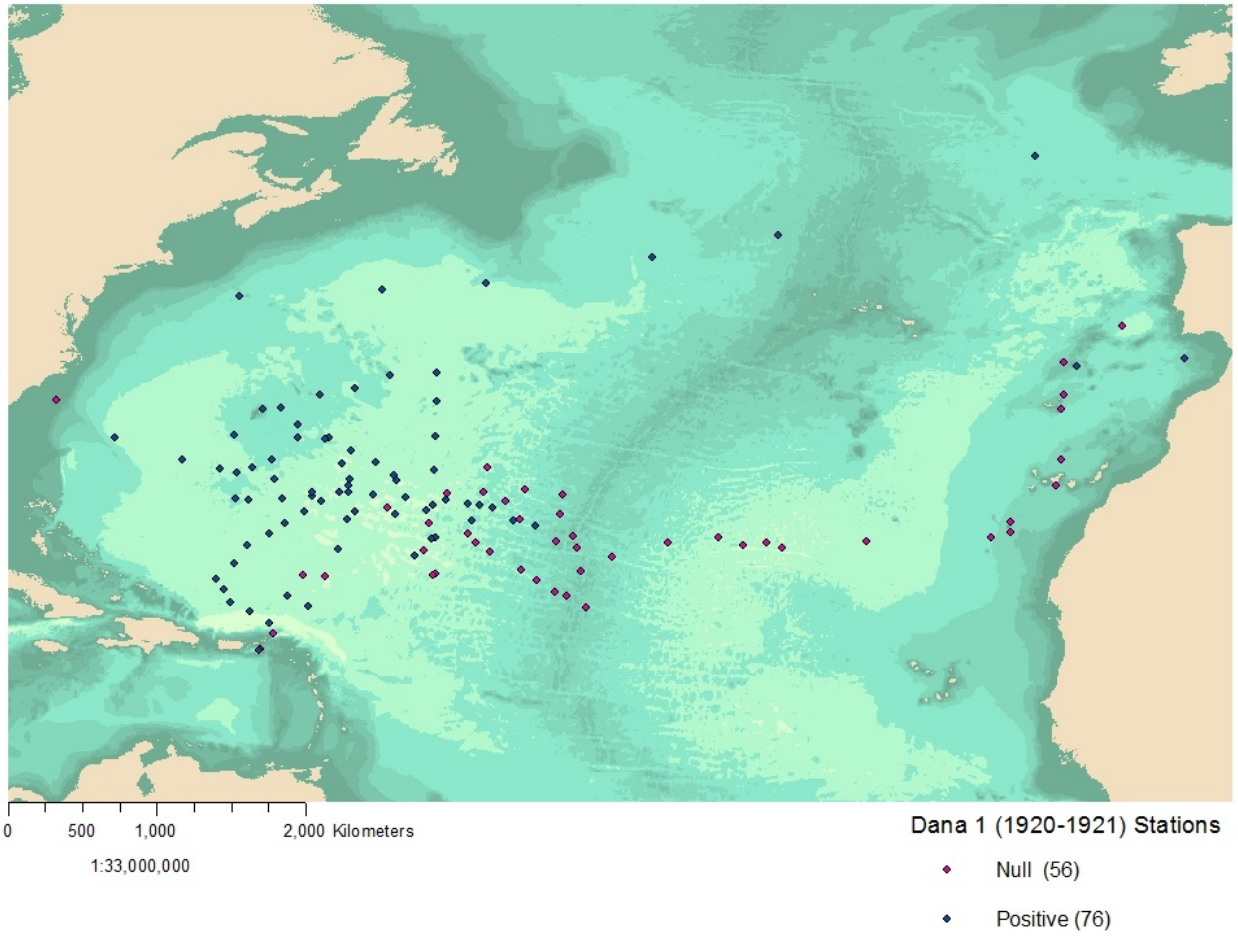

Figure F1. Dana 1 (1920–1921). The Dana I research vessel sampled at 132 stations under the direction of Johannes Schmidt from 1920 to 1921. Anguillid eel larvae were recorded present at 76 stations, but none were recorded at the other 56 stations.

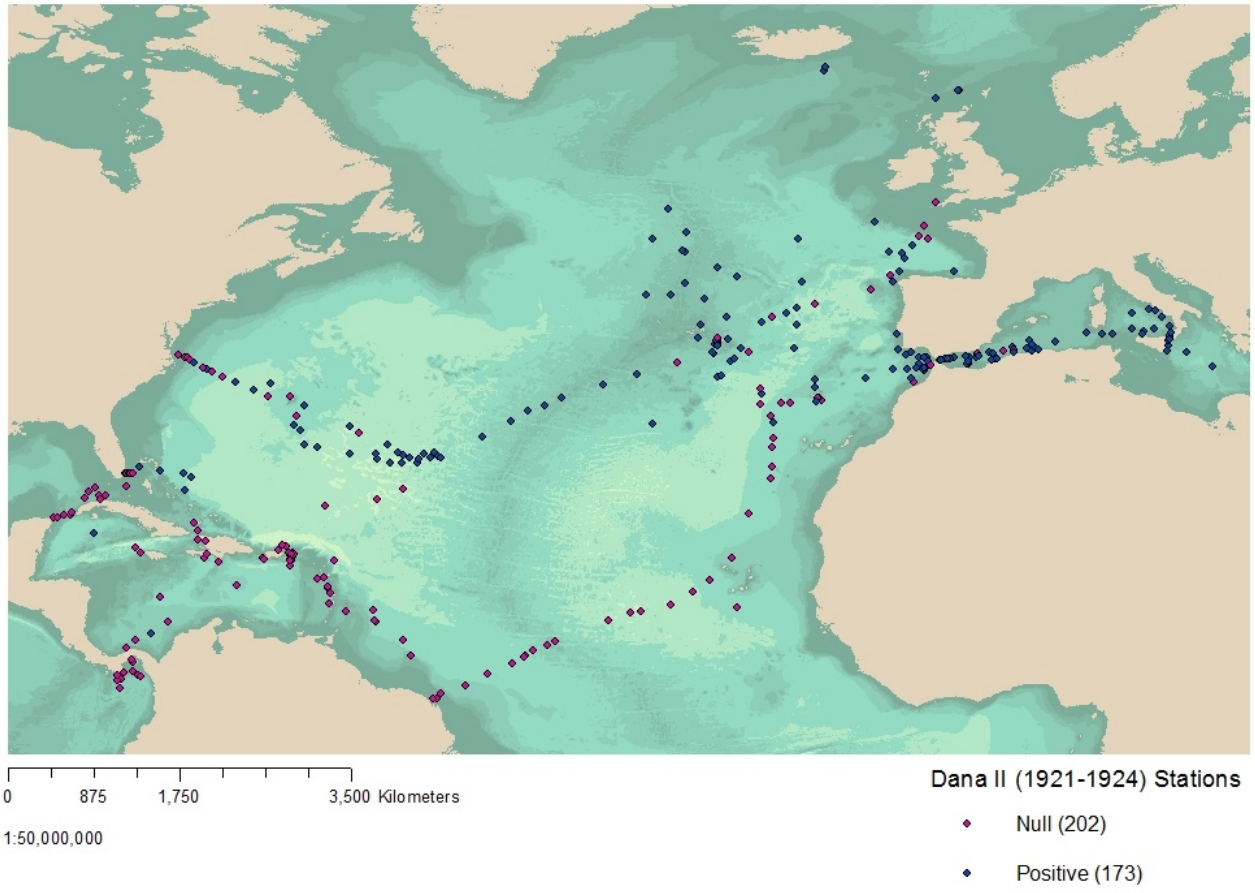

Figure F2. Dana II (1921–1924). The Dana II research vessel sampled at 375 stations under the direction of Johannes Schmidt from 1921 to 1934. Anguillid eel larvae were recorded present at 173 stations, but no larvae were recorded as present for the other 202 stations.

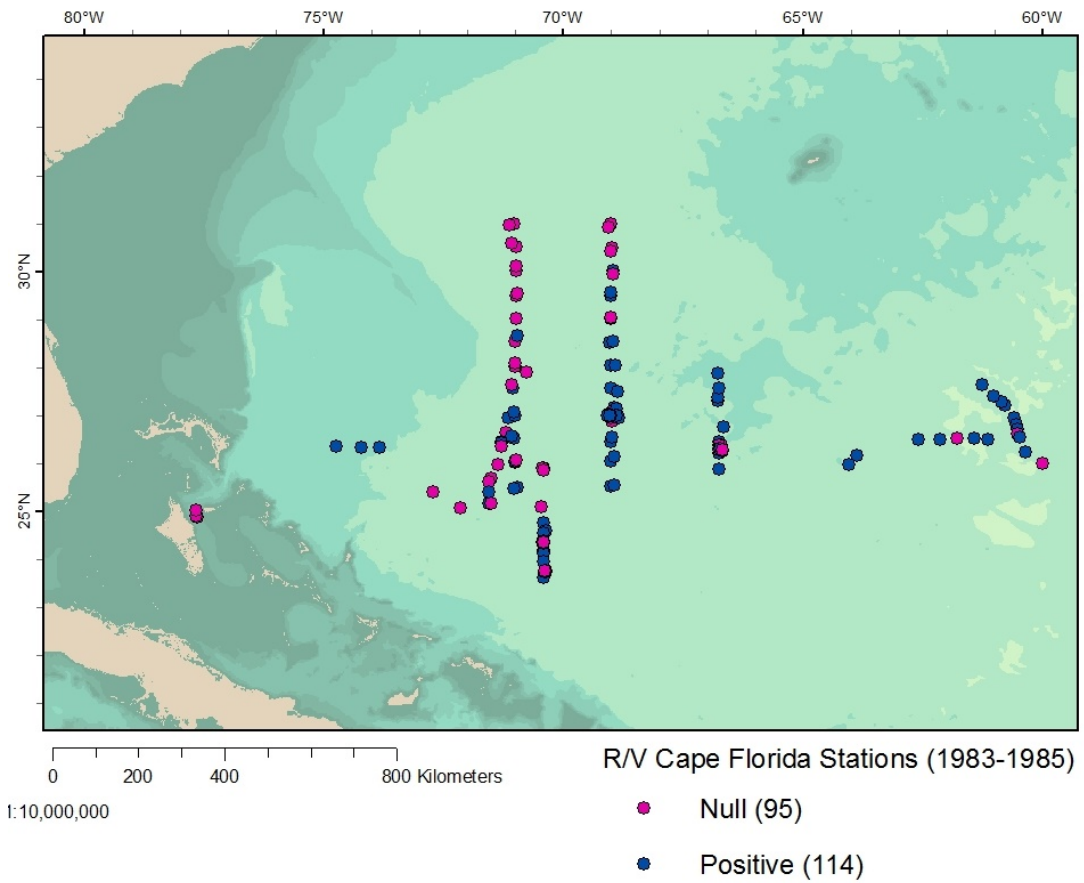

Figure F3. R/V Cape Florida (1983–1985). The Cape Florida sampled at 209 stations between 1983 and 1985. Anguillid larvae found at 114 stations and none reported at 95 stations.

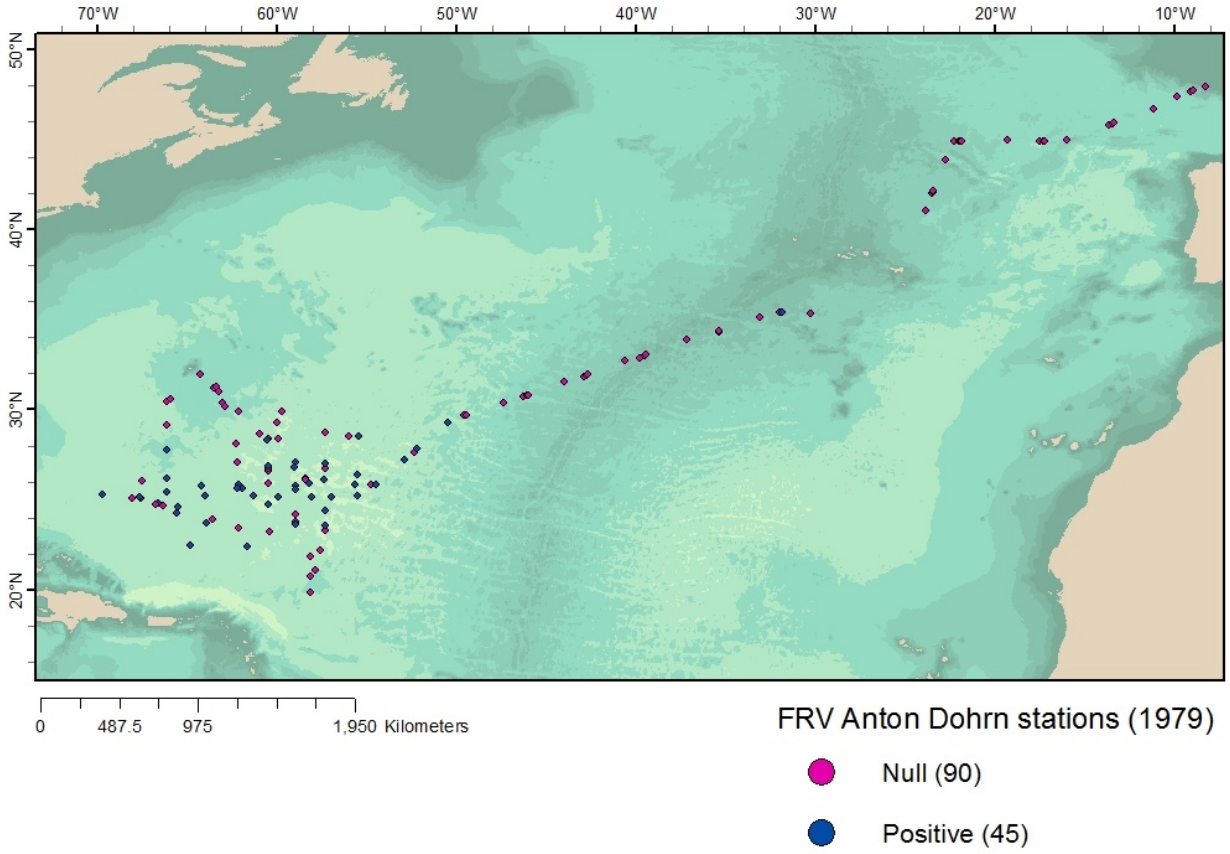

Figure F4. FRV Anton Dohrn (1979). The Fisheries Research Vessel (FRV) Anton Dohrn sampled at 135 stations in 1979. Anguillid larvae were found present at 45 of the stations. Ninety (90) stations did not record any positive finds.

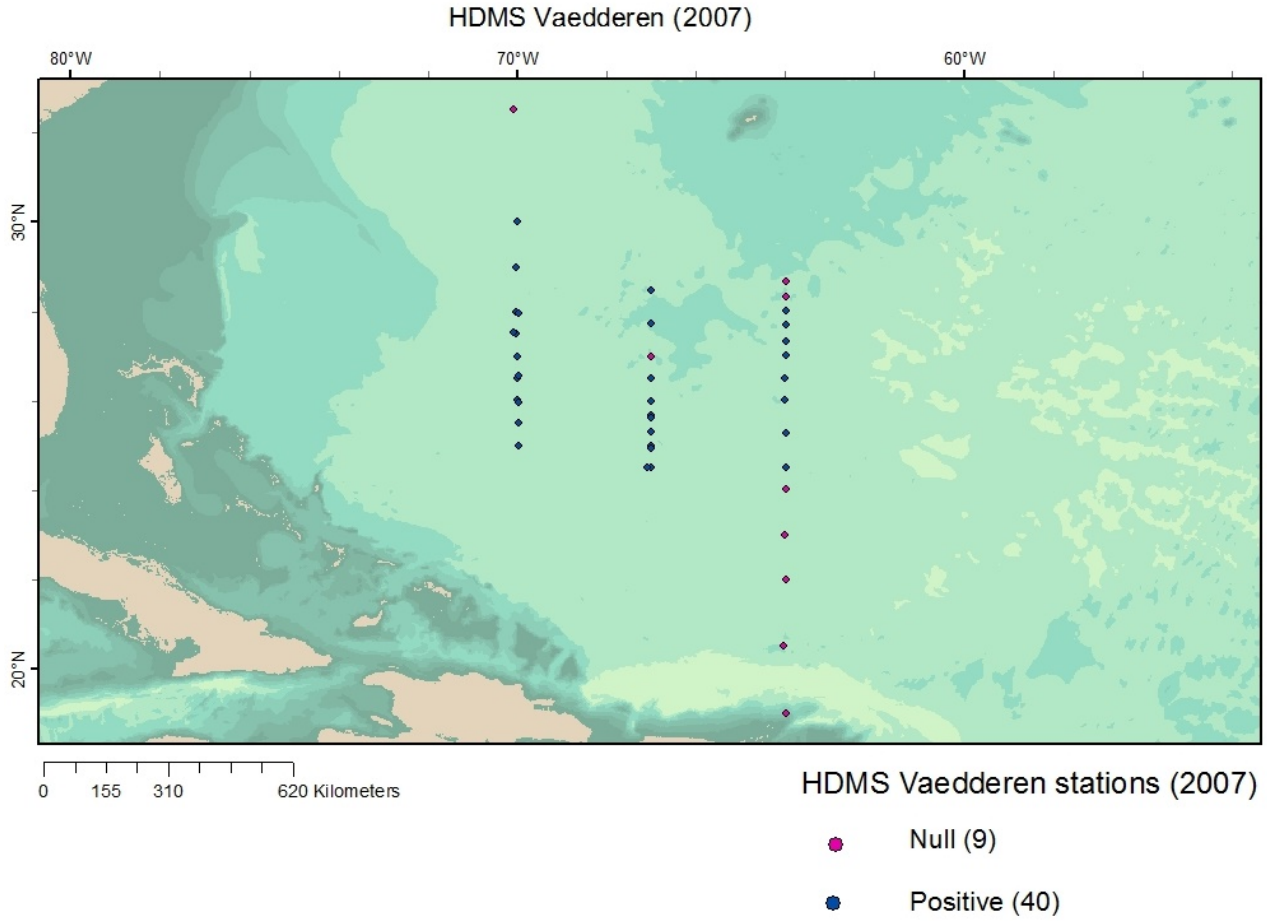

Figure F5. HDMS Vaedderen (2007). The HDMS Vaedderen sampled at 49 stations in 2007. Anguillid larvae were found present at 40 of the stations (blue). No larvae were found at (9) stations (purple).

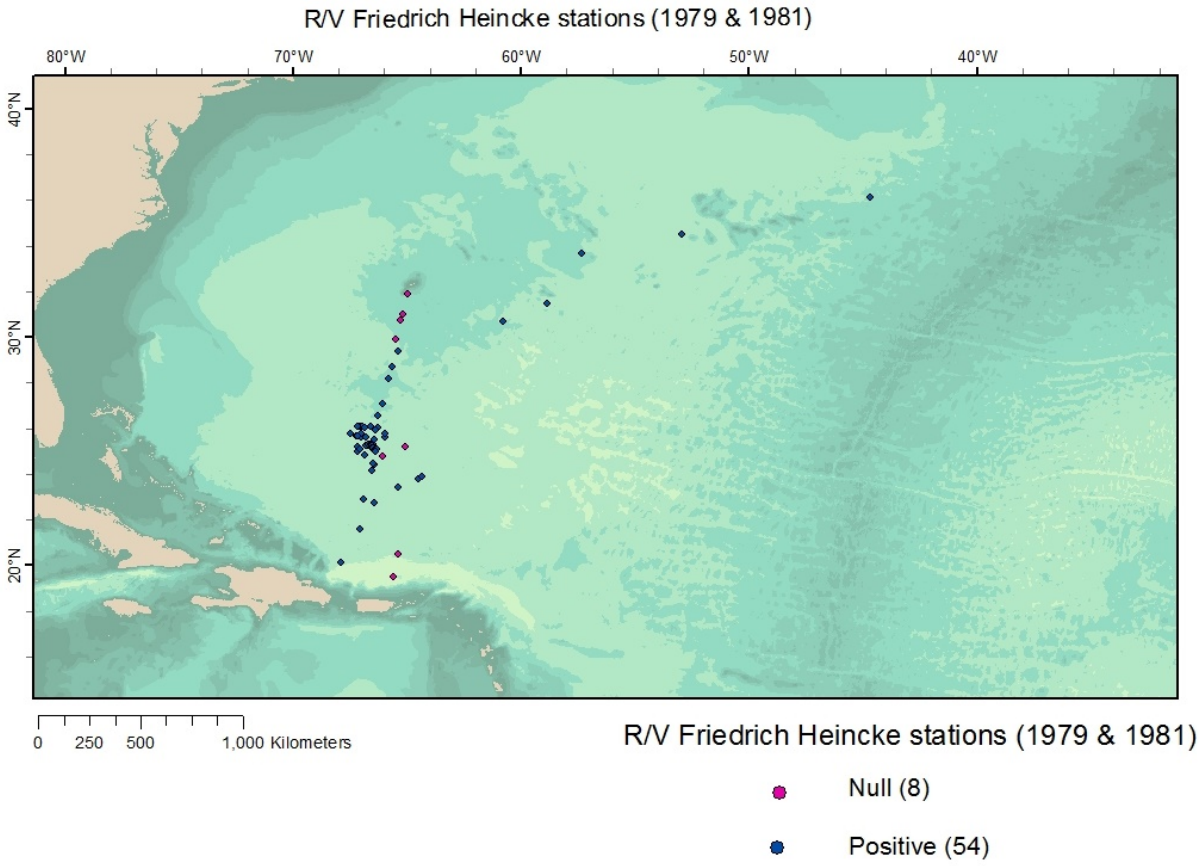

Figure F6. R/V Friedrich Heincke (1979 & 1981). The R/V Friedrich Heincke sampled at 62 stations in 1979 and 1981. Anguillid larvae were found present at 54 of the stations (blue). No larvae were found at (8) stations (purple).

Appendix G

Central Tendencies and Standard Distances of Size Groups

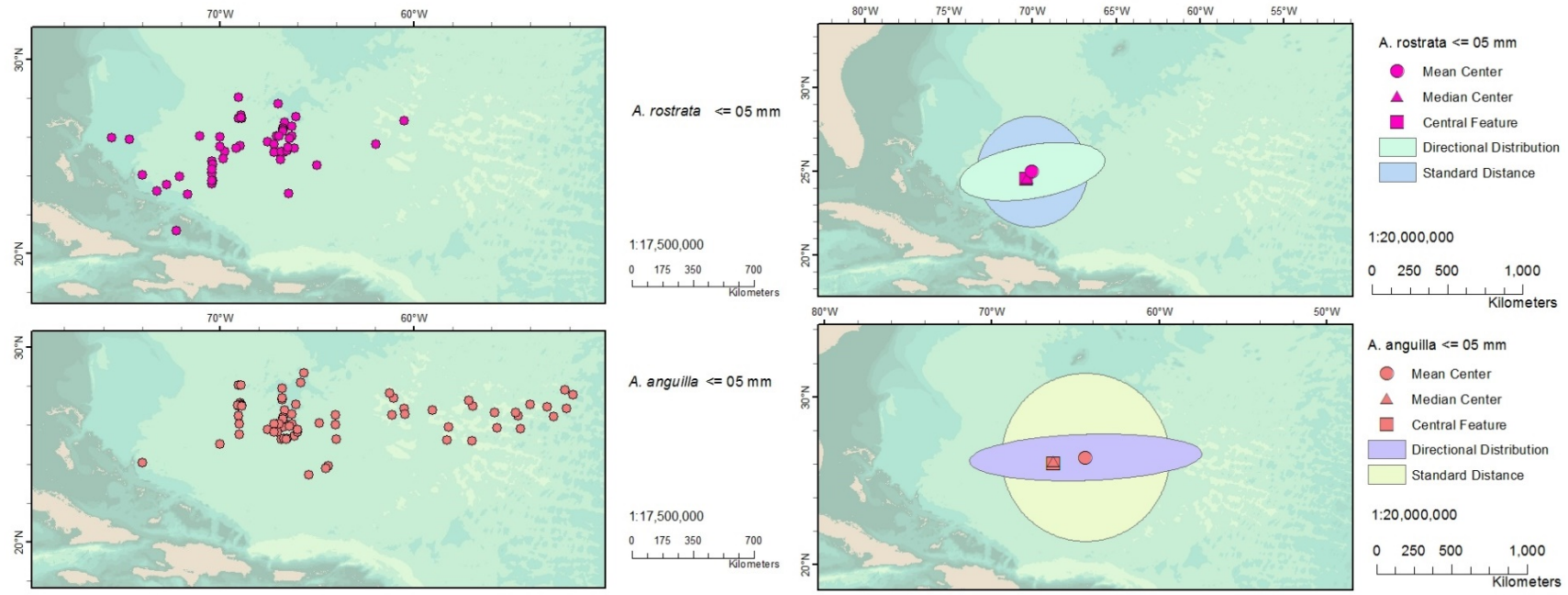

Figure G1. Geographic distribution and central tendencies (≤ 5 mm). Geographic distribution (left) and central tendencies (right) of American eel (above) and European eel (below) larvae (≤ 5 mm).

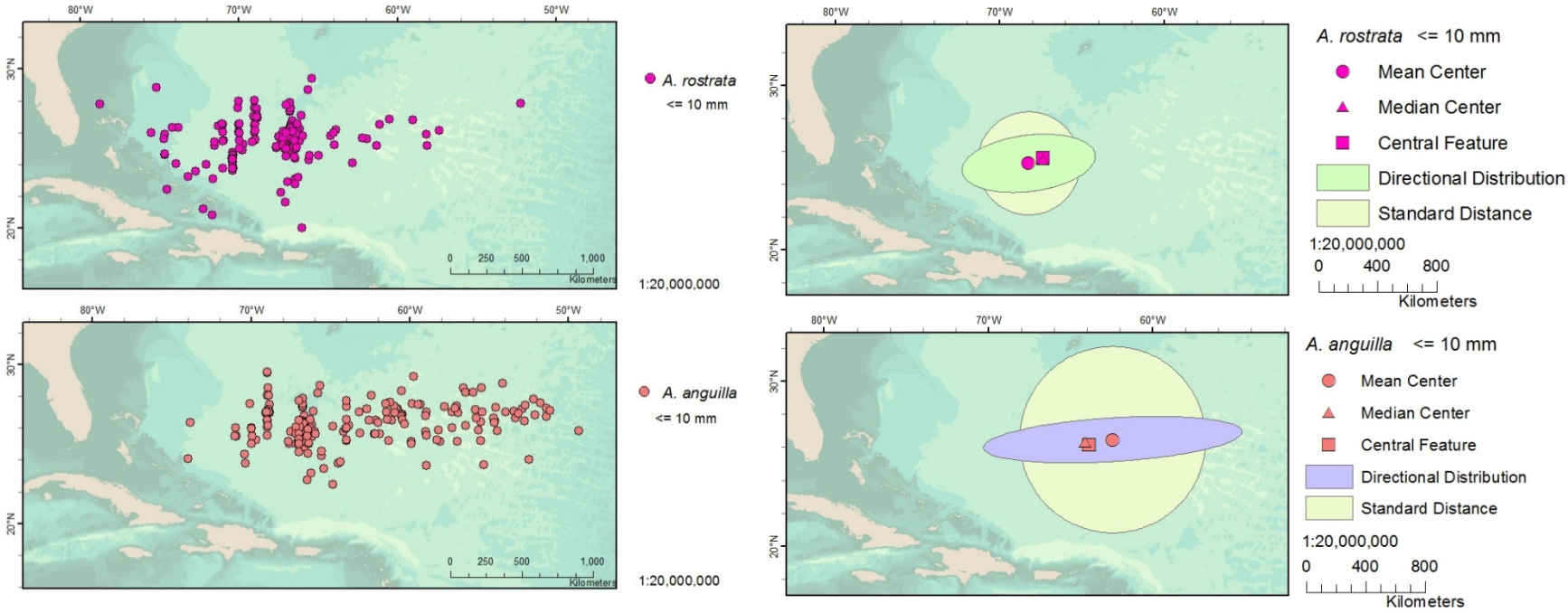

Figure G2. Geographic distribution and central tendencies (≤ 10 mm). Geographic distribution (left) and central tendencies (right) of American eel (above) and European eel (below) larvae (≤ 10 mm).

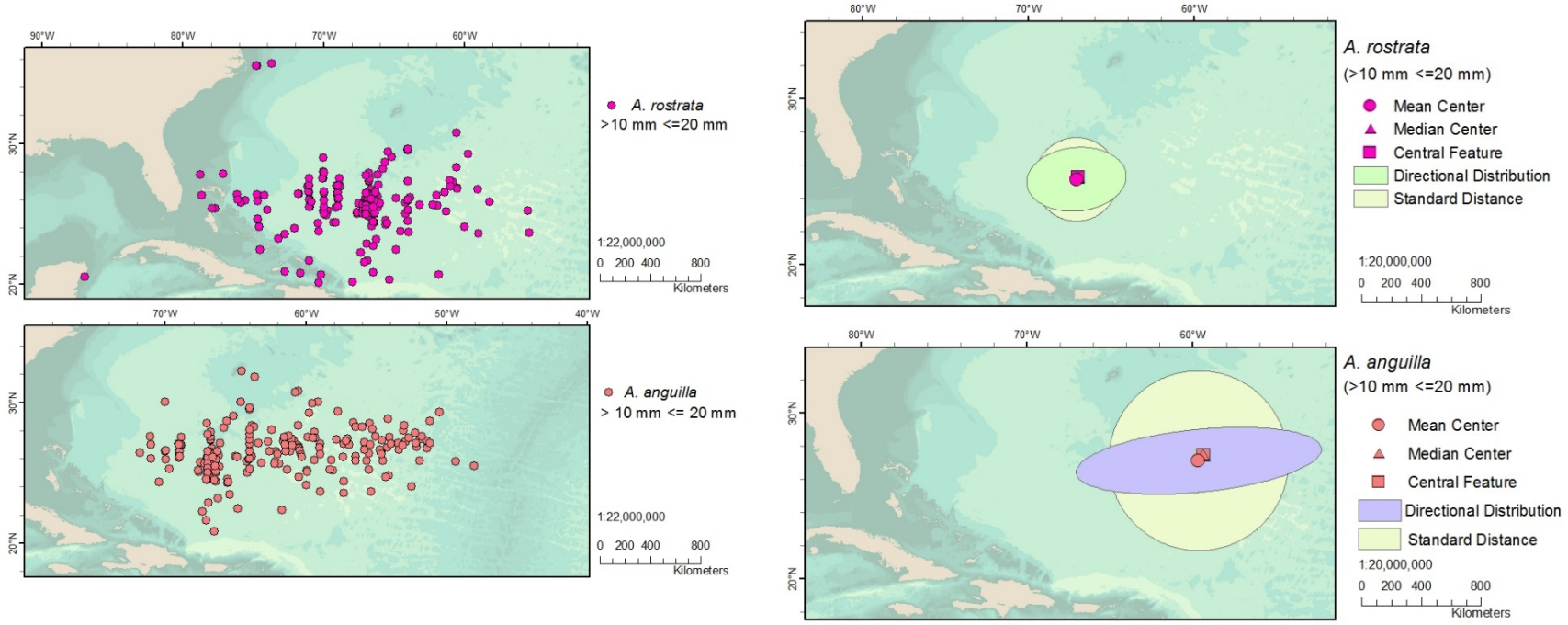

Figure G3. Geographic distribution and central tendencies (> 10 ≤ 20 mm). Geographic distribution (left) and central tendencies (right) of Asmerican eel (above) and European eel (below) larvae (> 10 ≤ 20 mm).

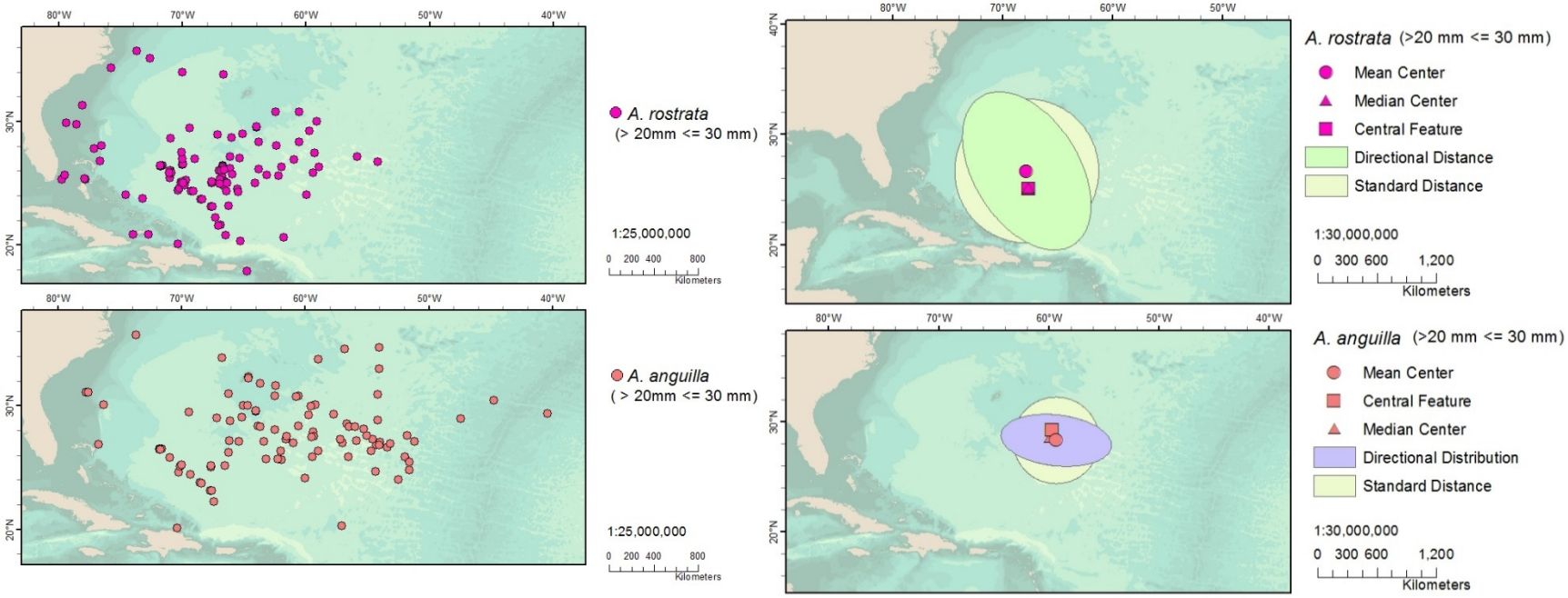

Figure G4. Geographic distribution and central tendencies (> 20 ≤ 30 mm). Geographic distribution (left) and central tendencies (right) of American eel (above) and European eel (below) larvae (> 20 ≤ 30 mm).

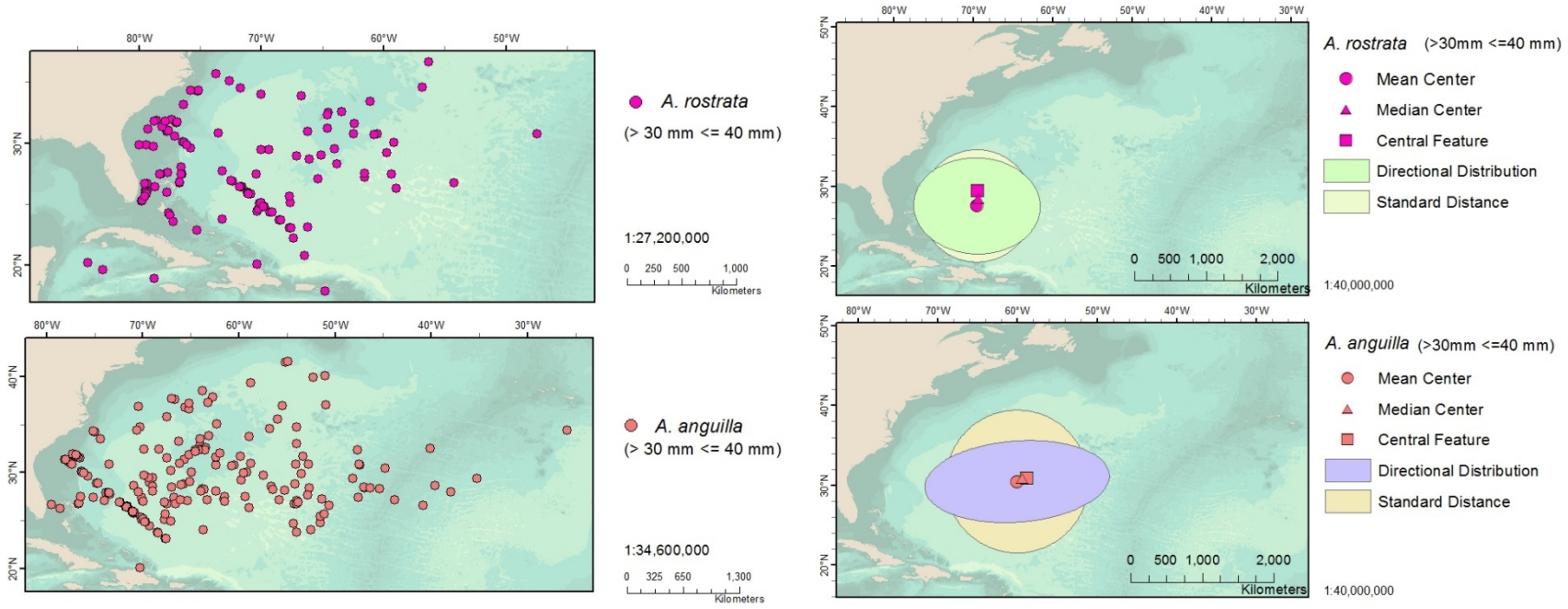

Figure G5. Geographic distribution and central tendencies (> 30 ≤ 40 mm). Geographic distribution (left) and central tendencies (right) of American eel (above) and European eel (below) larvae (> 30 ≤ 40 mm).

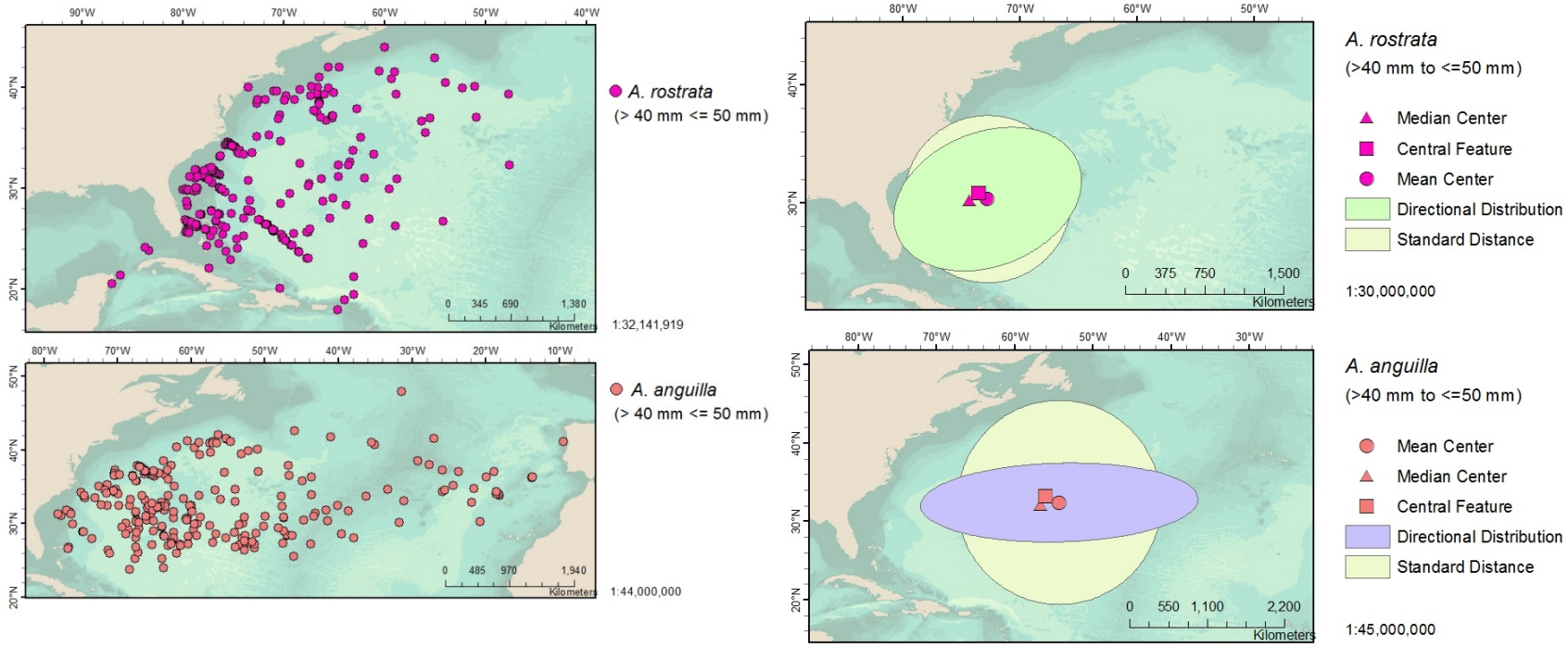

Figure G6. Geographic distribution and central tendencies (> 40 ≤ 50 mm). Geographic distribution (left) and central tendencies (right) of American eel (above) and European eel (below) larvae (> 40 ≤ 50 mm)

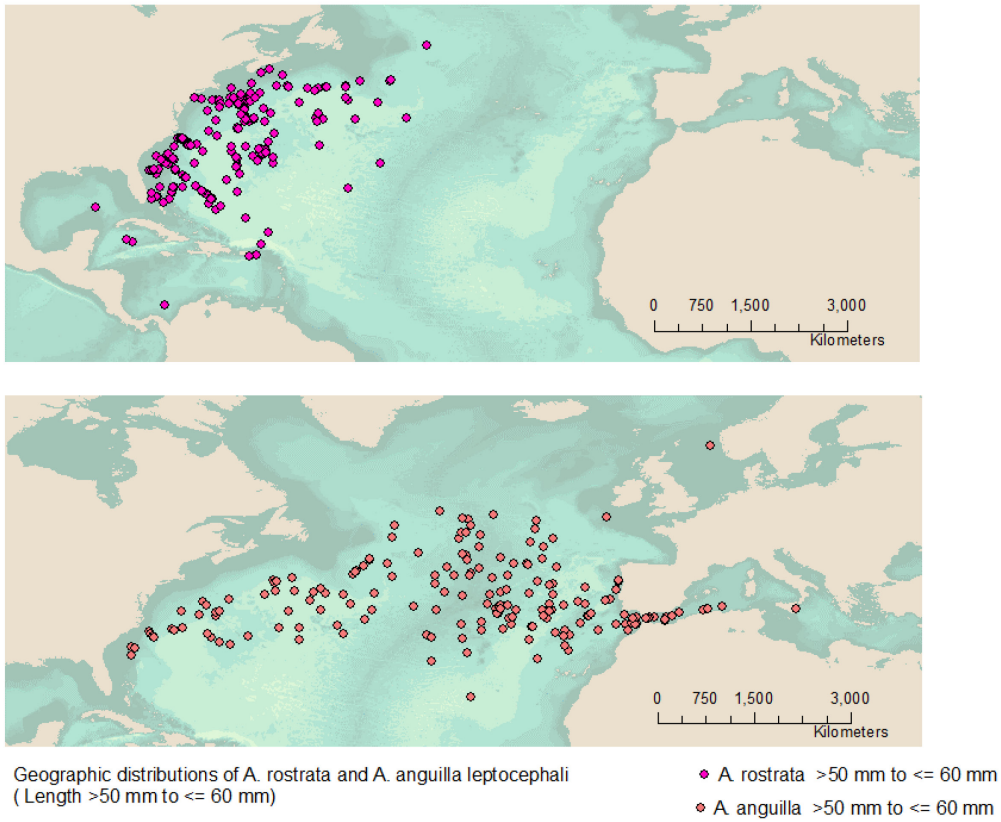

Figure G7. Geographic distribution and central tendencies (> 50 ≤ 60 mm). Geographic distribution (left) and central tendencies (right) of American eel (above) and European eel (below) larvae (> 50 ≤ 60 mm)

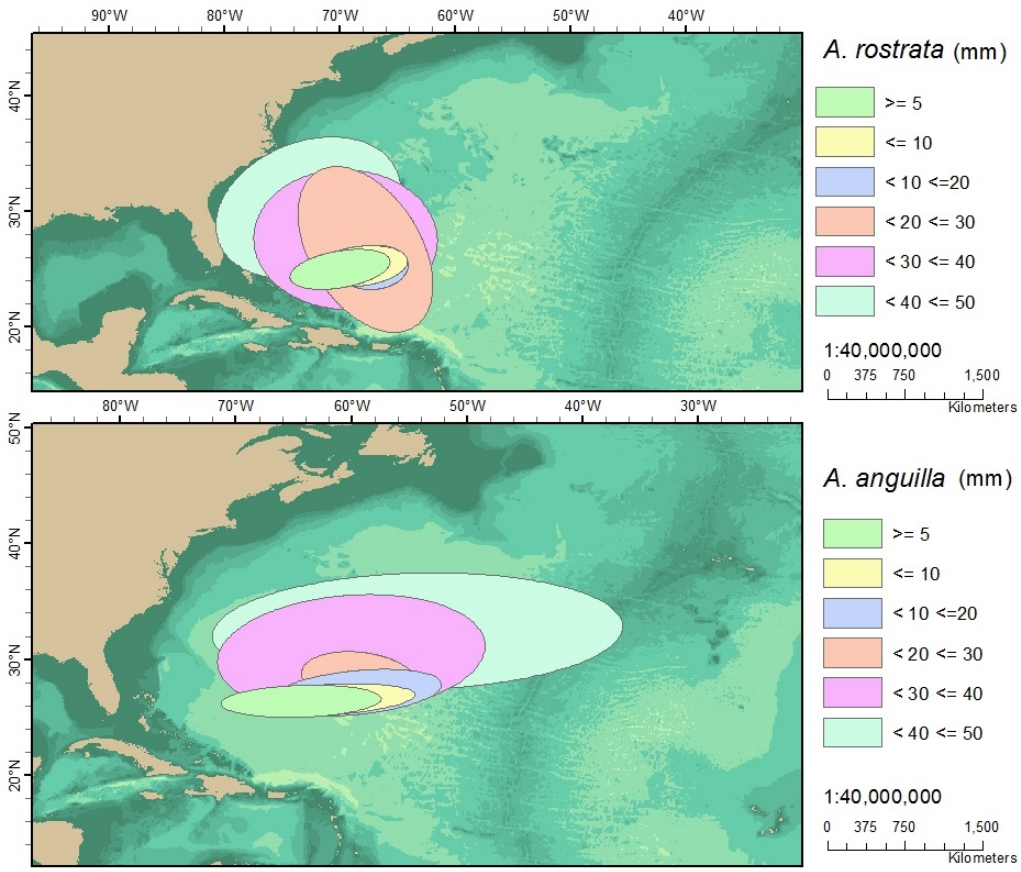

Figure G8. Comparison of directional tendencies of larva distributions. The directional tendencies of *A. rostrata* (above) and *A. anguilla* (below) are shown in 1 SD deviational ellipses for incremental size categories of ≤ 5 mm, ≤ 10 mm, 10 ≤ 20 mm, 20 ≤ 30 mm, 30 ≤ 40 mm and 40 ≤ 50 mm).

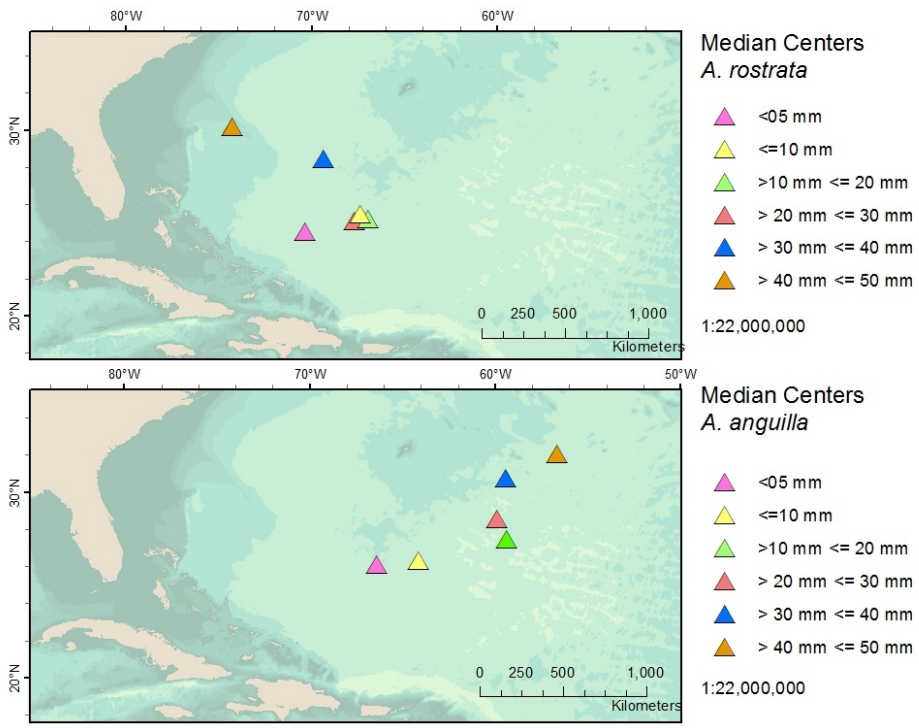

Figure G9. Comparison of central tendencies (≤ 10 mm). The deviational ellipses of the two eel species show their directional tendencies and one standard distance of their directional distribution. Locations of European eel larvae (below) were more laterally compact and oriented that that of American eel larvae (above). The directional ellipse of American eel larvae size category > 10 ≤ 20 mm rotated sharply from 84° to 148° (from "noon").

Appendix H

Supplementary Maps

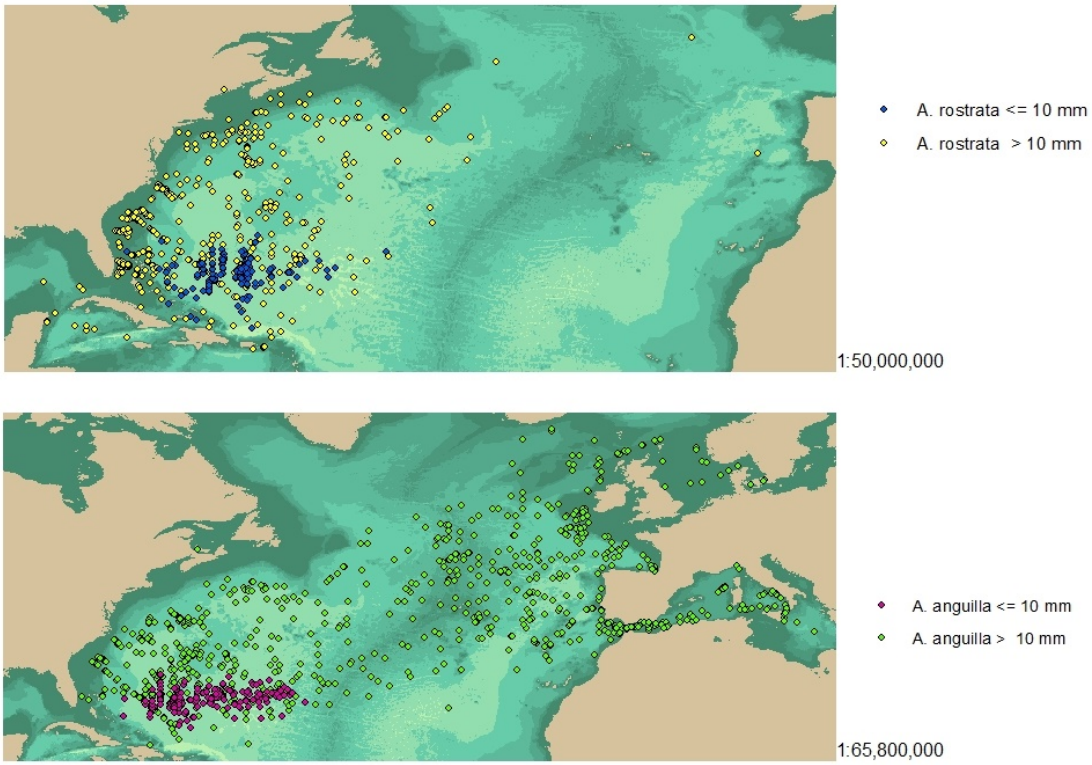

Figure H1. Geographic distribution of small larvae (≤ 10 mm) and larger larvae. The map gives an overview of the newer hatched larvae (≤ 10 mm) for *A. rostrata* (above in blue) and *A. anguilla* (below in purple) in the context of the overall distribution of their species (yellow for *A. rostrata* and green for *A. anguilla*).

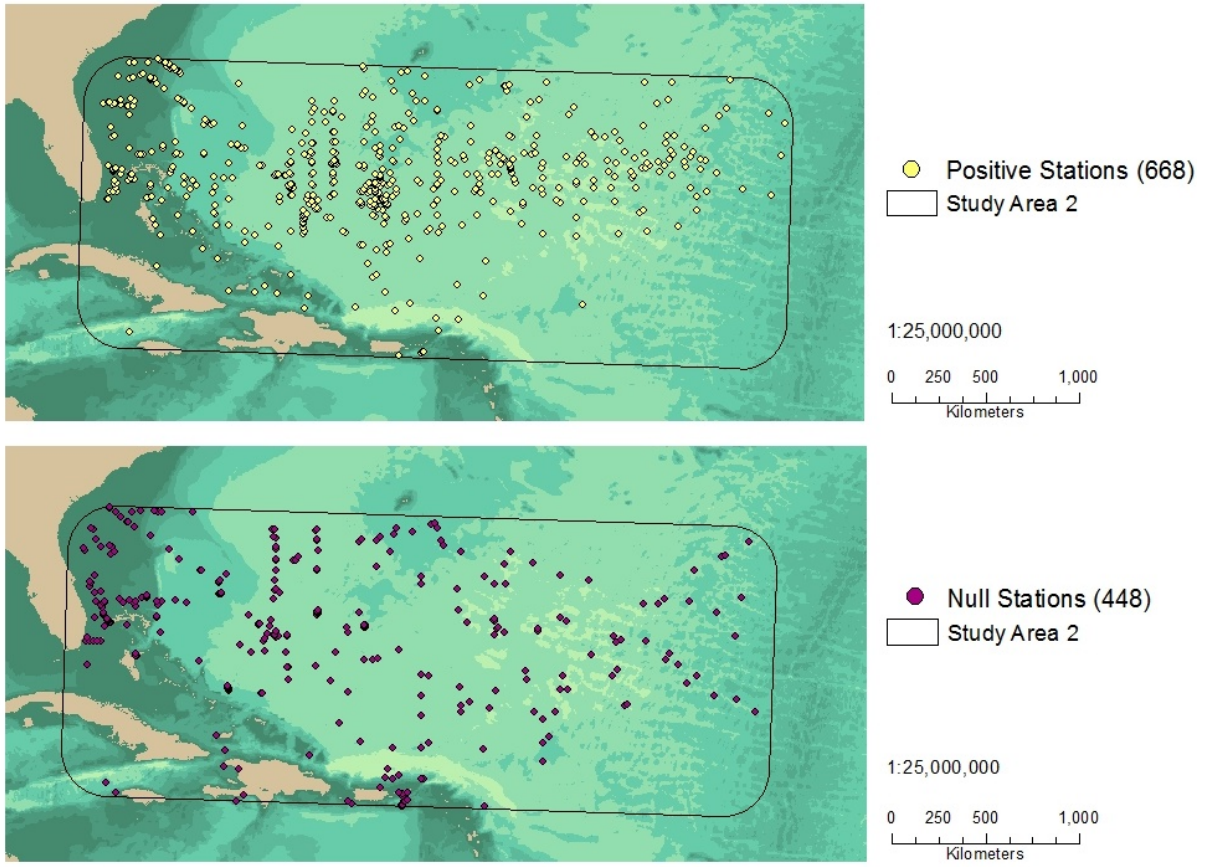

Figure H2. Positive and null stations (Study Area 2). The second study area had a total of 1,012 sampling locations of which 668 made positive larvae observations (above) and the other 448 were null stations (below) making no observations.

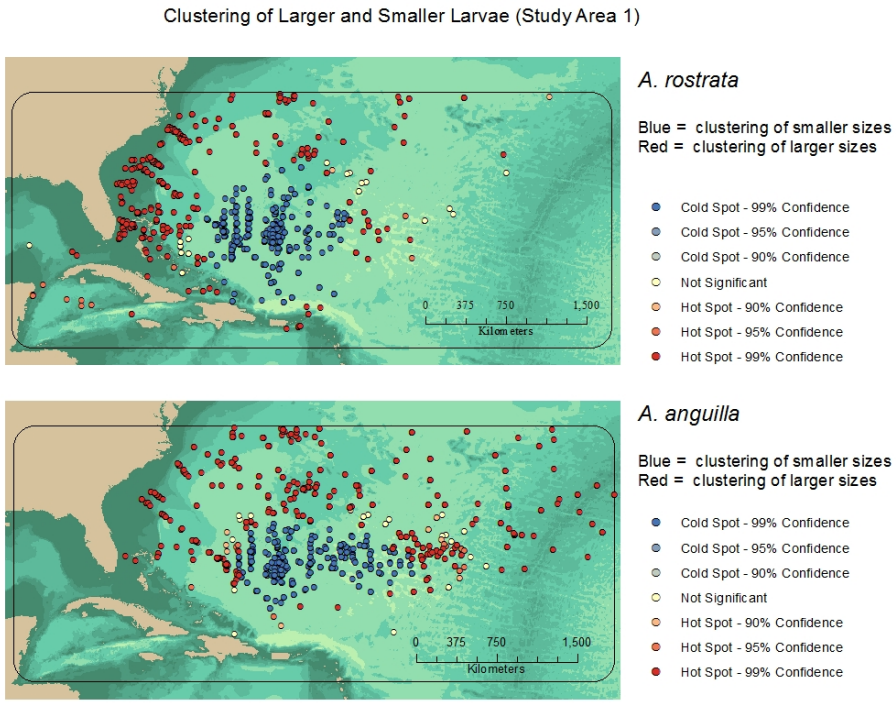

Figure H3. Hot Spot analysis of larval lengths (Study Area 1). The Getis-Ord GI* analysis provides confidence intervals (CIs) for clustering of *A. rostrata* (top) and *A. anguilla* (bottom) larvae clustering in Study Area 1, showing 90%, 95%, and 99% CIs for "cold spots" of smaller larvae (deepening shades of blue), and 90%, 95%, and 99% CIs for "hot spots" of larger larvae (deepening shades of red). Insignificant spatial occurrences are shown in white.